الجمهوريـة الجزائـريـة الديمقراطيـة الشعبيـة
People's Democratic Republic of Algeria
وزارة التعليـم العالـي والبحـث العلمـي
Ministry of Higher Education and Scientific Research

University of Mila

جـــامعة ميلـة

Faculty: Mathematics and Computer Science
Order No: …………………
Registration number: M97/2021

Department: Mathematics
Field: Mathematics
Specialty: Mathematics and applications

Thesis

Submitted for the degree of
Doctorate LMD

Asymptotic behavior of a system of parabolic quasi-variational inequalities

Presented by: Chebbah Samar

N°	Name and surname	Grade	University	Designation
1	Bencheikh Le Hocine Mohamed El Amine	Prof	University of Mila	Chairman
2	Haiour Mohamed	Prof	University of Annaba	Supervisor
3	Boudjedaa Badredine	Prof	University of Mila	Co-supervisor
4	Abdelouahab Mohamed Salah	Prof	University of Mila	Examiner
5	Boularouk Yakoub	MCA	University of Mila	Examiner
6	Dalah Mohamed	Prof	University of Constantine 1	Examiner
7	Merad Ahcene	Prof	University of Oum El Bouaghi	Examiner

University year: 2025 /2026

Acknowledgments

I would like to begin by expressing my sincere gratitude to Almighty God for granting me strength, patience, and perseverance to complete this work. I would like to extend my deepest appreciation to my supervisor, **Pr. Mohamed Haiour**, and my co-supervisor, **Pr. Badreddine Boudjedaa**, for their invaluable guidance, continuous support, and insightful advice throughout this research. Their patience, expertise, and encouragement have been a constant source of motivation. I am equally thankful to **Dr. Sofiane Madi** for his generous support, valuable recommendations, and sincere kindness throughout this research. I would like to sincerely thank the members of the jury for their time, careful reading, and constructive feedback: **Pr. Mohamed El Amine Bencheikh Le Hocine**, **Pr. Mohamed Dalah**, **Pr. Mohamed Salah Abdelouahab**, **Pr. Ahcene Merad**, and **Dr. Yakoub Boularouk**. I also owe a special thanks to my esteemed **Pr. Leïla Aït Kaki**, for her constant support, encouragement, and moral presence throughout this endeavor. Finally, to my dear mother, my brothers, and my sisters, your love and presence have always given me strength. A special remembrance goes to my late father, may his soul rest in peace, whose dream and vision have always guided me.

♡

Dedication

I dedicate this work, first and foremost, to my dear and irreplaceable father, Chebbah Chaabane (may his soul rest in peace). His dream has always been a guiding light in my life, and I thank God who granted me the strength to fulfill our shared dream.

To my beloved mother, Sellami Rebiha, whose prayers and unconditional love have accompanied every step of my academic path.

To my dear brothers: Karim, Yousef, and Yacine, whose presence and encouragement have always lifted my spirit.

To my dear sisters: Yassmine, Marwa, Safaa.

And especially my beloved sister Malak, along with her husband Dr. Bouguenna Bourhan Eddine and their lovely daughter Ayla Touline your love and kindness mean the world to me.

To my dear fiance, Boudraa Houssam, whose support, patience, and constant encouragement have been a source of strength and inspiration throughout this journey.

Chebbah Samar

Abstract

In this work, we investigated non-coercive parabolic quasi-variational inequality (qvi) systems associated with Hamilton–Jacobi–Bellman (HJB) equations. Our methodology consists of reformulating QVI systems directly into HJB equations and solving them, which represents a reversed perspective compared to most previous studies.

We focused on the analysis of the asymptotic behavior of these systems in both coercive and non-coercive cases, by considering continuous and discrete models. The discrete approximation was developed using finite element and finite difference methods.

Our approach relies on overlapping domain decomposition techniques of the alternating Schwarz type, first applied to two subdomains and then generalized to the case of q subdomains. Within this framework, we constructed two monotone sequences of lower and upper solutions and proved that they converge monotonically and geometrically to the unique discrete solution, while providing a sharp error estimate in the L^∞ norm.

Finally, we conducted several numerical experiments to study the asymptotic behavior of the computed solutions. The results demonstrated the stability and accuracy of the method, confirmed its efficiency in approximating the dynamics of parabolic Hamilton–Jacobi–Bellman equations, and underscored the crucial role of overlapping in accelerating convergence.

Keywords : asymptotic behavior, domain decomposition method, parabolic Hamilton-Jacobi-Bellman equations, geometric convergence, monotone convergence, finite elements, finite differences, lower and upper solution sequences, error estimation in the L^∞ norm.

Résumé

Dans ce travail, nous avons étudié les systèmes d'inéquations quasi-variationnelles (QVI) paraboliques non coercifs associés aux équations de Hamilton–Jacobi–Bellman (HJB). Notre méthodologie consiste à reformuler directement les systèmes de QVI en équations HJB et à les résoudre, ce qui constitue une orientation inverse par rapport à la majorité des travaux antérieurs.

Nous sommes concentrés sur l'étude du comportement asymptotique de ces systèmes dans les cas coercif et non coercif, à travers l'analyse des modèles continus et discrets. L'approximation discrète a été développée en s'appuyant sur les méthodes des éléments finis et des différences finies.

Notre approche repose sur des techniques de décomposition de domaine avec recouvrement de type Schwarz alterné, appliquées d'abord à deux sous-domaines puis généralisées au cas de q sous-domaines. Dans ce cadre, nous avons construit deux suites monotones de solutions inférieures et supérieures, et démontré qu'elles convergent monotone et géométriquement vers la solution discrète unique, tout en fournissant une estimation précise de l'erreur dans la norme L^∞.

Enfin, nous avons réalisé plusieurs expériences numériques afin d'étudier le comportement asymptotique des solutions calculées. Les résultats ont démontré la stabilité et la précision de la méthode, confirmé son efficacité pour approximer la dynamique des équations de Hamilton–Jacobi–Bellman paraboliques, et ont mis en évidence le rôle essentiel du recouvrement dans l'accélération de la convergence.

Mots-clés : comportement asymptotique, méthode de décomposition de domaine, équations de Hamilton–Jacobi–Bellman, systèmes d'inéquations quasi-variationnelles elliptiques et paraboliques, convergence géométrique et monotone, éléments finis, différences finies, suites de solutions inférieures et supérieures, estimation de l'erreur dans la norme L^∞.

ملخص

في هذا العمل، درسنا أنظمة المتباينات شبه المتغيرة غير القسرية (QVI) المرتبطة بمعادلات هاملتون–جاكوبي–بيلمان (HJB). وتكمن منهجيتنا في إعادة صياغة أنظمة QVI ذاتها على شكل معادلات HJB وحلها مباشرةً، وهو ما يمثل توجهاً عكسياً مقارنة بالمسار الذي اتبعته معظم الدراسات السابقة.

ركزنا على دراسة السلوك المقارب لهذه الأنظمة في الحالتين القسرية وغير القسرية، وذلك من خلال تحليل كل من النموذجين المتصل والمتقطع. وقد طوّرنا التقريب المتقطع بالاعتماد على منهجيتي العناصر المحدودة والفروق المحدودة.

ترتكز طريقتنا على تقنيات تقسيم المجالات المتداخلة من نوع شوارتز المتناوبة، حيث طُبّقت أولاً على مجالين فرعيين ثم عُمّمت إلى الحالة العامة لعدد q من المجالات الفرعية. في هذا الإطار، أنشأنا متتاليتين رتيبتين من الحلول السفلى والعليا، وأثبتنا أنهما تتقاربان رتيباً وهندسياً نحو الحل المنفصل الفريد، مع تقديم تقدير دقيق للخطأ في المعيار L^∞.

وأخيرا، أجرينا عدة تجارب عددية لدراسة السلوك التقاربي للحلول المحسوبة. أظهرت النتائج ثبات الطريقة ودقتها، وأكدت فعاليتها في تقريب ديناميكيات معادلات هاميلتون-جاكوبي-بيلمان المكافئة، وسلطت الضوء على الدور الحاسم للتداخل في تسريع التقارب.

الكلمات المفتاحية : السلوك المقارب ، طريقة تقسيم المجال، معادلات هاميلتون-جاكوبي-بيلمان ، أنظمة المتباينات شبه المتغيرة الإهليلجية والزمنية ، التقارب الهندسي والرتيب، العناصر المنتهية، الفروق المنتهية، متتاليات الحلول التحتية والفوقية، تقدير الخطأ في معيار L^∞.

Contents

List of Figures

List of Tables

List of abbreviations with symbols

$\mathbb{R}$	real numbers
$\mathbb{R}^N$	N-dimensional real vector space.
Ω	open, bounded set in $\mathbb{R}^N$.
$\bar{\Omega}$	the closure of Ω.
Γ	the boundary of Ω.
Ω_i	the subdomain $\mathfrak{i}$ of Ω.
$\partial\Omega_i$	the boundary of Ω_i.
$H^1(\Omega)$	sobolev space with square-integrable first derivatives.
$H_0^1(\Omega)$	sobolev space with zero trace on the boundary.
$L^2(\Omega)$	space of square-integrable functions.
$L^\infty(\Omega)$	space of essentially bounded functions.
$W^{2,p}(\Omega)$	sobolev space with second-order derivatives in L^p.
$W^{2,\infty}(\Omega)$	sobolev space with second-order derivatives in L^∞.
$C(\bar{\Omega})$	space of continuous functions on the closure of Ω.
$C^2(\bar{\Omega})$	space of functions with continuous second-order derivatives.
HJB	Hamilton-Jacobi-Bellman equation.
VI	variational inequality.
QVI	quasi-variational inequality.
FD	finite difference method.
FE	finite element method.
DDM	domain decomposition method.
DMP	discrete maximum principle.

General introduction

The evolution Hamilton–Jacobi–Bellman (HJB) equation is a nonlinear parabolic partial differential equation that arises naturally in optimal control theory to describe the time evolution of the optimal value function associated with a dynamic decision process. Rooted in Bellman's dynamic programming principle, it characterizes, at each instant of time, the optimal control strategy that optimizes a given performance criterion, taking into account the progressive nature of the system's evolution. From a mathematical perspective, its parabolic structure reflects the intrinsic dependence on time, making it a fundamental tool for modelling evolution phenomena where optimal decisions are continuously updated. This framework has become central in both theory and applications, particularly in economics and finance for time-dependent optimization under uncertainty, as well as in applied mathematics through its connections with parabolic variational inequalities, viscosity solutions, and differential games. Moreover, evolution HJB equations appear in a wide range of applied fields such as robotic motion planning, traffic flow evolution, image processing, and propagation phenomena in heterogeneous media.

In parallel to the extensive research on HJB equations, a substantial literature has been devoted to the study of **parabolic quasi-variational inequality (QVI) systems related to HJB problems**. These systems naturally arise in **stochastic control**, **impulse control**, and **energy management problems**, where the admissible control set depends on the state itself. Several works have provided existence, uniqueness, and asymptotic behavior results, together with finite element discretizations. For instance, in [5] the asymptotic behavior of parabolic QVI systems was analyzed, while [4] investigated finite element approximations for stochastic control models. In [6], further L^∞-error analysis was developed for QVIs associated with impulse control, extending earlier contributions on parabolic variational inequalities [3]. Other related studies examined error bounds, convergence rates, and the role of subsolution concepts in nonlinear settings [9, 12, 39]. These contributions demonstrate that QVI systems represent a natural and rich generalization of HJB equations, embedding them within a broader nonlinear variational framework.

From a computational perspective, **QVI systems related to HJB equations** have been approximated using numerical schemes based on finite difference and finite element methodologies. The finite element framework, in particular, has proven effective in handling mixed boundary conditions and nonlinear source terms while ensuring stable discretizations [11, 13]. In parallel, algorithmic strategies such as overlapping Schwarz methods and domain decomposition techniques have been adapted to these formulations, yielding convergence guarantees and a posteriori error estimates [10, 17, 19]. Extending these approaches to the **evolutionary HJB setting** introduces additional challenges, since the value function evolves over time and the governing PDE reflects a dynamic optimization over a continuous horizon. To address this parabolic case, several works employed finite element discretizations combined with implicit or semi-implicit time-stepping schemes, notably the backward Euler and theta methods, establishing well-posedness and convergence even in the presence of nonlinearities and complex boundary conditions [10, 13–15].

Further developments have addressed **parabolic quasi-variational inequalities** arising in impulse control, where discontinuous interventions alter the system trajectory and variational constraints amplify the nonlinear structure of the HJB formulation. To tackle these challenges, domain decomposition techniques most notably overlapping Schwarz algorithms have been employed, leading to L^∞-error bounds, monotone convergence results, and a posteriori error control specifically designed for time-dependent problems [16, 18, 20]. Beyond these advances, an additional layer of complexity emerges in the **non-coercive** case, where standard conditions ensuring existence, uniqueness, and stability may no longer hold due to degenerate or weakly dominant dynamics. In such settings, reliable numerical strategies typically rely on regularization procedures or reformulated variational principles to guarantee convergence and maintain stability [32, 34].

Domain decomposition techniques have themselves seen significant evolution since their introduction by Schwarz in the late 19th century [41, 45], with rapid developments over the last few decades driven by advancements in parallel computing. These methods not only decompose complex problems into simpler subproblems that are easier to handle computationally, but they also allow for a more flexible reformulation of boundary value problems posed on irregular geometries into equivalent problems defined on simpler domains [36].

A fundamental distinction among domain decomposition approaches concerns the treatment of subdomain interaction. According to this classification [36], subdomains can be:

- **Non-overlapping:** $\Omega_1 \cap \Omega_2 = \emptyset$ (see the right side of Figure (1));
- **Overlapping:** $\Omega_1 \cap \Omega_2 \neq \emptyset$ (see the left side of Figure (1)).

This distinction significantly affects the implementation and convergence of Schwarz-type algorithms.

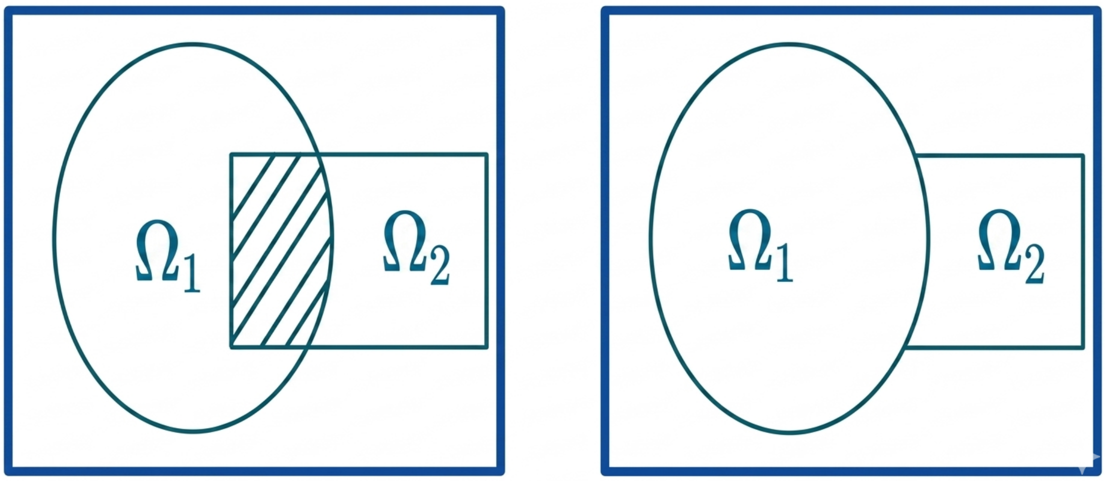

Figure 1: **Schwarz methods: overlapping vs non-overlapping subdomains**

Within the overlapping framework, Schwarz-type methods are commonly implemented in two principal forms:

- **Alternating Schwarz (Schwarz 1870):** subdomains are solved sequentially, each using the most recent boundary values from the neighboring domain [45]:

$$\begin{cases} -\Delta\vartheta_1^{k+1} = \mathbb{F} & \text{in } \Omega_1, \\ \vartheta_1^{k+1} = \vartheta_2^{k} & \text{on } \partial\Omega_1 \cap \Omega_2, \end{cases} \qquad \begin{cases} -\Delta\vartheta_2^{k+1} = \mathbb{F} & \text{in } \Omega_2, \\ \vartheta_2^{k+1} = \vartheta_1^{k+1} & \text{on } \partial\Omega_2 \cap \Omega_1. \end{cases}$$

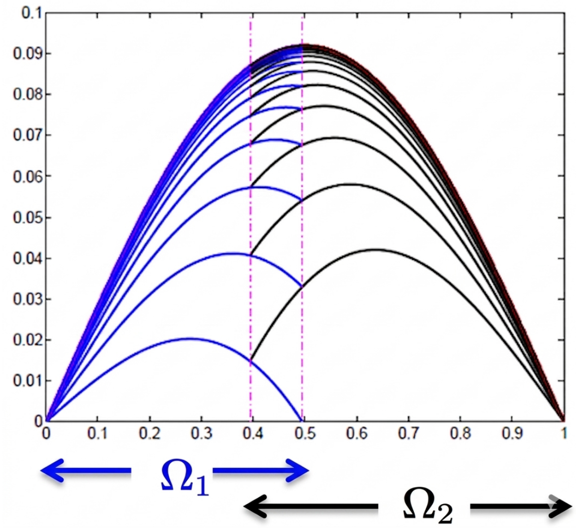

Figure 2: **Alternating Schwarz**

- **Parallel Schwarz (Lions 1988):** subdomains are solved concurrently using boundary data from the previous iteration [41]:

$$\begin{cases} -\Delta\vartheta_1^{k+1} = \mathbb{F} & \text{in } \Omega_1, \\ \vartheta_1^{k+1} = \vartheta_2^k & \text{on } \partial\Omega_1 \cap \Omega_2, \end{cases} \qquad \begin{cases} -\Delta\vartheta_2^{k+1} = \mathbb{F} & \text{in } \Omega_2, \\ \vartheta_2^{k+1} = \vartheta_1^k & \text{on } \partial\Omega_2 \cap \Omega_1. \end{cases}$$

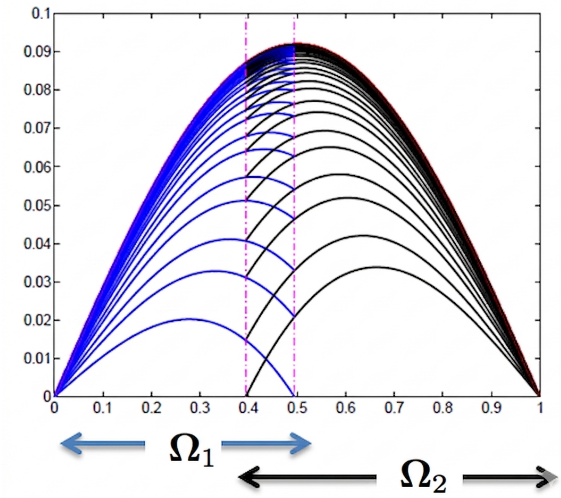

Figure 3: **Parallel Schwarz**

Both approaches may also be adapted to the non-overlapping setting, where appropriate **transmission conditions** such as Robin type interface constraints are introduced to preserve convergence guarantees.

In this study, we investigate the **asymptotic behavior of parabolic quasi-variational inequality (QVI) systems related to Hamilton Jacobi Bellman (HJB) equations**, formulated in the non-coercive setting as follows:

$$\begin{cases} \max\limits_{1\leq i\leq n}\left(\dfrac{\partial\vartheta}{\partial t}+\mathbb{A}^i\vartheta-\mathbb{F}^i\right)=0 & \text{in } \Omega\times[0,T], \\ \vartheta=0 & \text{on } \partial\Omega, \\ \vartheta(x,0)=\vartheta_0(x) & \text{in } \Omega. \end{cases}$$

The central objective is to characterize the long-time behavior of solutions, despite the non-linear and non-coercive structure that may generate significant analytical difficulties. To this end, the problem is first studied on two overlapping subdomains, where a backward Euler discretization in time reduces the parabolic formulation to a sequence of coercive elliptic problems. This strategy is then generalized to q overlapping subdomains by combining domain decomposition techniques with iterative sequences of sub- and super-solutions. We establish that these sequences converge monotonically and geometrically to the discrete solution, and we derive sharp L^∞-error estimates that capture the asymptotic profile of the system. Finally, numerical experiments using both finite difference and finite element discretizations confirm the theoretical predictions, underlining the efficiency of the method and the decisive role of overlap in accelerating convergence.

This thesis is organized into four main phases:

- **Chapter one** establishes the theoretical underpinnings essential for comprehending the whole structure. The discussion starts with a comprehensive examination of variational inequalities (VI) and quasi-variational inequalities (QVI), which provide the mathematical foundation for the analysis of Hamilton-Jacobi equations in non-traditional contexts. We examine the criteria for existence and uniqueness, together with qualitative attributes like monotonicity, regularity, and Lipschitz continuity. This context introduces the idea of subsolutions, and the investigation is extended to the discrete framework by examining approximations of the discrete issue and their convergence to the continuous case. This chapter is based on existing findings, especially those of Cortey-Dumont [33], whose work was crucial in the examination of uniform convergence in the $\|\cdot\|_\infty$ norm.

- **Chapter two** is exclusively focused on the coercive situation of the Hamilton-Jacobi-Bellman problem, resolved by the overlapping Schwarz technique over two subdomains in its sequential format. We formulate a numerical technique using sequences of sub- and supersolutions for the discrete issue and demonstrate that these sequences converge monotonically and geometrically to the actual solution. A numerical example is shown to verify the approach and illustrate its effectiveness. This phase emphasizes the beneficial impact of domain overlap on expediting numerical convergence and illustrates how coercivity contributes to solution stability.

- **Chapter three** advances this analytical trajectory by examining the non-coercive scenario, which presents more challenges owing to the absence of classical contraction features. The numerical sequence is recreated using procedures similar to those in the preceding chapter; however, the study of stability and convergence need more sophisticated reasoning. A comprehensive theoretical analysis is provided, corroborated by numerical simulations that illustrate the method's efficacy despite the lack of coercivity. Particular emphasis is placed on the selection of overlap parameters and their impact on convergence speed and quality. This chapter is an innovative addition to the thesis, considering the limited research on non-coercive solutions using the Schwarz approach.

- In the **fourth chapter**, we study the **asymptotic behavior of a system of quasi-variational inequalities related to a non-coercive parabolic Hamilton–Jacobi–Bellman (HJB) problem**. Starting from the backward time discretization, the system is reformulated into a sequence of coercive elliptic HJB equations. This framework first enables the analysis in the case of two overlapping subdomains, where existence, uniqueness, and convergence are established through monotonicity arguments. The study is then extended to the general case of q overlapping subdomains, where we establish monotone and geometric convergence of the iterative sequences. Moreover, we study the asymptotic behavior of the solution and derive optimal error estimates in the uniform norm for the considered problem.

Finally, we verify the asymptotic behavior computationally through several numerical experiments, rather than only theoretical results. These simulations confirm the error estimates, illustrate the monotone convergence, and demonstrate the efficiency and stability of the proposed overlapping domain decomposition method for time-dependent non-coercive HJB systems.

Chapter one :

Preliminaries on variational and quasi-variational inequality problems and systems

In this chapter, we present the mathematical framework of variational and quasi-variational inequalities. We introduce the functional setting, study the continuous and discrete formulations, and establish the main results concerning existence, uniqueness, and approximation properties. Finally, we extend the analysis to systems of quasi-variational inequalities.

Contents

1.1 Mathematical preliminaries and function spaces

In order to build the theoretical framework of this work, we first recall some basic notions concerning function spaces. The discussion focuses on Lebesgue spaces and, in particular, on their structure as Banach or Hilbert spaces depending on the choice of the parameter p [24].

1.1.1 Definition of lebesgue spaces

- For a real exponent $1 \leq p < \infty$, the Lebesgue space $L^p(\Omega)$ is the collection of measurable functions $f : \Omega \to \mathbb{R}$ such that:

$$\int_\Omega |f(x)|^p \, dx < \infty.$$

- The norm that turns this set into a Banach space is defined by:

$$\|f\|_{L^p} = \left(\int_\Omega |f(x)|^p \, dx \right)^{\frac{1}{p}}.$$

- When $p = \infty$, one considers the space of essentially bounded measurable functions:

$$L^\infty(\Omega) = \left\{ f : \Omega \to \mathbb{R} \;\middle|\; \sup_{x \in \Omega} \mathrm{ess}\, |f(x)| < \infty \right\}.$$

- The natural norm on this space is given by:

$$\|f\|_{L^\infty} = \sup_{x \in \Omega} |f(x)|.$$

1.1.2 Hilbert space $L^2(\Omega)$

- For $p = 2$, the space acquires the structure of a Hilbert space, equipped with the inner product:

$$\langle f, g \rangle_{L^2} = \int_\Omega f(x)\, g(x)\, dx.$$

- The associated norm is induced in the usual way from this scalar product.

1.1.3 Sobolev-type function spaces

We now recall the definition and the main properties of Sobolev spaces, which play a central role in the variational framework of partial differential equations.

- Let $m \geq 1$ be an integer and $p \geq 1$ a real number.
- The Sobolev space $W^{m,p}(\Omega)$ consists of all functions $u \in L^p(\Omega)$ such that all weak derivatives up to order m also belong to $L^p(\Omega)$:

$$W^{m,p}(\Omega) = \left\{ u \in L^p(\Omega) \;\middle|\; D^\alpha u \in L^p(\Omega),\ \forall \alpha \text{ with } |\alpha| \leq m \right\}.$$

- The space becomes a Banach space under the norm:

$$\|u\|_{W^{m,p}(\Omega)} = \left(\sum_{|\alpha| \leq m} \|D^\alpha u\|^p_{L^p(\Omega)} \right)^{1/p}.$$

- For $p = 2$, the Sobolev space is usually denoted by $H^m(\Omega)$.
- It contains all $u \in L^2(\Omega)$ with weak derivatives up to order m in $L^2(\Omega)$:

$$H^m(\Omega) = \left\{ u \in L^2(\Omega) \;\middle|\; D^\alpha u \in L^2(\Omega),\ |\alpha| \le m \right\}.$$

- The inner product that endows $H^m(\Omega)$ with a Hilbert structure is:

$$\langle u, v \rangle_{H^m(\Omega)} = \sum_{|\alpha| \le m} \langle D^\alpha u, D^\alpha v \rangle.$$

- A fundamental subspace is:

$$H_0^1(\Omega) = \left\{ u \in H^1(\Omega) \;\middle|\; u_{|\partial\Omega} = 0 \right\},$$

  where the boundary condition is understood in the trace sense.
- Being closed in $H^1(\Omega)$, this space is itself a Hilbert space.

1.1.4 Integral bounds via hölder-type inequalities

Theorem 1.1.1: [24]

Let $\Omega \subset \mathbb{R}^N$ be a measurable set, and consider two functions $f \in L^p(\Omega)$ and $g \in L^q(\Omega)$, where the exponents $p, q > 0$ satisfy the conjugacy relation:

$$\frac{1}{p} + \frac{1}{q} = 1.$$

Then, for $1 \le p \le \infty$, the standard Hölder inequality asserts that:

$$\int_\Omega |f(x)\, g(x)|\, dx \le \|f\|_{L^p(\Omega)}\, \|g\|_{L^q(\Omega)}.$$

1.2 The variational inequalities

This section introduces the analytical framework of variational inequalities in both continuous and discrete settings. The study is based on elliptic boundary value problems formulated in Sobolev spaces and their finite-dimensional approximations.

1.2.1 Continuous variational inequalities

Mathematical preliminaries and structural hypotheses

Let $\Omega \subset \mathbb{R}^N$ be a bounded convex domain with sufficiently smooth boundary $\partial\Omega$. The variational framework is developed in the space $H_0^1(\Omega)$, together with the standard assumptions ensuring the well-posedness of the problem.

The associated bilinear form is defined for all $u, v \in H^1(\Omega)$ by:

$$a(v,u) = \int_\Omega \left(\sum_{z,s=1}^{N} a_{zs}(x)\,\frac{\partial v}{\partial x_z}\,\frac{\partial u}{\partial x_s} + \sum_{s=1}^{N} b_s(x)\,\frac{\partial v}{\partial x_s}\,u + a_0(x)\,v\,u \right) dx, \tag{1.1}$$

which corresponds to a second-order differential operator defined by:

$$\mathscr{A}u = \sum_{z,s=1}^{N} a_{zs}(x)\frac{\partial^2 u}{\partial x_z \partial x_s} + \sum_{s=1}^{N} b_s(x)\frac{\partial u}{\partial x_s} + a_0(x)u. \tag{1.2}$$

The coefficients are assumed to satisfy standard structural hypotheses ensuring the well-posedness of the model. In particular, the zeroth-order term is assumed to be strictly positive, namely:

$$a_0(x) \geq \gamma > 0, \quad \forall x \in \Omega, \tag{1.3}$$

while the diffusion matrix is uniformly elliptic in the sense that there exists $\delta > 0$ such that:

$$\sum_{z,s=1}^{N} a_{zs}(x)\,\xi_z \xi_s \geq \delta|\xi|^2, \quad \forall \xi \in \mathbb{R}^N,\ x \in \overline{\Omega}, \tag{1.4}$$

and the coefficients are assumed to be symmetric:

$$a_{zs}(x) = a_{sz}(x). \tag{1.5}$$

Under these assumptions, the bilinear form is continuous and coercive, which guarantees the existence of a constant $\lambda > 0$ such that:

$$a(u,u) \geq \lambda \|u\|^2_{H^1(\Omega)}, \quad \forall u \in H^1(\Omega). \tag{1.6}$$

The external forcing is represented by a linear functional $\mathbb{F} \in L^\infty(\Omega)$ defined by:

$$\langle \mathbb{F}, u \rangle = \int_\Omega \mathbb{F}(x)\,u(x)\,dx, \quad \mathbb{F} \geq 0, \tag{1.7}$$

while the obstacle function is assumed to belong to $W^{2,\infty}(\Omega)$ and satisfy:

$$\Psi > 0 \quad \text{on } \partial\Omega. \tag{1.8}$$

This leads to the definition of the admissible convex set:

$$\mathbb{K} = \{u \in H_0^1(\Omega) \mid 0 \leq u \leq \Psi \text{ in } \Omega\}. \tag{1.9}$$

Finally, the continuous variational inequality problem consists in finding $\vartheta \in \mathbb{K}$ such that:

$$a(\vartheta, u - \vartheta) \geq \langle \mathbb{F}, u - \vartheta \rangle, \quad \forall u \in \mathbb{K}. \tag{1.10}$$

Existence, uniqueness, and regularity of the continuous solution

Theorem 1.2.1: [7]

Under the assumptions introduced previously, the variational inequality problem (1.10) admits a unique solution ϑ. Moreover, this solution satisfies the regularity property:

$$\vartheta \in W^{2,p}(\Omega), \quad 1 \leq p < \infty.$$

Proof

The proof is divided into two parts: uniqueness and existence.

- **Uniqueness:** Let $\vartheta_1, \vartheta_2 \in \mathbb{K}$ be two solutions of (1.10). Then

$$a\langle \vartheta_1, u - \vartheta_1 \rangle \geq \langle \mathbb{F}, u - \vartheta_1 \rangle, \quad \forall u \in \mathbb{K},$$
$$a\langle \vartheta_2, u - \vartheta_2 \rangle \geq \langle \mathbb{F}, u - \vartheta_2 \rangle, \quad \forall u \in \mathbb{K}.$$

Taking $u = \vartheta_2$ in the first inequality yields

$$a\langle \vartheta_1, \vartheta_2 - \vartheta_1 \rangle \geq \langle \mathbb{F}, \vartheta_2 - \vartheta_1 \rangle.$$

Since

$$\vartheta_2 - \vartheta_1 = -(\vartheta_1 - \vartheta_2),$$

we obtain:

$$-a\langle \vartheta_1, \vartheta_1 - \vartheta_2 \rangle \geq -\langle \mathbb{F}, \vartheta_1 - \vartheta_2 \rangle.$$

Multiplying by -1, it follows that:

$$a\langle \vartheta_1, \vartheta_1 - \vartheta_2 \rangle \leq \langle \mathbb{F}, \vartheta_1 - \vartheta_2 \rangle. \tag{1.11}$$

Similarly, choosing $u = \vartheta_1$ in the second inequality gives:

$$a\langle \vartheta_2, \vartheta_1 - \vartheta_2 \rangle \geq \langle \mathbb{F}, \vartheta_1 - \vartheta_2 \rangle. \tag{1.12}$$

Combining the two relations (1.11) and (1.12), we deduce that:

$$a\langle \vartheta_1, \vartheta_1 - \vartheta_2 \rangle - a\langle \vartheta_2, \vartheta_1 - \vartheta_2 \rangle \leq 0.$$

Using the linearity of the bilinear form with respect to the first variable, we obtain:

$$a\langle \vartheta_1 - \vartheta_2, \vartheta_1 - \vartheta_2 \rangle \leq 0.$$

Since the bilinear form a is coercive, there exists a constant $\lambda > 0$ such that:

$$a\langle v, v \rangle \geq \lambda \|v\|^2.$$

Consequently,

$$0 \leq \lambda \|\vartheta_1 - \vartheta_2\|^2 \leq a\langle \vartheta_1 - \vartheta_2, \vartheta_1 - \vartheta_2 \rangle \leq 0,$$

which implies:

$$\vartheta_1 = \vartheta_2.$$

- **Existence:** We introduce the projection operator T and consider the fixed-point formulation:
$$\vartheta = T\big(\vartheta - \rho(\mathbb{A}\vartheta - \mathbb{F})\big), \quad \rho > 0.$$
This formulation is equivalent to the variational inequality (1.10), since it satisfies:
$$\langle \mathbb{A}\vartheta - \mathbb{F}, u - \vartheta\rangle \geq 0, \quad \forall u \in \mathbb{K}.$$
Using the non-expansiveness of the projection operator, for all $u, v \in H_0^1$, we obtain:
$$\|T(u - \rho(\mathbb{A}u - \mathbb{F})) - T(v - \rho(\mathbb{A}v - \mathbb{F}))\|^2 \leq \|u - v - \rho\mathbb{A}(u - v)\|^2.$$
Expanding the right-hand side gives:
$$\|u - v\|^2 - 2\rho\, a(u - v, u - v) + \rho^2\|\mathbb{A}(u - v)\|^2.$$
Using coercivity and boundedness of $\mathbb{A}$, we obtain:
$$(1 - 2\rho\lambda + \rho^2 C_*^2)\|u - v\|^2,$$
where $\lambda > 0$ is the coercivity constant and C_* is the continuity constant of $\mathbb{A}$. Choosing:
$$\rho < \frac{2\lambda}{C_*^2}$$
ensures that the mapping is a contraction. Hence, Banach's fixed-point theorem guarantees the existence and uniqueness of $\vartheta \in \mathbb{K}$.

The existence and uniqueness of the solution ϑ are classical results that can be found in the literature. Furthermore, the solution satisfies the following a priori estimate:

$$\|\vartheta\|_{W^{2,p}(\Omega)} \leq C\left(\|\mathbb{F}\|_\infty + \|\mathbb{A}\Psi\|_\infty\right), \tag{1.13}$$

where C is a positive constant depending only on the geometry of Ω and the coefficients of the operator $\mathbb{A}$.

Expression of the continuous solution in terms of lower solutions

To better understand the structure of the solutions to the variational inequality (1.10), we now present a characterization involving subsolutions. This perspective provides an alternative formulation and introduces a comparison principle, according to which the exact solution can be described as the upper bound of all subsolutions.

Definition 1.2.1: [7]

Let X denote the set of subsolutions to the variational inequality (1.10). An element $\mathfrak{z} \in H_0^1(\Omega)$ belongs to X if it satisfies:

$$\begin{cases} a\langle \mathfrak{z}, u\rangle \leq \langle \mathbb{F}, u\rangle, & \forall u \in H_0^1(\Omega), \\ \mathfrak{z} \leq \Psi, & \text{with } u \geq 0. \end{cases}$$

We may now establish a fundamental result connecting the unique solution ϑ of problem (1.10) with the set X.

Theorem 1.2.2: [7]

Under the standing assumptions, the solution ϑ of the variational inequality (1.10) is the greatest element of the set X.

Properties of the obstacle mapping

Let us introduce the mapping:

$$\begin{aligned} \Upsilon : L^\infty(\Omega) &\longrightarrow L^\infty(\Omega), \\ \Psi &\longmapsto \Upsilon(\Psi) = \vartheta, \end{aligned} \tag{1.14}$$

where ϑ denotes the unique solution of the variational inequality (1.10) associated with the obstacle Ψ.

Proposition 1.2.1: [22]

The mapping Υ is increasing, concave, and lipschitz continuous with respect to Ψ.

Proof

Let us verify the main properties of the operator Υ:

1. **Monotonicity:** let $\Psi, \tilde{\Psi} \in L^\infty(\Omega)$ be such that $\Psi \leq \tilde{\Psi}$ almost everywhere.
   - By definition, $\Upsilon(\Psi)$ is the unique solution of the variational inequality with obstacle Ψ.
   - Since $\Upsilon(\Psi) \leq \Psi \leq \tilde{\Psi}$, the function $\Upsilon(\Psi)$ satisfies the inequality constraint associated with $\tilde{\Psi}$.
   - Therefore, $\Upsilon(\Psi)$ is a subsolution for the variational inequality with obstacle $\tilde{\Psi}$.
   - From theorem 1.2.2, the solution corresponding to an obstacle is the greatest subsolution.
   - Hence, $\Upsilon(\Psi) \leq \Upsilon(\tilde{\Psi})$, proving that Υ is monotone.
2. **Concavity:** let $\Psi, \tilde{\Psi} \in L^\infty(\Omega)$ and let $\theta \in [0, 1]$. Define:

$$\Psi_\theta = \theta\Psi + (1-\theta)\tilde{\Psi}.$$

   - Let $\Upsilon_\theta = \Upsilon(\Psi_\theta)$ denote the solution associated with the convex combination Ψ_θ.
   - Consider the convex combination of solutions:

$$\theta\Upsilon(\Psi) + (1-\theta)\Upsilon(\tilde{\Psi}).$$

   - Since $\Upsilon(\Psi) \leq \Psi$ and $\Upsilon(\tilde{\Psi}) \leq \tilde{\Psi}$, their convex combination satisfies:

$$\theta\Upsilon(\Psi) + (1-\theta)\Upsilon(\tilde{\Psi}) \leq \Psi_\theta.$$

- Therefore, this convex combination is a subsolution for the variational inequality with obstacle Ψ_θ.
- Again, by theorem 1.2.2, we conclude:

$$\Upsilon(\Psi_\theta) \geq \theta\Upsilon(\Psi) + (1-\theta)\Upsilon(\tilde{\Psi}),$$

which proves the concavity of Υ.

3. **Lipschitz continuity:**

- Let $\Psi, \tilde{\Psi} \in L^\infty(\Omega)$ be two obstacle functions, and denote by $\vartheta = \Upsilon(\Psi)$ and $\tilde{\vartheta} = \Upsilon(\tilde{\Psi})$ their corresponding solutions.
- Set $\Phi = \|\Psi - \tilde{\Psi}\|_\infty$. This quantity represents the maximum pointwise deviation between the two obstacles over the domain.
- Observe that, since $\vartheta \leq \Psi$, shifting the solution downward by Φ yields $\vartheta - \Phi \leq \Psi - \Phi$.
- Given that $\Psi - \Phi \leq \tilde{\Psi}$, it follows that $\vartheta - \Phi \leq \tilde{\Psi}$, meaning that the function $\vartheta - \Phi$ respects the obstacle constraint associated with $\tilde{\Psi}$.
- This shifted function thus qualifies as a subsolution to the variational inequality defined by the obstacle $\tilde{\Psi}$. By applying the comparison principle from theorem 1.2.2, we conclude that:

$$\vartheta - \Phi \leq \tilde{\vartheta}, \quad \text{which implies} \quad \vartheta \leq \tilde{\vartheta} + \Phi.$$

- Reversing the roles of Ψ and $\tilde{\Psi}$, the same argument gives:

$$\tilde{\vartheta} \leq \vartheta + \Phi.$$

- Combining both inequalities, we obtain:

$$\|\vartheta - \tilde{\vartheta}\|_\infty \leq \Phi = \|\Psi - \tilde{\Psi}\|_\infty,$$

which confirms that Υ is lipschitz continuous with lipschitz constant equal to 1.

Monotonicity of the continuous solution

Let us examine the solution operator $\partial(\mathbb{F}, \Psi)$ related to the variational inequality issue (1.10). Let us consider two source terms $\mathbb{F}, \tilde{\mathbb{F}} \in L^\infty(\Omega)$ and two obstacles $\Psi, \tilde{\Psi} \in L^\infty(\Omega)$. The objective is to determine a monotonicity characteristic of the solution for this facts.

Proposition 1.2.2: [22]

Under the assumptions that $\mathbb{F} \leq \tilde{\mathbb{F}}$ and $\Psi \leq \tilde{\Psi}$, the corresponding solutions satisfy the inequality

$$\partial(\mathbb{F}, \Psi) \leq \partial(\tilde{\mathbb{F}}, \tilde{\Psi}). \tag{1.15}$$

Proof

- We begin by introducing the two solutions: let $\vartheta = \partial(\mathbb{F}, \Psi)$ and $\tilde{\vartheta} = \partial(\tilde{\mathbb{F}}, \tilde{\Psi})$, which correspond respectively to the data sets $(\mathbb{F}, \Psi)$ and $(\tilde{\mathbb{F}}, \tilde{\Psi})$.
- Since $\mathbb{F} \leq \tilde{\mathbb{F}}$, we observe that for any nonnegative test function $v \geq 0$, the variational inequality satisfied by ϑ yields
$$a\langle \vartheta, v\rangle \leq \langle \mathbb{F}, v\rangle \leq \langle \tilde{\mathbb{F}}, v\rangle.$$
- In parallel, since $\Psi \leq \tilde{\Psi}$, it holds that the constraint set defined by the obstacle Ψ is more restrictive than that associated with $\tilde{\Psi}$, and in particular, any function lying below Ψ also lies below $\tilde{\Psi}$.
- These observations imply that ϑ satisfies the obstacle constraint corresponding to Ψ, and simultaneously satisfies the variational inequality (in the weak sense) associated with $\tilde{\mathbb{F}}$. Hence, ϑ acts as a subsolution to the variational inequality defined by the pair $(\tilde{\mathbb{F}}, \Psi)$.
- Let us denote by $u = \partial(\tilde{\mathbb{F}}, \Psi)$ the unique solution to this intermediate problem. Since the solution is maximal among all subsolutions, it follows that:
$$\vartheta \leq u.$$
- At this stage, we have related the solution of the first problem to the solution of an intermediate one with updated right-hand side but fixed obstacle. To proceed further, we invoke the known monotonicity of the solution with respect to the obstacle function, which ensures that:
$$\partial(\tilde{\mathbb{F}}, \Psi) \leq \partial(\tilde{\mathbb{F}}, \tilde{\Psi}).$$
- By transitivity, combining the two previous inequalities, we conclude that:
$$\partial(\mathbb{F}, \Psi) = \vartheta \leq u \leq \tilde{\vartheta} = \partial(\tilde{\mathbb{F}}, \tilde{\Psi}),$$
which confirms the desired monotonicity result.
- To express this property more generally, we may define the mapping:
$$\begin{aligned} \partial : L^\infty(\Omega) &\to L^\infty(\Omega), \\ (\mathbb{F}, \Psi) &\mapsto \partial(\mathbb{F}, \Psi) = \vartheta, \end{aligned}$$
where ϑ denotes the unique solution to the variational inequality problem (1.10), and which inherits the monotonicity in both arguments.

Proposition 1.2.3: [22]

Let $c > 0$ be a given constant. Then, the solution associated with the shifted data satisfies the translation invariance property:
$$\partial\left(\mathbb{F} + a_0 c, \Psi + c\right) = \partial(\mathbb{F}, \Psi) + c. \tag{1.16}$$

Proof

We proceed in two main steps to establish the identity.

- **Step 1:** let us define :

$$\tilde{\vartheta} = \partial\left(\mathbb{F} + \mathfrak{a}_0 \mathfrak{c}, \Psi + \mathfrak{c}\right) \quad \text{and} \quad \vartheta = \partial(\mathbb{F}, \Psi).$$

Given that any solution to the variational inequality (1.10) also qualifies as a lower solution, it follows that:

$$\begin{cases} a\langle \vartheta, u\rangle \leq \langle \mathbb{F}, u\rangle, & \forall u \in H_0^1(\Omega), \\ \vartheta \leq \Psi, \quad u \geq 0. \end{cases}$$

By adding the constant c to both sides of each inequality, we obtain:

$$\begin{cases} a\langle \vartheta + c, u\rangle \leq \langle \mathbb{F} + a_0 c, u\rangle, & \forall u \in H_0^1(\Omega), \\ \vartheta + c \leq \Psi + c, \quad u \geq 0. \end{cases}$$

This demonstrates that $\vartheta + c$ constitutes a lower solution for the problem with shifted data $(\mathbb{F} + a_0 c, \Psi + c)$. Since the solution is characterized as the greatest among all lower solutions, it necessarily holds that:

$$\vartheta + c \leq \tilde{\vartheta} \quad \Rightarrow \quad \partial(\mathbb{F}, \Psi) + c \leq \partial\left(\mathbb{F} + a_0 c, \Psi + c\right). \tag{1.17}$$

- **Step 2:**consider the properties of $\tilde{\vartheta}$. By definition of solution, we have:

$$\begin{cases} a\langle \tilde{\vartheta}, u\rangle \leq \langle \mathbb{F} + a_0 c, u\rangle, & \forall u \in H_0^1(\Omega), \\ \tilde{\vartheta} \leq \Psi + c, \quad u \geq 0. \end{cases}$$

Subtracting c from both sides in the inequalities above gives:

$$\begin{cases} a\langle \tilde{\vartheta} - c, u\rangle \leq \langle \mathbb{F}, u\rangle, & \forall u \in H_0^1(\Omega), \\ \tilde{\vartheta} - c \leq \Psi, \quad u \geq 0. \end{cases}$$

This confirms that $\tilde{\vartheta} - c$ is a valid lower solution for the original problem with data $(\mathbb{F}, \Psi)$. Invoking the maximality property of ϑ, we deduce:

$$\tilde{\vartheta} - c \leq \vartheta \quad \Rightarrow \quad \partial(\mathbb{F}, \Psi) + c \geq \partial\left(\mathbb{F} + a_0 c, \Psi + c\right). \tag{1.18}$$

By combining inequalities (1.17) and (1.18), we conclude that the two sides are equal:

$$\partial\left(\mathbb{F} + a_0 c, \Psi + c\right) = \partial(\mathbb{F}, \Psi) + c.$$

Lipschitz continuity property of the continuous solution

We next establish a lipschitz-type estimate, the stability of the continuous solution with respect to perturbations in both the source term and the obstacle. This property ensures that small variations in the data lead to proportionally bounded changes in the solution.

Proposition 1.2.4: [22]

Under the previous assumptions and notations, the following estimate is satisfied:

$$\|\vartheta - \tilde{\vartheta}\|_{L^\infty(\Omega)} \leq \|\Psi - \tilde{\Psi}\|_{L^\infty(\Omega)} + ca_0\|\mathbb{F} - \tilde{\mathbb{F}}\|_{L^\infty(\Omega)},$$

where c denotes a constant independent of the right-hand side and the obstacle, chosen so that:

$$ca_0(x) \geq 1.$$

Proof

We proceed in several steps:

- Define the auxiliary bound:

$$\Phi = \|\Psi - \tilde{\Psi}\|_{L^\infty(\Omega)} + ca_0\|\mathbb{F} - \tilde{\mathbb{F}}\|_{L^\infty(\Omega)}.$$

- By the triangle inequality, the following pointwise relations hold:

$$\tilde{\Psi} \leq \Psi + \Phi, \qquad \tilde{\mathbb{F}} \leq \mathbb{F} + \Phi.$$

- Using the monotonicity of the solution operator $\partial(\cdot, \cdot)$ together with the property (1.16), we deduce:

$$\partial(\tilde{\mathbb{F}}, \tilde{\Psi}) \leq \partial(\mathbb{F}, \Psi) \leq \partial(\mathbb{F} + \mathsf{a}_0\Phi, \Psi + \Phi).$$

- Applying again the translation identity (1.16), one has:

$$\partial(\mathbb{F} + a_0\Phi, \Psi + \Phi) = \partial(\mathbb{F}, \Psi) + \Phi.$$

- Combining the inequalities yields:

$$\partial(\tilde{\mathbb{F}}, \tilde{\Psi}) - \partial(\mathbb{F}, \Psi) \leq \Phi.$$

- Taking absolute values leads to:

$$|\partial(\tilde{\mathbb{F}}, \tilde{\Psi}) - \partial(\mathbb{F}, \Psi)| \leq \Phi.$$

- Reversing the roles of $(\mathbb{F}, \Psi)$ and $(\tilde{\mathbb{F}}, \tilde{\Psi})$ yields the symmetric inequality:

$$\partial(\mathbb{F}, \Psi) - \partial(\tilde{\mathbb{F}}, \tilde{\Psi}) \leq \Phi.$$

- Finally, passing to the supremum norm gives:

$$\|\vartheta - \tilde{\vartheta}\|_{L^\infty(\Omega)} \leq \Phi,$$

  which completes the proof.

1.2.2 Discrete variational inequality

Discrete formulation and finite element method principle

Let τ_h be a regular triangulation of the closure $\overline{\Omega}$ of the domain Ω, formed by a family of triangular elements

$$K_1, K_2, \ldots, K_N.$$

The mesh is assumed to satisfy the standard conformity and regularity assumptions of finite element theory. In particular,

$$\overline{\Omega} = \bigcup_{K \in \tau_h} \overline{K},$$

and for any two distinct elements K_z and K_s, their intersection is either empty, a common vertex, or a common edge.

Associated with this triangulation, we introduce the finite element space:

$$V_h = \left\{ u_h \in C(\Omega) \cap H_0^1(\Omega) \; ; \; u_h|_K \in P_1, \quad \forall K \in \tau_h \right\},$$

where P_1 denotes the space of polynomial functions of degree one. The parameter $h > 0$ represents the mesh size associated with the triangulation.

Let A_z, $z = 1, \ldots, N(h)$, be the interior nodes of the mesh. For each node A_z, we associate the usual nodal basis function $\varphi_z \in V_h$ satisfying:

$$\varphi_z(A_s) = \delta_{zs},$$

where δ_{zs} denotes the Kronecker symbol.

Any discrete function $u_h \in V_h$ can therefore be expressed in the form:

$$u_h(x) = \sum_{z=1}^{N(h)} u_h(A_z)\varphi_z(x).$$

We further define the Lagrange interpolation operator:

$$r_h : C(\Omega) \cap H_0^1(\Omega) \longrightarrow V_h,$$
$$u(x) \longmapsto r_h u(x) = \sum_{z=1}^{N(h)} u(A_z)\varphi_z(x),$$

The discrete counterpart of the bilinear form is represented through the stiffness matrix:

$$\mathscr{A} \in \mathbb{R}^{N(h)\times N(h)},$$

whose coefficients are defined by:

$$\mathscr{A}_{zs} = a\langle \varphi_z, \varphi_s \rangle.$$

Definition 1.2.2: [29, 31]

An invertible matrix: $\mathscr{A} \in M_N(\mathbb{R})$ is called an M-matrix if its off-diagonal entries satisfy:

$$a_{zs} \le 0, \quad z \ne s,$$

and if its inverse exists and has nonnegative entries.

This property leads to the discrete maximum principle stated below.

Definition 1.2.3: [29,31]

Let $\mathscr{A}$ be an M-matrix and let $u, v \in V_h$ satisfy:

$$\mathscr{A}u \geq \mathscr{A}v \quad \text{in } \Omega.$$

Then:

$$u \geq v \quad \text{in } \overline{\Omega}.$$

Existence and uniqueness of the discrete solution

Using these constructions, the discrete variational inequality associated with the continuous problem (1.10) is formulated as follows:

$$\begin{cases} \text{Find } \vartheta_h \in \mathbb{K}_h \text{ such that:} \\ a\langle \vartheta_h, u_h - \vartheta_h \rangle \geq \langle \mathscr{F}, u_h - \vartheta_h \rangle, & \forall u_h \in \mathbb{K}_h, \end{cases} \tag{1.19}$$

where the discrete admissible set is defined by:

$$\mathbb{K}_h = \{u_h \in V_h \; ; \; u_h \leq r_h \Psi\}.$$

Theorem 1.2.3: [31,37]

Under the previous assumptions, the discrete variational inequality (1.19) admits a unique solution.

Characterization via Subsolutions

To provide a constructive view of the discrete solution, we introduce the set of discrete subsolutions X_h, defined by:

$$\begin{cases} a\langle \mathfrak{z}_h, \varphi_t \rangle \leq \langle \mathscr{F}, \varphi_z \rangle, & \forall z = 1, \dots, N(h), \\ \mathfrak{z}_h \leq r_h \Psi. \end{cases}$$

Theorem 1.2.4: [31]

The discrete solution ϑ_h of (1.19) is uniquely characterized as the supremum of all functions belonging to X_h.

Discrete solution mapping and its main properties

In analogy with the continuous framework, we introduce the operator:

$$\begin{aligned} \Upsilon_h : L^\infty(\Omega) &\longrightarrow V_h, \\ \Psi &\longmapsto \Upsilon_h(\Psi) = \vartheta_h, \end{aligned} \tag{1.20}$$

Assuming that the discrete maximum principle is satisfied, the operator Υ_h inherits the main properties of its continuous counterpart Υ defined in (1.14).

Proposition 1.2.5: [31]

The operator Υ_h is increasing, concave, and lipschitz continuous with respect to Ψ.

We examine here the monotonicity of the operator $\partial_h(\mathscr{F}, r_h\Psi)$, which maps the data $(\mathscr{F}, \Psi)$ to the corresponding discrete solution.

Proposition 1.2.6: [31]

If $\mathscr{F} \leq \widetilde{\mathscr{F}}$ and $\Psi \leq \widetilde{\Psi}$, then:

$$\partial_h(\mathscr{F}, r_h\Psi) \leq \partial_h(\widetilde{\mathscr{F}}, r_h\widetilde{\Psi}).$$

The operator also enjoys a stability property under constant shifts in the data.

Proposition 1.2.7: [31]

For any positive constant c, one has:

$$\partial_h(\mathscr{F} + a_0 c, r_h(\Psi + c)) = \partial_h(\mathscr{F}, r_h\Psi) + c.$$

Having established monotonicity, we now turn to the lipschitz continuity of the discrete solution map, which ensures the stability of the solution under small perturbations in the data.

Proposition 1.2.8

The solution map ∂_h is lipschitz continuous in the L^∞-norm:

$$\|\vartheta_h - \widetilde{\vartheta}_h\|_{L^\infty(\Omega)} \leq \|r_h\Psi - r_h\widetilde{\Psi}\|_{L^\infty(\Omega)} + ca_0\|\mathscr{F} - \widetilde{\mathscr{F}}\|_{L^\infty(\Omega)}.$$

To conclude this subsection, we present a regularity result for the discrete solution that quantifies the boundedness of the bilinear form when applied to the solution and the nodal basis functions. This result plays a significant role in further numerical analysis [30].

Theorem 1.2.5: [30]

There exists a constant C, independent of the mesh size h, such that

$$|a\langle\vartheta_h, \varphi_z\rangle| \leq C\|\varphi_z\|_{L^1(\Omega)}, \qquad \forall z = 1, \ldots, N(h).$$

Error estimate in the L^∞ norm

To assess the accuracy of the proposed numerical scheme, we now establish an a priori error estimate in the uniform norm. Specifically, we compare the exact continuous solution ϑ of problem (1.10) with its discrete counterpart ϑ_h, defined by (1.19). The following result quantifies the convergence rate of the discrete approximation with respect to the mesh size.

Theorem 1.2.6: [31]

Assuming that conditions (1.1)–(1.9) are satisfied and that the discrete maximum principle and the regularity condition (1.13) holds, the approximation error in the L^∞-norm is bounded by:

$$\|\vartheta - \vartheta_h\|_{L^\infty(\Omega)} \leq Ch^2|\log h|^2.$$

1.3 The quasi-variational inequalities

In this section, we address the quasi-variational inequalities (QVI) problem in both continuous and discrete frameworks.

1.3.1 Continuous quasi-variational inequality

We consider a class of elliptic quasi-variational inequalities characterized by the fact that the admissible set depends on the unknown solution itself. In this framework, we seek a function ϑ defined on a bounded smooth domain $\Omega \subset \mathbb{R}^N$, governed by the coupled system:

$$\begin{cases} \mathbb{A}\vartheta - \mathbb{F} \leq 0, \quad \vartheta - M\vartheta \leq 0, \quad \text{in } \Omega, \\ \langle \mathbb{A}\vartheta - \mathbb{F}\rangle\langle \vartheta - M\vartheta\rangle = 0 \quad \text{in } \Omega, \end{cases} \tag{1.21}$$

The formulation (1.21) has a structure analogous to that of the classical obstacle problem (1.10). The main difference lies in the fact that the obstacle is defined implicitly through the solution of the problem itself. Where $\mathbb{A}$ is a uniformly elliptic second-order differential operator acting on Ω,and M is an operator defined by:

$$\begin{aligned} M : L^\infty(\Omega) &\longrightarrow L^\infty(\Omega), \\ \vartheta &\longmapsto M\vartheta. \end{aligned}$$

The operator $M\vartheta$ represents the obstacle associated with impulse control and corresponds to the cost incurred by an intervention. As a key component of quasi-variational inequalities, it satisfies several important analytical properties, such as monotonicity and concavity, which are crucial in the theoretical analysis of the problem [23, 32]:

- Lipschitz continuity in the sense that:

$$\|Mu - Mv\| \leq \|u - v\|, \quad \forall u, v.$$

- Monotonicity, meaning that:

$$u \leq v \quad \text{implies} \quad Mu \leq Mv.$$

- Concavity and the following property:

$$M(u + c) = Mu + c, \quad \forall c > 0.$$

Since the constraint depends on the unknown solution, the problem can be rewritten as a fixed point variational inequality. We thus look for $\vartheta \in \mathbb{K}(\vartheta)$ such that:

$$\mathbb{K}(\vartheta) = \Big\{ u \in H_0^1(\Omega) \;\Big|\; 0 \leq u \leq M\vartheta \text{ in } \Omega \Big\}.$$

$$\begin{cases} \text{Find } \vartheta \in \mathbb{K}(\vartheta) \text{ such that:} \\ a\langle \vartheta, u - \vartheta\rangle \geq \langle \mathbb{F}, u - \vartheta\rangle, \quad \forall u \in \mathbb{K}(\vartheta), \end{cases} \tag{1.22}$$

Theorem 1.3.1: [8]

Under the stated assumptions, problem (1.22) admits a unique solution. Moreover, the solution satisfies the regularity property:

$$\vartheta \in W^{2,p}(\Omega), \quad 2 \leq p < \infty.$$

1.3.2 Discrete quasi-variational inequality

We extend the framework of quasi-variational inequalities to the discrete setting using the same triangulation introduced for the variational inequality.

Let us define the discrete admissible set:

$$\mathbb{K}(\vartheta_h) = \{u_h \in V_h \ : \ u_h \leq r_h M_h u_h \quad \text{in } \tau_h\},$$

where r_h is the lagrange interpolation operator. The associated discrete quasi-variational inequality is then formulated as:

$$\begin{cases} \text{Find } \vartheta_h \in \mathbb{K}(\vartheta_h) \text{ such that:} \\ a\langle \vartheta_h, u_h - \vartheta_h \rangle \geq \langle \mathscr{F}, u_h - \vartheta_h \rangle, \quad \forall u_h \in \mathbb{K}(\vartheta_h). \end{cases} \tag{1.23}$$

This formulation reveals the fixed point nature of the problem, since the admissible set depends on the unknown solution through the operator M_h.

Theorem 1.3.2: [8]

Under the discrete maximum principle, problem (1.23) admits a unique solution in V_h.

1.4 Quasi-variational inequality systems related to HJB

In this section, we provide both the continuous and discrete formulations of quasi-variational inequality (QVI) systems. The focus is placed on the mathematical structure of the coupled problem, the role of bilinear forms, and the analysis of existence and uniqueness of solutions via fixed-point methods. We also discuss the essential properties of the solutions in both settings.

1.4.1 Continuous quasi-variational inequality systems

We study a system of $n \in \mathbb{N}$ coupled quasi-variational inequalities, where each component involves an elliptic operator and is linked to the others through inequality constraints.

The objective is to determine a vector-valued function:

$$\vartheta = (\vartheta^1, \ldots, \vartheta^n) \in \left(H_0^1(\Omega)\right)^n,$$

that satisfies the system of inequalities stated below. For each index $i \in \{1, \ldots, n\}$:

- **Elliptic operator:** $\mathbb{A}^i$ is given in (1.2).
- **Bilinear form:** $a^i\langle \cdot, \cdot \rangle$, associated with $\mathbb{A}^i$ (see (1.1)).

- **Coefficients:** $a^i_{zs}, a^i_s, a^i_0 \in C^2(\bar{\Omega})$, satisfying (1.3), (1.4), and (1.5).
- **Source term:** $\mathbb{F}^i \in C^2(\bar{\Omega})$, with $\mathbb{F}^i \geq 0$ in Ω (see (1.7)).
- If $M\vartheta = \kappa + \vartheta$ with $\kappa > 0$, in (1.21), then the system is given by the following weak formulation:

$$\begin{cases} \text{Find } \vartheta = (\vartheta^1, \dots, \vartheta^n) \in \left(H^1_0(\Omega)\right)^n \text{ such that for each } i = 1, \dots, n: \\ a^i\langle \vartheta^i, u - \vartheta^i \rangle \geq \langle \mathbb{F}^i, u - \vartheta^i \rangle, \quad \forall u \in H^1_0(\Omega), \\ \vartheta^i \leq \kappa + \vartheta^{i+1}, \quad \text{with } u \leq \kappa + \vartheta^{i+1}, \\ \vartheta^{n+1} = \vartheta^1, \quad \kappa > 0. \end{cases} \tag{1.24}$$

Theorem 1.4.1: [22]

Let the assumptions and notations introduced in (1.1) and (1.7) be satisfied. Then, the system described in (1.24) admits a unique solution in the product Sobolev space:

$$\vartheta = (\vartheta^1, \dots, \vartheta^n), \quad \text{with } \vartheta^i \in W^{2,p}(\Omega), \quad 1 < p < \infty, \quad i = 1, \dots, n.$$

A fixed point mapping associated with the system of QVIs

In order to analyze and approximate the system (1.24), it is convenient to recast it as a fixed-point problem. The reformulation is organized as follows:

$$H^+ = \prod_{i=1}^{n} L^\infty_+(\Omega),$$

where each component belongs to the cone of nonnegative essentially bounded functions on Ω. For any vector:

$$V = (v^1, \dots, v^n) \in H^+,$$

define:

$$\begin{aligned} T : H^+ &\longrightarrow H^+, \\ V &\longmapsto TV = (\vartheta^1, \dots, \vartheta^n). \end{aligned} \tag{1.25}$$

Each component ϑ^i is obtained as the unique solution of:

$$\begin{cases} a^i\langle \vartheta^i, u - \vartheta^i \rangle \geq \langle \mathbb{F}^i, u - \vartheta^i \rangle, \quad \forall u \in H^1_0(\Omega), \\ \vartheta^i \leq \kappa + v^{i+1}, \quad u \leq \kappa + v^{i+1}, \\ \text{with } \vartheta^{n+1} = \vartheta^1. \end{cases} \tag{1.26}$$

The solution of problem (1.26) satisfies:

$$\vartheta^i = \Upsilon(\kappa + v^{i+1}). \tag{1.27}$$

The formula (1.27) can be verified as follows:

$$TV = \left[\Upsilon(\kappa + v^2), \Upsilon(\kappa + v^3), \dots, \Upsilon(\kappa + v^n), \Upsilon(\kappa + v^1)\right]. \tag{1.28}$$

This fixed point setting makes it possible to construct iterative procedures based on repeated applications of T. Under suitable assumptions, such as monotonicity or contraction properties, these iterations converge reliably to the unique solution of the quasi-variational system.

Some properties of the mapping T

In order to analyze the iterative behavior of the operator T, it is useful to introduce an auxiliary function. Define

$$\hat{\vartheta}^0 = (\hat{\vartheta}^{1,0}, \dots, \hat{\vartheta}^{n,0}),$$

where each component is obtained as the unique solution of the following independent variational problem:

$$a^i\langle \hat{\vartheta}^{i,0}, u\rangle = \langle \mathbb{F}^i, u\rangle, \quad \forall u \in H_0^1(\Omega), \quad 1 \le i \le n. \tag{1.29}$$

The assumptions stated in (1.1)–(1.9) guarantee the existence of a unique positive solution, with the additional regularity

$$\hat{\vartheta}^{i,0} \in W^{2,\infty}(\Omega),$$

for all indices i.

Proposition 1.4.1: [22]

For any $V, U \in H^+$, the following properties hold:

$$TV \le TU \quad \text{whenever } V \le U, \tag{1.30}$$

$$TV \ge 0, \quad \forall V \in H^+, \tag{1.31}$$

$$TV \le \hat{\vartheta}^0, \quad \forall V \in H^+. \tag{1.32}$$

Proposition 1.4.2: [22]

The operator T is concave and Lipschitz continuous on the space H^+, that is,

$$\|TU - TV\|_\infty \le \|U - V\|_\infty, \quad U, V \in H^+.$$

Continuous iterative scheme

To approximate the solution of the quasi-variational inequality system introduced in (1.24), we consider a continuous iterative procedure that exploits the monotonicity of the operator T. The idea is to generate two sequences, starting from an upper and a lower solution of the system, and to update them recursively through successive applications of T.

We begin with the initial upper solution $\hat{\vartheta}^0$, which is known to solve the auxiliary problem (1.29), and with the trivial lower solution given by the zero function $\check{\vartheta}^0 = 0$. The sequences are then constructed as:

$$\hat{\vartheta}^{k+1} = T\hat{\vartheta}^k, \quad k = 0, 1, \dots, \tag{1.33}$$

and

$$\check{\vartheta}^{k+1} = T\check{\vartheta}^k, \quad k = 0, 1, \dots. \tag{1.34}$$

In order to analyze the convergence of this scheme, we introduce the positive cone in H^+,

$$\mathbb{K} = \left\{ U \in H^+ \text{ such that } 0 \le U \le \hat{\vartheta}^0 \right\}.$$

The next lemma provides a key lower bound that compares the action of T at the zero function with the initial upper solution. This estimate plays a central role in ensuring that the iterative sequences remain well controlled.

Lemma 1.4.1: [22]

Assume that: $0 < \nu < \inf\left(\frac{\kappa}{\|\hat{\vartheta}^0\|_\infty}, 1\right)$. Then the following inequality holds: $T(0) \geq \nu\hat{\vartheta}^0$.

Building on this estimate, the following proposition combines the concavity and monotonicity of T (see proposition 1.4.2) with the lower bound estimate in lemma 1.4.1 to derive a sharper comparison inequality between two elements of the cone $\mathbb{K}$.

Proposition 1.4.3: [22]

Let $\varrho \in [0,1]$ be such that, for any $U, \tilde{U} \in \mathbb{K}$, the relation (1.35) holds:

$$U - \tilde{U} \leq \varrho U \tag{1.35}$$

Then, combining the monotonicity of T with the lower bound estimate in lemma 1.4.1, one obtains:

$$TU - T\tilde{U} \leq \varrho(1-\nu)TU. \tag{1.36}$$

Convergence of the continuous iterative scheme

The next result shows that the iterative sequences constructed in (1.33)–(1.34) are stable, remain bounded within the cone $\mathbb{K}$, and converge monotonically toward the unique solution of the quasi-variational inequality system. The proof relies on the monotonicity property (1.30), the upper bound property (1.32), and the refined comparison inequality of proposition 1.4.3.

Proposition 1.4.4

Let $(\hat{\vartheta}^k)$ and $(\check{\vartheta}^k)$ be the sequences generated by the iterative scheme (1.33)–(1.34). Then, both sequences remain in the set K and converge monotonically from above and below, respectively, toward the unique solution of the quasi-variational inequality system (1.24).

Proof

The proof is structured in four steps.

- **Step 1. Monotonicity and boundedness of** $(\hat{\vartheta}^k)$
  From the definition of the iterative process (1.33) and the variational inequality formulation (1.26), for each $k \geq 1$ the vector :
  $$\hat{\vartheta}^k = \left(\hat{\vartheta}^{1,k}, \dots, \hat{\vartheta}^{n,k}\right),$$
  satisfies the system:
  $$\begin{cases} a^i\langle\hat{\vartheta}^{i,k}, u - \hat{\vartheta}^{i,k}\rangle \geq \langle\mathbb{F}^i, u - \hat{\vartheta}^{i,k}\rangle, & \forall u \in H_0^1(\Omega), \\ \hat{\vartheta}^{i,k} \leq \kappa + \hat{\vartheta}^{i+1,k-1}, \quad u \leq \kappa + \hat{\vartheta}^{i+1,k-1}, & i = 1, 2, \dots, n, \\ \hat{\vartheta}^{n+1,k} = \hat{\vartheta}^{1,k}. \end{cases} \tag{1.37}$$
  Since $\mathbb{F}^i \geq 0$ and the initial guess satisfies $\hat{\vartheta}^{i,0} \geq 0$, the comparison principle for variational inequalities implies that:
  $$\hat{\vartheta}^k \geq 0, \quad \forall k \geq 0. \tag{1.38}$$

Moreover, proposition 1.4.2 ensures the monotonicity of the operator T. Hence, by the recursive definition (1.33), one obtains:

$$\hat{\vartheta}^1 = T\hat{\vartheta}^0 \le \hat{\vartheta}^0.$$

Iterating this inequality yields the nested sequence:

$$0 \le \hat{\vartheta}^{k+1} = T\hat{\vartheta}^k \le \hat{\vartheta}^k \le \cdots \le \hat{\vartheta}^0, \quad \forall k \ge 0, \tag{1.39}$$

which establishes both the non-negativity and the monotone decay of the iterates. Consequently, the sequence $(\hat{\vartheta}^k)$ remains bounded inside the cone $\mathbb{K}$, thus setting the basis for convergence analysis in the next steps.

- **Step 2. Convergence of $(\hat{\vartheta}^k)$ to a limit function**
From the monotonicity and boundedness properties established in (1.38)–(1.39), the sequence $(\hat{\vartheta}^k)$ converges pointwise almost everywhere in Ω. Hence, for each component $i = 1, \ldots, n$, there exists a function $\bar{\vartheta}^i \in \mathbb{K}$ such that:

$$\lim_{k\to\infty} \hat{\vartheta}^{i,k}(x) = \bar{\vartheta}^i(x), \quad x \in \Omega, \quad \text{with } \bar{\vartheta}^i \in \mathbb{K}. \tag{1.40}$$

To reinforce this convergence, we derive energy estimates from the variational inequality (1.37). Choosing the admissible test function $u = 0$, we obtain:

$$a^i\langle\hat{\vartheta}^{i,k}, -\hat{\vartheta}^{i,k}\rangle \ge \langle\mathbb{F}^i, -\hat{\vartheta}^{i,k}\rangle,$$

which after rearrangement gives:

$$a^i\langle\hat{\vartheta}^{i,k}, \hat{\vartheta}^{i,k}\rangle \le \left\|\mathbb{F}^i\right\|_{L^2(\Omega)} \left\|\hat{\vartheta}^{i,k}\right\|_{H^1(\Omega)}.$$

By the coercivity of the bilinear form a^i, there exists $\lambda > 0$ such that:

$$\lambda \left\|\hat{\vartheta}^{i,k}\right\|^2_{H^1(\Omega)} \le a^i\langle\hat{\vartheta}^{i,k}, \hat{\vartheta}^{i,k}\rangle.$$

Thus,

$$\lambda \left\|\hat{\vartheta}^{i,k}\right\|^2_{H^1(\Omega)} \le \left\|\mathbb{F}^i\right\|_{L^2(\Omega)} \left\|\hat{\vartheta}^{i,k}\right\|_{H^1(\Omega)},$$

which implies the uniform estimate:

$$\left\|\hat{\vartheta}^{i,k}\right\|_{H^1(\Omega)} \le \frac{1}{\lambda}\left\|\mathbb{F}^i\right\|_{L^2(\Omega)} = C,$$

for some constant C independent of k. Consequently, the sequence $(\hat{\vartheta}^{i,k})$ is uniformly bounded in $H^1(\Omega)$, and we obtain the weak convergence

$$\lim_{k\to\infty} \hat{\vartheta}^{i,k} = \bar{\vartheta}^i \quad \text{weakly in } H^1(\Omega). \tag{1.41}$$

This weak convergence, combined with the pointwise convergence in (1.40), ensures that : $\bar{\vartheta} = (\bar{\vartheta}^1, \ldots, \bar{\vartheta}^n)$ is a candidate solution of the quasi-variational inequality system (1.24).

- **Step 3. Verification that the limit satisfies the QVI system**
  We now show that the limit function $\bar{\vartheta} = (\bar{\vartheta}^1, \ldots, \bar{\vartheta}^n)$ satisfies the quasi-variational inequality system (1.24).

  From the iterative scheme we have, for each component:

  $$\hat{\vartheta}^{i,k}(x) \leq \kappa + \hat{\vartheta}^{i+1,k-1}(x).$$

  Passing to the limit as $k \to \infty$ and using the pointwise convergence in (1.40), we deduce:

  $$\bar{\vartheta}^i(x) \leq \kappa + \bar{\vartheta}^{i+1}(x), \quad \text{for a.e. } x \in \Omega, \quad i = 1, \ldots, n.$$

  This confirms that the obstacle constraints of the system are satisfied.

  Let $u \in H_0^1(\Omega)$ with $u \leq \kappa + \bar{\vartheta}^{i+1}$. Since $\hat{\vartheta}^{i+1,k-1} \to \bar{\vartheta}^{i+1}$ monotonically from above, we have : $u \leq \kappa + \hat{\vartheta}^{i+1,k-1}$ for all sufficiently large k. Hence, u is admissible as a test function in the discrete variational inequality (1.37).

  Using the weak convergence in (1.41), the pointwise convergence in (1.40), and the weak lower semicontinuity of the bilinear form a^i, we can pass to the limit in (1.37) to obtain:

  $$a^i\langle\bar{\vartheta}^i, u - \bar{\vartheta}^i\rangle \geq \langle\mathbb{F}^i, u - \bar{\vartheta}^i\rangle, \quad \forall u \in H_0^1(\Omega),\ u \leq \kappa + \bar{\vartheta}^{i+1}.$$

  This is exactly the variational inequality defining the solution of the system.

  Therefore, the limit function satisfies the quasi-variational inequality system, and by uniqueness of the solution we conclude:

  $$\vartheta = \bar{\vartheta} = (\bar{\vartheta}^1, \ldots, \bar{\vartheta}^n).$$

- **Step 4. Convergence of the lower sequence**
  The monotonicity of the sequence $\left(\check{\vartheta}^k\right)$ can be established by an argument analogous to that used in Step 1 for the sequence $\left(\hat{\vartheta}^k\right)$.

  To prove convergence toward the unique solution of the system (1.24), we exploit inequalities (1.35) and (1.36) with the specific choice:

  $$U = \hat{\vartheta}^0, \quad \tilde{U} = \check{\vartheta}^0, \quad \varrho = 1.$$

  Applying inequality (1.35) gives:

  $$T\hat{\vartheta}^0 - T\check{\vartheta}^0 \leq (1 - \nu)T\hat{\vartheta}^0,$$

  which leads to the bound:

  $$0 \leq \hat{\vartheta}^1 - \check{\vartheta}^1 \leq (1 - \nu)\hat{\vartheta}^1.$$

Using inequality (1.36), this estimate propagates recursively:

$$0 \leq \hat{\vartheta}^2 - \check{\vartheta}^2 \leq (1-\nu)^2 \hat{\vartheta}^2,$$

and by induction:

$$0 \leq \hat{\vartheta}^k - \check{\vartheta}^k \leq (1-\nu)^k \hat{\vartheta}^k \leq (1-\nu)^k \hat{\vartheta}^0 \leq (1-\nu)^k \left\| \hat{\vartheta}^0 \right\|_\infty, \quad \forall k \geq 0.$$

The difference between the two sequences thus decays exponentially:

$$\hat{\vartheta}^k - \check{\vartheta}^k \longrightarrow 0 \quad \text{a.e. in } \Omega, \quad \text{as } k \to \infty.$$

Since $\hat{\vartheta}^k \to \vartheta$, we deduce:

$$\check{\vartheta}^k \longrightarrow \underline{\vartheta} = \vartheta,$$

where ϑ is the unique solution to the quasi-variational inequality system (1.24).

Remark 1.4.1

From the result established above, it is evident that the solution ϑ of the system (1.24) is a fixed point of the operator T, that is:

$$\vartheta = T\vartheta. \tag{1.42}$$

The following estimates provide a quantitative description of the convergence behavior of the iterative schemes defined by (1.33) and (1.34). These results will play a crucial role in the forthcoming analysis of error estimates in the context of finite element discretization.

Geometric convergence of the iterative scheme

Proposition 1.4.5: [22]

There exists a constant $(0 < \rho < 1)$ such that the iterates $\hat{\vartheta}^k$ and $\check{\vartheta}^k$ satisfy the following geometric convergence estimates:

$$\left\| \hat{\vartheta}^k - \vartheta \right\|_\infty \leq \rho^k \left\| \hat{\vartheta}^0 \right\|_\infty, \tag{1.43}$$

$$\left\| \check{\vartheta}^k - \vartheta \right\|_\infty \leq \rho^k \left\| \hat{\vartheta}^0 \right\|_\infty. \tag{1.44}$$

Proof

To establish the geometric convergence, we divide the argument into successive steps. From (1.39)–(1.40), we have:

$$0 \leq \vartheta \leq \hat{\vartheta}^0,$$

which implies:

$$0 \leq \hat{\vartheta}^0 - \vartheta \leq \hat{\vartheta}^0.$$

Applying inequality (1.36) with $\varrho = 1$, we obtain:

$$0 \leq T\hat{\vartheta}^0 - T\vartheta \leq (1-\nu)\,T\hat{\vartheta}^0.$$

Using identity (1.42) and the definition (1.33), this leads to:

$$0 \leq \hat{\vartheta}^1 - \vartheta \leq (1-\nu)\,\hat{\vartheta}^1.$$

Repeating the argument with (1.36) and $\varrho = 1-\nu$, we get:

$$0 \leq \hat{\vartheta}^2 - \vartheta \leq (1-\nu)^2\hat{\vartheta}^2.$$

By induction, one deduces:

$$0 \leq \hat{\vartheta}^k - \vartheta \leq (1-\nu)^k\hat{\vartheta}^k \leq (1-\nu)^k\hat{\vartheta}^0.$$

Taking the supremum norm yields (1.43). The proof of (1.44) follows analogously for the sequence $(\check{\vartheta}^k)$ and is therefore omitted.

1.4.2 Discrete quasi-variational inequality systems

We now turn to the discrete counterpart of the quasi-variational inequality (QVI) system, obtained through finite element approximation of the continuous problem. The aim is to establish a rigorous discrete formulation and confirm that essential properties such as stability, monotonicity, and uniqueness are preserved after discretization.

Let $V_h \subset H_0^1(\Omega)$ be a conforming finite element subspace, constructed on a mesh of size h. For each index $i = 1, \ldots, n$, the discrete analogue of the continuous QVI system (1.24) reads as follows: find $\vartheta_h^i \in V_h$ such that:

$$\begin{cases} a^i\langle \vartheta_h^i, u_h - \vartheta_h^i\rangle \geq \langle \mathscr{F}^i, u_h - \vartheta_h^i\rangle, \quad \forall u_h \in V_h, \\ \vartheta_h^i \leq r_h(\kappa + \vartheta_h^{i+1}), \quad u_h \leq r_h(\kappa + \vartheta_h^{i+1}), \quad \text{for } i = 1, \ldots, n, \\ \vartheta_h^{n+1} = \vartheta_h^1. \end{cases} \tag{1.45}$$

Here, the discrete bilinear forms $a^i\langle\cdot,\cdot\rangle$ are represented by the stiffness matrices $\mathscr{A}^i$. We assume that each $\mathscr{A}^i$ satisfies the discrete maximum principle, i.e., it is an M-matrix in the sense of [29]. This structural property guarantees that the discrete formulation inherits fundamental qualitative features of the continuous problem, such as stability, positivity, and monotonicity. Since the proofs of these properties follow closely the continuous arguments, they are omitted here for brevity.

Theorem 1.4.2: [22]

If each stiffness matrix $\mathscr{A}^i$ satisfies the discrete maximum principle, then the quasi-variational inequality system defined by (1.45) admits a unique solution.

Discrete fixed point operator for the QVI system

To construct an iterative resolution method for the discrete quasi-variational inequality system, we associate it with a nonlinear operator defined through auxiliary discrete variational inequalities. This operator plays the role of a fixed-point mapping.

We introduce:

$$\begin{aligned} T_h : H^+ &\longrightarrow (V_h)^n, \\ V &\longmapsto T_h V = (\vartheta_h^1, \ldots, \vartheta_h^n), \end{aligned} \tag{1.46}$$

where each component ϑ_h^i is uniquely determined as the solution of the constrained discrete variational inequality:

$$\begin{cases} a^i\langle \vartheta_h^i, u_h - \vartheta_h^i\rangle \geq \langle \mathscr{F}^i, u_h - \vartheta_h^i\rangle, \quad \forall u_h \in V_h, \\ \vartheta_h^i \leq r_h(\kappa + v^{i+1}), \quad u_h \leq r_h(\kappa + v^{i+1}), \\ \text{with } \vartheta_h^{n+1} = \vartheta_h^1. \end{cases}$$

The solution of problem (1.4.2) satisfies:

$$\vartheta_h^i = \Upsilon_h(\kappa + v^{i+1}), \tag{1.47}$$

The formula (1.47) can be verified as follows:

$$T_h V = \left[\Upsilon_h(\kappa + v^2),\, \Upsilon_h(\kappa + v^3),\, \ldots,\, \Upsilon_h(\kappa + v^n),\, \Upsilon_h(\kappa + v^1)\right].$$

We choose as initial guess the discrete vector:

$$\hat{\vartheta}_h^0 = \left(\hat{\vartheta}_h^{1,0}, \ldots, \hat{\vartheta}_h^{n,0}\right),$$

which is obtained as the finite element approximation of the continuous supersolution introduced earlier. It is defined through:

$$a^i\langle \hat{\vartheta}_h^{i,0}, u_h\rangle = \langle \mathscr{F}^i, u_h\rangle, \quad \forall u_h \in V_h, \quad 1 \leq i \leq n. \tag{1.48}$$

From the correspondence between the continuous and discrete problems, it follows that T_h admits a unique fixed point. Moreover, the discrete maximum principle together with the positivity of the data $\mathscr{F}^i$ guarantees that the starting iterate satisfies:

$$\hat{\vartheta}_h^0 \geq 0.$$

Fundamental properties of the discrete mapping T_h

We next analyze the main features of the discrete operator T_h introduced in (1.46). Its behavior closely parallels that of the continuous counterpart T defined in (1.25)–(1.28). In particular, the discrete mapping preserves three essential qualitative properties: monotonicity, non-negativity, and boundedness. These are gathered in the following statement.

Proposition 1.4.6: [22]

For any $U, V \in H^+$, the operator T_h satisfies:

$$\begin{aligned} &U \leq V \implies T_h U \leq T_h V, \\ &T_h V \geq 0, \\ &T_h V \leq \hat{\vartheta}_h^0. \end{aligned}$$

Beyond the above features, the operator T_h retains further regularity properties analogous to those established in the continuous case (cf. proposition 1.4.2). These can be summarized as follows.

Proposition 1.4.7: [22]

The mapping T_h is concave on H^+. In addition, it is Lipschitz continuous with constant one, namely:

$$\|T_h U - T_h V\|_\infty \leq \|U - V\|_\infty\,, \quad U, V \in H^+. \tag{1.49}$$

Iterative procedure for the discrete QVI system

To approximate the solution of the discrete quasi-variational inequality system given in (1.45), we introduce an iterative method that repeatedly applies the discrete operator T_h. Beginning with an initial estimate, this approach generates a sequence of approximations converging to the unique fixed point of the operator.

Let the starting point $\hat{\vartheta}_h^0$ be determined from the solution of the variational problem (1.48), or alternatively, consider the zero initialization:

$$\check{\vartheta}_h^0 = (0, 0, \ldots, 0).$$

We then define the iterative sequences as follows:

$$\hat{\vartheta}_h^{k+1} = T_h \hat{\vartheta}_h^k, \quad k = 0, 1, 2, \ldots \tag{1.50}$$

and similarly,

$$\check{\vartheta}_h^{k+1} = T_h \check{\vartheta}_h^k, \quad k = 0, 1, 2, \ldots$$

In order to maintain the iterations within a well-defined functional framework, we restrict the sequence to a convex and bounded set:

$$\mathbb{K}_h = \left\{ U \in H^+ \;\middle|\; 0 \leq U \leq \hat{\vartheta}_h^0 \right\}.$$

A key element for understanding the behavior of these iterates is a lower bound on the image of the zero element under T_h.

Lemma 1.4.2: [22]

Let ν be a positive constant such that: $0 < \nu < \min\left(\frac{\kappa}{\|\hat{\vartheta}_h^0\|_\infty}, 1 \right)$. Then the operator satisfies: $T_h(0) \geq \nu \hat{\vartheta}_h^0$.

Finally, we state a contraction-type property that is fundamental in estimating the convergence speed of the iterative scheme. This result shows that, under a suitable smallness condition, T_h behaves as a contraction on $\mathbb{K}_h$.

Proposition 1.4.8: [22]

Assume there exists a constant $\varrho \in [0, 1]$ such that:

$$U - \tilde{U} \leq \varrho U, \quad \forall\, U, \tilde{U} \in \mathbb{K}_h.$$

Then, the following inequality holds:

$$T_h U - T_h \tilde{U} \leq \varrho(1 - \nu)\, T_h U.$$

Convergence analysis of the discrete iterative procedure

With the discrete iterative framework in place, we now turn to the study of the convergence behavior of the sequences it generates. The following result ensures that these sequences converge monotonically towards the unique solution of the discrete quasi-variational inequality system.

Proposition 1.4.9: [22]

The iterative sequences $\left(\hat{\vartheta}_h^k\right)$ and $(\check{\vartheta}_h^k)$ remain well-defined within the set $\mathbb{K}_h$ and converge monotonically to the unique discrete solution of system (1.45). More specifically, the sequence $\left(\hat{\vartheta}_h^k\right)$ approaches the solution from above, whereas $(\check{\vartheta}_h^k)$ approaches it from below.

Remark 1.4.2

As a direct implication of Proposition 1.4.9 , the discrete solution of (1.45) can be equivalently characterized as a fixed point of the operator T_h, i.e.,

$$\vartheta_h = T_h \vartheta_h.$$

Quantitative geometric convergence

Beyond mere convergence, it is important to quantify the speed at which the iterative sequences approach the fixed point. The next proposition establishes that this convergence occurs at a geometric rate, guaranteeing a rapid reduction of the approximation error measured in the supremum norm.

Proposition 1.4.10: [22]

There exists a constant $0 < \rho < 1$ such that the sequences $\left(\hat{\vartheta}_h^k\right)$ and $(\check{\vartheta}_h^k)$ satisfy the following geometric convergence estimates:

$$\left\|\hat{\vartheta}_h^k - \vartheta_h\right\|_\infty \leq \rho^k \left\|\hat{\vartheta}_h^0\right\|_\infty, \tag{1.51}$$

$$\left\|\check{\vartheta}_h^k - \vartheta_h\right\|_\infty \leq \rho^k \left\|\hat{\vartheta}_h^0\right\|_\infty. \tag{1.52}$$

1.4.3 Finite element approximation in the L^∞ norm

This section is devoted to the analysis of the approximation properties of the finite element scheme in the $L^\infty(\Omega)$ norm. Using classical finite element approximation results and a local comparison between the continuous and discrete subsolutions, we derive the following estimate.

Theorem 1.4.3: [28, 44]

Let $\hat{\vartheta}^{i,0}$ (respectively, $\hat{\vartheta}_h^{i,0}$) denote the solution of the continuous problem (1.29) (respectively, its discrete approximation (1.48)). Then, for each subdomain $i = 1, 2, \dots, n$, the following estimate holds:

$$\left\| \hat{\vartheta}^{i,0} - \hat{\vartheta}_h^{i,0} \right\|_{L^\infty(\Omega)} \leq C\, h^2 |\log h|^{3/2}. \tag{1.53}$$

Auxiliary iterative sequence for variational inequalities

To facilitate a more detailed analysis of the approximation error, we define an auxiliary sequence:

$$\tilde{\vartheta}_h^k = \left(\tilde{\vartheta}_h^{1,k}, \ldots, \tilde{\vartheta}_h^{n,k} \right),$$

which acts as an intermediate step connecting the discrete solution to the fixed-point formulation of the system. For each iteration $k \geq 1$, the component $\tilde{\vartheta}_h^{i,k}$ is characterized as the unique solution of the following variational inequality: [22]

$$\begin{cases} a^i \langle \tilde{\vartheta}_h^{i,k}, u - \hat{\vartheta}^{i,k} \rangle \geq \langle \mathbb{F}^i, u - \hat{\vartheta}^{i,k} \rangle, \quad \forall u \in H_0^1(\Omega), \\ \tilde{\vartheta}_h^{i,k} \leq \kappa + \hat{\vartheta}^{i+1,k-1}, \quad u \leq \kappa + \hat{\vartheta}^{i+1,k-1}, \quad i = 1, 2, \ldots, n, \\ \tilde{\vartheta}_h^{n+1,k} = \tilde{\vartheta}_h^{1,k}, \quad \text{and} \quad \tilde{\vartheta}_h^{i,0} = \hat{\vartheta}_h^{i,0}, \end{cases}$$

where the vector $\hat{\vartheta}^k = (\hat{\vartheta}^{1,k}, \ldots, \hat{\vartheta}^{n,k})$ is as defined in (1.33). Equivalently, this sequence can be interpreted operatorially as:

$$\tilde{\vartheta}_h^k = T_h \hat{\vartheta}^k, \quad \tilde{\vartheta}_h^0 = \hat{\vartheta}_h^0. \tag{1.54}$$

This auxiliary sequence clarifies the structure of the fixed-point operator T_h and provides a tool to control the regularity of iterates throughout the discrete procedure. The following proposition confirms that both $\hat{\vartheta}^{i,k}$ and $\tilde{\vartheta}^{i,k}$ remain uniformly bounded in $W^{2,p}(\Omega)$, which is essential for establishing uniform error estimates.

Proposition 1.4.11: [28, 44]

Under the hypotheses (1.1)–(1.9) and the regularity condition (1.13), there exists a constant C, independent of k, such that:

$$\max \left(\|\hat{\vartheta}^{i,k}\|_{W^{2,p}(\Omega)}, \|\tilde{\vartheta}^{i,k}\|_{W^{2,p}(\Omega)} \right) \leq C, \quad i = 1, 2, \ldots, n, \quad 1 \leq p < \infty.$$

Proposition 1.4.12

Within the established framework, the auxiliary sequence satisfies the uniform error bound

$$\|\hat{\vartheta}^k - \tilde{\vartheta}_h^k\|_\infty \leq C\, h^2 |\log h|^2. \tag{1.55}$$

The following lemma plays a crucial role in connecting the exact sequence $\hat{\vartheta}^k$ with the discrete iterates $\hat{\vartheta}_h^k$, allowing us to quantify the total error using the auxiliary sequence:

Lemma 1.4.3: [22]

For all $k \geq 0$, the inequality (1.56) holds:

$$\|\hat{\vartheta}^k - \hat{\vartheta}_h^k\|_\infty \leq \sum_{p=0}^{k} \|\hat{\vartheta}^p - \tilde{\vartheta}_h^p\|_\infty \tag{1.56}$$

Proof

The proof proceeds by mathematical induction on the iteration index k.

- **Base case** $(k = 1)$.
  From definitions (1.50) and (1.54), we have:
  $$\hat{\vartheta}_h^1 = T_h \hat{\vartheta}_h^0, \quad \tilde{\vartheta}_h^1 = T_h \hat{\vartheta}^0.$$
  By the triangle inequality,
  $$\left\|\hat{\vartheta}^1 - \hat{\vartheta}_h^1\right\|_\infty \leq \left\|\hat{\vartheta}^1 - \tilde{\vartheta}_h^1\right\|_\infty + \left\|\tilde{\vartheta}_h^1 - \hat{\vartheta}_h^1\right\|_\infty \leq \left\|\hat{\vartheta}^1 - \tilde{\vartheta}_h^1\right\|_\infty + \left\|\hat{\vartheta}^1 - \tilde{\vartheta}_h^1\right\|_\infty + \left\|T_h \hat{\vartheta}_h^0 - T_h \hat{\vartheta}_h^0\right\|_\infty.$$
  Using the lipschitz continuity of T_h (proposition 1.4.7 and inequality (1.49)) gives:
  $$\left\|\tilde{\vartheta}_h^1 - \hat{\vartheta}_h^1\right\|_\infty \leq \left\|\hat{\vartheta}^1 - \tilde{\vartheta}_h^1\right\|_\infty + \left\|\hat{\vartheta}^0 - \tilde{\vartheta}_h^0\right\|_\infty.$$
  Hence,
  $$\left\|\hat{\vartheta}^1 - \hat{\vartheta}_h^1\right\|_\infty \leq \sum_{p=0}^{1} \left\|\hat{\vartheta}^p - \tilde{\vartheta}_h^p\right\|_\infty.$$

- **Inductive step.**
  Assume that for some $k-1$,
  $$\left\|\hat{\vartheta}^{k-1} - \hat{\vartheta}_h^{k-1}\right\|_\infty \leq \sum_{p=0}^{k-1} \left\|\hat{\vartheta}^p - \tilde{\vartheta}_h^p\right\|_\infty.$$
  We prove the result for k. From the recursive definitions,
  $$\tilde{\vartheta}_h^k = T_h \hat{\vartheta}^{k-1}, \quad \hat{\vartheta}_h^k = T_h \hat{\vartheta}_h^{k-1}.$$
  Thus,
  $$\begin{aligned}
  \left\|\hat{\vartheta}^k - \hat{\vartheta}_h^k\right\|_\infty &\leq \left\|\hat{\vartheta}^k - \tilde{\vartheta}_h^k\right\|_\infty + \left\|\tilde{\vartheta}_h^k - \hat{\vartheta}_h^k\right\|_\infty \\
  &\leq \left\|\hat{\vartheta}^k - \tilde{\vartheta}_h^k\right\|_\infty + \left\|T_h \hat{\vartheta}^{k-1} - T_h \hat{\vartheta}_h^{k-1}\right\|_\infty \\
  &\leq \left\|\hat{\vartheta}^k - \tilde{\vartheta}_h^k\right\|_\infty + \left\|\hat{\vartheta}^{k-1} - \hat{\vartheta}_h^{k-1}\right\|_\infty \\
  &\leq \left\|\hat{\vartheta}^k - \tilde{\vartheta}_h^k\right\|_\infty + \sum_{p=0}^{k-1} \left\|\hat{\vartheta}^p - \tilde{\vartheta}_h^p\right\|_\infty.
  \end{aligned}$$
  Using the inductive hypothesis yields:
  $$\left\|\hat{\vartheta}^k - \hat{\vartheta}_h^k\right\|_\infty \leq \sum_{p=0}^{k} \left\|\hat{\vartheta}^p - \tilde{\vartheta}_h^p\right\|_\infty.$$
  This completes the proof.

Combining Propositions (1.4.5), (1.4.10), (1.4.12), lemma 1.4.3, and theorem 1.4.3, we are now in a position to derive the main convergence result for the fully discretized quasi-variational inequality system.

L^∞-error estimate for the system of QVIs

In this subsection, we establish a uniform error bound in the L^∞-norm between the exact solution ϑ and its numerical approximation ϑ_h. This result describes the asymptotic behavior of the discretization scheme with respect to the mesh size h, providing a rigorous measure of accuracy as $h \to 0$.

Theorem 1.4.4: [22]

There exists a constant $C > 0$, independent of h, such that the numerical solution satisfies the following global error estimate:

$$\|\vartheta - \vartheta_h\|_\infty \leq Ch^2 |\log h|^3.$$

Proof

To establish the uniform L^∞-error bound, we decompose the proof into clear stages.

- **Step 1.**
We split the total error as follows:

$$\|\vartheta - \vartheta_h\|_\infty \leq \left\|\vartheta - \hat{\vartheta}^k\right\|_\infty + \left\|\hat{\vartheta}^k - \hat{\vartheta}_h^k\right\|_\infty + \left\|\hat{\vartheta}_h^k - \vartheta_h\right\|_\infty.$$

- **Step 2.**
Using the contraction properties,

$$\left\|\vartheta - \hat{\vartheta}^k\right\|_\infty \leq \rho^k \left\|\hat{\vartheta}^0\right\|_\infty, \quad \left\|\hat{\vartheta}_h^k - \vartheta_h\right\|_\infty \leq \rho^k \left\|\hat{\vartheta}_h^0\right\|_\infty.$$

- **Step 3.**
By lemma 1.4.3,

$$\left\|\hat{\vartheta}^k - \hat{\vartheta}_h^k\right\|_\infty \leq \left\|\hat{\vartheta}^0 - \hat{\vartheta}_h^0\right\|_\infty + \sum_{p=1}^{k} \left\|\hat{\vartheta}^p - \tilde{\vartheta}_h^p\right\|_\infty.$$

Using (1.53), (1.55), (1.51), (1.56), we obtain:

$$\left\|\hat{\vartheta}^0 - \hat{\vartheta}_h^0\right\|_\infty \leq Ch^2 |\log h|^{3/2}, \quad \left\|\hat{\vartheta}^p - \tilde{\vartheta}_h^p\right\|_\infty \leq Ch^2 |\log h|^2.$$

- **Step 4.**
Combining all contributions,

$$\|\vartheta - \vartheta_h\|_\infty \leq \rho^k \|\hat{\vartheta}^0\|_\infty + \rho^k \|\hat{\vartheta}_h^0\|_\infty + Ch^2 |\log h|^{3/2} + kCh^2 |\log h|^2.$$

- **Step 5.**
Choosing k such that $\rho^k \sim h^2$, i.e. $k \sim |\log h|$, we obtain:

$$\|\vartheta - \vartheta_h\|_\infty \leq Ch^2 |\log h|^3.$$

This completes the proof.

Chapter two :

Overlapping domain decomposition methods for coercive HJB equations

This chapter investigates the coercive Hamilton–Jacobi–Bellman problem in both continuous and discrete settings. Existence, uniqueness, and convergence are established using monotone iterative sequences combined with overlapping domain decomposition methods. The analysis is validated by finite element simulations and a comparison between overlapping and non-overlapping decomposition strategies.

Contents

2.1 Analysis of the HJB problem

This section studies the coercive Hamilton–Jacobi–Bellman problem in both continuous and discrete settings. Existence, uniqueness, and convergence results are established using finite element approximations together with L^∞-error estimates.

2.1.1 The continuous HJB problem

Mathematical formulation of the HJB problem

We investigate a class of deterministic optimal control problems whose value function is characterized as the unique viscosity solution to a fully nonlinear elliptic partial differential equation of Hamilton-Jacobi-Bellman type. Specifically, we consider the boundary value problem given by:

$$\begin{cases} \max\limits_{1\leq i\leq n} \left(\mathbb{A}^i\vartheta - \mathbb{F}^i\right) = 0 & \text{in } \Omega, \\ \vartheta = 0 & \text{on } \partial\Omega, \end{cases} \tag{2.1}$$

where $\Omega \subset \mathbb{R}^N$ is a bounded open domain with smooth boundary, and ϑ is the unknown function. The differential operators $\mathbb{A}^i$, which reflect the dynamics and costs associated with different control modes, are defined by:

$$\mathbb{A}^i\vartheta = \sum_{1\leq z,s\leq N} a^i_{zs}(x)\frac{\partial^2\vartheta}{\partial x_z\partial x_s} + \sum_{1\leq s\leq N} a^i_s(x)\frac{\partial\vartheta}{\partial x_s} + a^i_0(x)\vartheta, \tag{2.2}$$

and their bilinear forms are associated with $\mathbb{A}^i$, for $v, u \in H^1(\Omega)$:

$$a^i\langle v,u\rangle = \int_\Omega \left(\sum_{z,s=1}^N a^i_{zs}(x)\frac{\partial v}{\partial x_z}\frac{\partial u}{\partial x_s} + \sum_{s=1}^N a^i_s(x)\frac{\partial v}{\partial x_s}u + a^i_0(x)vu\right)dx. \tag{2.3}$$

Throughout, we assume that the coefficients of the operators satisfy the following structural and regularity conditions:

- For each $i \in \{1,\dots,n\}$, the functions a^i_{zs}, a^i_s, a^i_0 belong to $C^2(\overline{\Omega})$.
- The symmetric part of the matrix (a^i_{zs}) is uniformly positive definite, that is,

$$\sum_{z,s=1}^N a^i_{zs}(x)\xi_z\xi_s \geq \delta|\xi|^2 \quad \text{for all } \xi\in\mathbb{R}^N, \text{ and } x\in\overline{\Omega}, \text{ with } \delta>0. \tag{2.4}$$

- The coefficients satisfy the symmetry condition

$$a^i_{zs}(x) = a^i_{sz}(x), \tag{2.5}$$

  and the zeroth-order term is uniformly coercive:

$$a^i_0(x) \geq \gamma > 0. \tag{2.6}$$

- The source terms $\mathbb{F}^i \in C^2(\overline{\Omega})$ and are non-negative:

$$\mathbb{F}^i \geq 0. \tag{2.7}$$

Existence, uniqueness and regularity of the solution

The properties of existence and uniqueness for the solution of (2.1) follow from the structure of the maximum operator combined with the uniform ellipticity and coercivity of each $\mathbb{A}^i$. In previous studies [42], to simplify computations, the Hamilton-Jacobi-Bellman equation was approximated by a quasi-variational system (1.24).

Theorem 2.1.1: [42]

As $\kappa \to 0$, each component of the system (1.24) converges uniformly in $C(\overline{\Omega})$ to the solution ϑ of the HJB equation (2.1). Additionally, the system (1.24) or (2.1) admits a unique solution that belongs to the Sobolev space $(W^{2,p}(\Omega))^n$, where $2 \leq p < \infty$.

2.1.2 The discrete HJB problem

In this part, we address the discrete approximation of the coercive Hamilton-Jacobi-Bellman problem. The continuous domain Ω is discretized through a triangulation process, and the solution is approximated using finite element methods. We follow a systematic discretization strategy that ensures stability and convergence while preserving the structural properties of the original system.

Discretization by finite element method

Let $\Omega \subset \mathbb{R}^N$ be a polygonal domain covered by a family of conforming, quasi-uniform triangular meshes denoted by τ^h, where $h > 0$ indicates the mesh parameter. On this triangulation, we construct the finite element space

$$V_h = \left\{ u_h \in C(\Omega) \cap H_0^1(\Omega) : u_h|_K \in P_1,\ \forall K \in \tau_h \right\},$$

where P_1 denotes the set of polynomials of degree one. The functions in V_h are continuous and piecewise affine, vanishing on the boundary. Let $\{\varphi_z\}_{z=1}^{N(h)}$ be the nodal basis of this space. The discrete operators $\mathscr{A}^i \in \mathbb{R}^{N(h)\times N(h)}$, corresponding to the bilinear forms $a^i\langle\cdot,\cdot\rangle$, are defined by:

$$\mathscr{A}^i_{zs} = a^i\langle \varphi_z, \varphi_s\rangle, \quad 1 \leq z, s \leq N(h), \quad 1 \leq i \leq n.$$

The right-hand side vector approximating the source term is given by:

$$\mathscr{F}^i_z = \langle \mathscr{F}^i, \varphi_z\rangle, \quad 1 \leq z \leq N(h), \quad 1 \leq i \leq n.$$

With these notations, the finite element discretization of the HJB problem leads to the following discrete system:

$$\begin{cases} \text{Find} \quad \vartheta_h \in V_h \quad \text{solution to:} \\ \max\limits_{1\leq i\leq n} (\mathscr{A}^i \vartheta_h - \mathscr{F}^i) = 0. \end{cases} \tag{2.8}$$

The matrices $\mathscr{A}^i$ are designed to satisfy the discrete maximum principle and possess the structure of M-matrices, as detailed in [29].

Existence, uniqueness, and convergence of the discrete solution

Due to the coercivity and regularity properties inherited from the continuous setting, and assuming that the dmp condition is satisfied, the discretized HJB system (2.8) is well-posed. It can be alternatively interpreted as a limit of a family of discrete quasi-variational inequality problems parameterized by $\kappa > 0$, as discussed in [33]. This perspective provides a convenient framework to establish stability and convergence.

Theorem 2.1.2: [33]

Assume the discrete maximum principle holds. Then, the discrete problem (2.8), or equivalently the quasi-variational system (1.45), admits a unique solution $\vartheta_h \in V_h$. Moreover, as $\kappa \to 0$, the approximating sequence of solutions to (1.45) converges uniformly in $C(\overline{\Omega})$ to ϑ_h.

2.1.3 L^∞-error estimate for the discretized coercive HJB equation

We now turn our attention to the analysis of the discretization error associated with the finite element solution of the coercive Hamilton-Jacobi-Bellman equation. In particular, we aim to establish a convergence estimate in the uniform norm that quantifies how well the discrete approximation ϑ_h replicates the exact solution ϑ as the mesh is refined.

Theorem 2.1.3: [22]

Let ϑ be the unique solution of the continuous HJB problem (2.1), and let ϑ_h denote the discrete solution obtained from (2.8). Then, there exists a constant $C > 0$, independent of the mesh size h, such that:

$$\|\vartheta - \vartheta_h\|_{L^\infty(\Omega)} \leq Ch^2 |\log h|^3.$$

Proof

We begin by decomposing the total error between the continuous and discrete solutions into three distinct components. This decomposition will allow us to isolate the contributions from different sources of error. We proceed as follows:

$$\begin{aligned}\|\vartheta - \vartheta_h\|_{L^\infty(\Omega)} &\leq \max_{1\leq i\leq n} \left(\|\vartheta^i - \vartheta\|_{L^\infty(\Omega)} + \|\vartheta^i - \vartheta_h^i\|_{L^\infty(\Omega)} + \|\vartheta_h^i - \vartheta_h\|_{L^\infty(\Omega)}\right), \\ &\leq \max_{1\leq i\leq n} \left(\|\vartheta^i - \vartheta\|_{L^\infty(\Omega)}\right) + \max_{1\leq i\leq n} \left(\|\vartheta^i - \vartheta_h^i\|_{L^\infty(\Omega)}\right) + Ch^2 |\log h|^3,\end{aligned}$$

Using the estimate established in theorem (2.1.1), together with the result of theorem 1.4.5. and the discrete maximum principle stated in theorem (2.1.2), we obtain the following overall error estimate:

$$\|\vartheta - \vartheta_h\|_{L^\infty(\Omega)} \leq Ch^2 |\log h|^3,$$

where C is a constant that does not depend on the mesh size h.

2.2 Overlapping domain decomposition approach for HJB problems

In this part, we investigate the use of overlapping domain decomposition techniques for the resolution of Hamilton–Jacobi–Bellman (HJB) equations, following the framework introduced in [46]. The computational domain is partitioned into several overlapping subregions, and iterative constructions based on upper and lower solution bounds are employed. This procedure guarantees the monotone convergence of the iterative sequences toward the exact solution of the discrete HJB formulation.

2.2.1 Domain partitioning and transmission boundaries

Let $\Omega \subset \mathbb{R}^2$ be a bounded domain with smooth boundary. To implement the overlapping decomposition strategy, we divide Ω into two subregions, denoted by Ω_1 and Ω_2, in such a way that the overlap between them is nontrivial:

$$\Omega = \Omega_1 \cup \Omega_2, \qquad \Omega_1 \cap \Omega_2 \neq \varnothing.$$

For each subdomain Ω_j, we denote its boundary by Γ_j, where:

$$\Gamma_j = \partial\Omega_j, \quad j \in \{1, 2\}.$$

The portion of the boundary shared with the neighboring subdomain is referred to as the interface:

$$\Sigma_j = \partial\Omega_j \cap \Omega_l, \qquad l \neq j.$$

These transmission boundaries Σ_j ensure the proper exchange of information between the two subproblems and are essential for maintaining consistency of the global solution.

In the numerical experiments considered here, the computational domain is chosen to be the unit square $[0, 1] \times [0, 1]$. The overlapping decomposition is constructed by defining:

$$\Omega_1 = [0, \beta] \times [0, 1], \qquad \Omega_2 = [\alpha, 1] \times [0, 1],$$

with parameters $0 < \alpha < \beta < 1$, so that Ω_1 and Ω_2 overlap on the vertical strip $[\alpha, \beta] \times [0, 1]$.

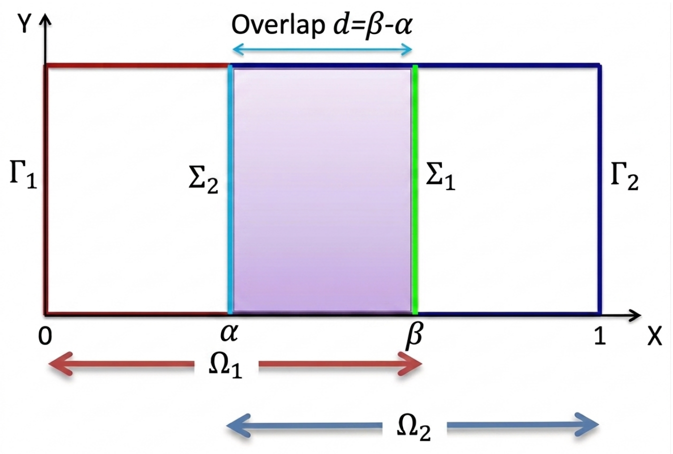

Figure 2.1: **The domain Ω and its decomposition into two overlapping subdomains**

We introduce the index set $\{1, \ldots, N\}$ and divide it into two disjoint subsets:

$$\{1, \ldots, \beta - 1\} \qquad \text{and} \qquad \{\alpha + 1, \ldots, N\}.$$

Here, the integer parameter:

$$d = \beta - \alpha$$

measures the size of the overlap between the two subdomains. In terms of the mesh size h, the physical length of this overlapping portion can be expressed as:

$$\sigma(h) = d\,h.$$

This factor $\sigma(h)$ quantifies the geometric extent of the shared region and will play a role in the analysis of convergence.

2.2.2 Discrete block matrix representation of the system

The discretized Hamilton–Jacobi–Bellman system can be written in a block structure by means of a bilinear form $a^i(u,v)$ associated with the stiffness matrices $\mathscr{A}^i$. The global unknown vector ϑ_h is partitioned according to the decomposition of the computational domain:

$$\vartheta_h = \begin{pmatrix} \vartheta_{1h} \\ \vartheta_{2h} \end{pmatrix},$$

where each block represents the discrete solution restricted to one of the subdomains.

The system matrix naturally acquires a block form:

$$\mathscr{A}^i = \begin{pmatrix} \mathscr{A}^i_{11} & -\mathscr{A}^i_{12} \\ -\mathscr{A}^i_{21} & \mathscr{A}^i_{22} \end{pmatrix},$$

with diagonal blocks corresponding to the internal contributions of each subdomain, while the off-diagonal blocks encode the coupling across the overlapping interfaces.

Similarly, the right-hand side vector is decomposed into two components:

$$\mathscr{F}^i = \begin{pmatrix} \mathscr{F}^i_1 \\ \mathscr{F}^i_2 \end{pmatrix}.$$

The entries of the subvectors are given by the nodal values associated with the mesh points of each subdomain, namely

$$\vartheta_{1h} = \big((\vartheta_{1h})_1, \ldots, (\vartheta_{1h})_{\beta-1}\big)^T, \qquad \vartheta_{2h} = \big((\vartheta_{2h})_{\alpha+1}, \ldots, (\vartheta_{2h})_N\big)^T.$$

This block formulation reflects both the local structure of each subproblem and the interdependence created by the overlapping decomposition.

2.2.3 Decompositions of the matrix $\mathscr{A}^i$

We now investigate two different block decompositions of the global matrix $\mathscr{A}^i$, which are central to the domain decomposition approach for Hamilton–Jacobi–Bellman equations. Such decompositions simplify the algebraic structure of the system, allow an efficient implementation of the iterative process, and contribute to the proof of convergence.

First decomposition

On the subdomain $[0,\beta]$, the matrix $\mathscr{A}^i$ can be written in the following block form:

$$\mathscr{A}^i = \begin{pmatrix} \mathscr{A}^i_{1,1} & -\mathscr{A}^i_{1,2} \\ \mathscr{C}^i_1 & \mathscr{D}^i_1 \end{pmatrix}.$$

Here, the blocks are defined as follows:

- $\mathscr{A}^i_{1,1} \in \mathbb{R}^{(\beta-1)\times(\beta-1)}$ represents the contribution of the first subdomain Ω_1.
- $\mathscr{D}^i_1 \in \mathbb{R}^{(N-\beta+1)\times(N-\beta+1)}$ corresponds to the remaining part of the domain outside Ω_1.
- The coupling blocks are given by:

  $$\mathscr{A}^i_{1,2} \in \mathbb{R}^{(\beta-1)\times(N-\beta+1)}, \qquad \mathscr{C}^i_1 \in \mathbb{R}^{(N-\beta+1)\times(\beta-1)},$$

  and they ensure the interaction between the two subdomains across the overlap.

Second decomposition:

An alternative factorization of the matrix $\mathscr{A}^i$ is obtained by splitting it into block components over the interval $[\alpha, 1]$. The structure takes the form

$$\mathscr{A}^i = \begin{pmatrix} \mathscr{D}_2^i & \mathscr{C}_2^i \\ -\mathscr{A}_{2,1}^i & \mathscr{A}_{2,2}^i \end{pmatrix}.$$

The interpretation of each block is as follows:

- The diagonal submatrices $\mathscr{D}_2^i \in \mathbb{R}^{\alpha\times\alpha}$ and $\mathscr{A}_{2,2}^i \in \mathbb{R}^{(N-\alpha)\times(N-\alpha)}$ act, respectively, on the degrees of freedom inside the first portion of the interval and on those of the subdomain Ω_2.
- The off-diagonal components $\mathscr{C}_2^i \in \mathbb{R}^{\alpha\times(N-\alpha)}$ and $\mathscr{A}_{2,1}^i \in \mathbb{R}^{(N-\alpha)\times\alpha}$ encode the transmission terms across the interface, ensuring communication between the overlapping parts of the decomposition.
- In the limiting configuration where $\beta = \alpha + 1$, the overlap shrinks to a single point. In this case one has the identities $\mathscr{A}_{1,1}^i = \mathscr{D}_2^i$ and $\mathscr{A}_{2,2}^i = \mathscr{D}_1^i$. Hence, the geometric overlap is minimal and the algebraic coupling vanishes completely.

Matrix extension for boundary compatibility

To maintain a consistent coupling between overlapping subdomains, the off-diagonal blocks $\mathscr{A}_{1,2}^i$ and $\mathscr{A}_{2,1}^i$ are extended by adding zero rows or columns. This zero-padding procedure aligns the blocks with the global indexing of the interface and guarantees compatibility for any overlap size.

The construction of the extended blocks is as follows:

- **Extension from Ω_2 to Ω_1:**

$$\tilde{\mathscr{A}}_{1,2}^i = \begin{bmatrix} 0_{(\beta-1)\times(d-1)} & \mathscr{A}_{1,2}^i \end{bmatrix}, \qquad \tilde{\mathscr{A}}_{1,2}^i \in \mathbb{R}^{(\beta-1)\times(N-\alpha)}.$$

  - ❖ The leading zero block corresponds to the indices outside the overlap.
  - ❖ The active block $\mathscr{A}_{1,2}^i$ transfers information from Ω_2 into the unknowns of Ω_1.

- **Extension from Ω_1 to Ω_2:**

$$\tilde{\mathscr{A}}_{2,1}^i = \begin{bmatrix} \mathscr{A}_{2,1}^i & 0_{(N-\alpha)\times(d-1)} \end{bmatrix}, \qquad \tilde{\mathscr{A}}_{2,1}^i \in \mathbb{R}^{(N-\alpha)\times(\beta-1)}.$$

  - ❖ The trailing zero block represents the part of Ω_2 outside the overlap.
  - ❖ The active block $\mathscr{A}_{2,1}^i$ enforces the coupling with Ω_1.

With this construction, the structure of the global operator is preserved, and the information exchange across the overlapping interface remains consistent for any value of the overlap parameter.

Reformulated system over the extended domain

By introducing the extended coupling blocks, the discrete problem can be rewritten as a global augmented system. The reformulated system takes the form

$$\begin{cases} \max\limits_{1\le i\le n} \left(\tilde{\mathscr{A}}^i\,\vartheta_h - \mathscr{F}^i\right) = 0, & \text{in } \Omega, \\ \vartheta_h = 0, & \text{on } \partial\Omega. \end{cases}$$

This extended formulation guarantees that information is properly transmitted across the overlap and preserves the continuity of the solution between subdomains. The construction becomes particularly relevant when the overlap covers more than a single grid node.

❖ Special case: minimal overlap

- When the overlap is minimal, i.e., $d = 1$, the zero-padding vanishes, and the augmented matrices coincide with the original local blocks.
- In this situation, the extended operator $\tilde{\mathscr{A}}^i$ reduces exactly to the initial block structure $\mathscr{A}^i$:

$$\tilde{\mathscr{A}}^i = \begin{pmatrix} \mathscr{A}^i_{1,1} & -\tilde{\mathscr{A}}^i_{1,2} \\ -\tilde{\mathscr{A}}^i_{2,1} & \mathscr{A}^i_{2,2} \end{pmatrix} = \begin{pmatrix} \mathscr{A}^i_{1,1} & -\mathscr{A}^i_{1,2} \\ -\mathscr{A}^i_{2,1} & \mathscr{A}^i_{2,2} \end{pmatrix} = \mathscr{A}^i.$$

This confirms that the extension procedure is conservative: it coincides with the original formulation when no additional degrees of freedom are introduced by the overlap.

2.2.4 Iterative strategy based on overlapping subdomains

To tackle the discrete Hamilton–Jacobi–Bellman (HJB) problem (2.8), we employ an iterative scheme rooted in the principle of overlapping domain decomposition. The global computational domain is partitioned into two partially superposed subregions, Ω_1 and Ω_2, which enables localized solution updates while preserving the global coupling. This framework not only enhances parallelism but also improves the convergence properties of the method.

Local updates on subdomains

The algorithm proceeds in an iterative manner. At iteration $k+1$, the solution is updated alternately on each subdomain, with interface data exchanged between neighboring regions.

- **Update on Ω_1 :** The discrete problem restricted to the first subdomain reads

$$\begin{cases} \max\limits_{1\le i\le n} \left(\mathscr{A}^i_{1,1}\vartheta^{k+1}_{1h} - \mathscr{F}^i_1\right) = 0, & \text{in } \Omega_1, \\ \left(\vartheta^{k+1}_{1h}\right)_\beta = \left(\vartheta^{k}_{2h}\right)_\beta, & \text{on } \Sigma_1, \end{cases}$$

  where the boundary condition along the interface Σ_1 is supplied by the previous iterate on the adjacent subdomain.

- **Update on Ω_2 :** Once ϑ^{k+1}_{1h} is available, the solution on Ω_2 is computed from:

$$\begin{cases} \max\limits_{1\le i\le n} \left(\mathscr{A}^i_{2,2}\vartheta^{k+1}_{2h} - \mathscr{F}^i_2\right) = 0, & \text{in } \Omega_2, \\ \left(\vartheta^{k+1}_{2h}\right)_\alpha = \left(\vartheta^{k+1}_{1h}\right)_\alpha, & \text{on } \Sigma_2. \end{cases}$$

- **Compact representation :** By incorporating the interfacial transmission conditions, the coupled updates can be expressed more succinctly as

$$\begin{cases} \max\limits_{1\le i\le n}\left\{\mathscr{A}^i_{1,1}\vartheta^{k+1}_{1h} - \tilde{\mathscr{A}}^i_{1,2}\vartheta^{k}_{2h} - \mathscr{F}^i_1\right\} = 0, & \text{in } \Omega_1,\\ \max\limits_{1\le i\le n}\left\{\mathscr{A}^i_{2,2}\vartheta^{k+1}_{2h} - \tilde{\mathscr{A}}^i_{2,1}\vartheta^{k+1}_{1h} - \mathscr{F}^i_2\right\} = 0, & \text{in } \Omega_2, \end{cases}$$

where the tilde-blocks explicitly encode the overlap-induced coupling across the interface.

Block formulation and Gauss–Seidel interpretation

The iterative procedure can be reformulated in a block-matrix setting. Defining the global update vector

$$\vartheta_h^{k+1} = \begin{pmatrix} \vartheta_{1h}^{k+1} \\ \vartheta_{2h}^{k+1} \end{pmatrix},$$

the iteration is written as:

$$\underbrace{\begin{pmatrix} \mathscr{A}^i_{1,1} & 0 \\ -\mathscr{A}^i_{2,1} & \mathscr{A}^i_{2,2} \end{pmatrix}}_{\text{Left Gauss–Seidel Block}} \begin{pmatrix} \vartheta_{1h} \\ \vartheta_{2h} \end{pmatrix}^{k+1} = \underbrace{\begin{pmatrix} \mathscr{A}^i_{1,2} & 0 \\ 0 & 0 \end{pmatrix}}_{\text{Right-hand coupling from } \vartheta^k} \begin{pmatrix} \vartheta_{1h} \\ \vartheta_{2h} \end{pmatrix}^{k} + \begin{pmatrix} \mathscr{F}^i_1 \\ \mathscr{F}^i_2 \end{pmatrix}. \tag{2.9}$$

This formulation corresponds to the block Gauss–Seidel iteration for the global linear system

$$\mathscr{A}^i\vartheta = \mathscr{F}^i,$$

where the standard splitting

$$(\mathscr{L} + \mathscr{D})\vartheta^{k+1} = -\mathscr{U}\vartheta^k + \mathscr{F}$$

is applied with the blocks:

- $\mathscr{D}$: diagonal blocks $(\mathscr{A}_{1,1}, \mathscr{A}_{2,2})$,
- $\mathscr{L}$: lower block $(-\mathscr{A}_{2,1})$,
- $\mathscr{U}$: upper block $(\mathscr{A}_{1,2})$.

In general, the Gauss–Seidel iteration is given by

$$\begin{cases} \vartheta^{(0)} \in \mathbb{R}^N, \\ \mathscr{A}_{z,z}\,\vartheta_z^{(k+1)} = -\sum\limits_{s<z}^{N} \mathscr{A}_{z,s}\,\vartheta_s^{(k+1)} - \sum\limits_{s>z}^{N} \mathscr{A}_{z,s}\,\vartheta_s^{(k)} + \mathscr{F}_z, \quad z = 1,\dots,N. \end{cases} \tag{2.10}$$

Thus, the overlapping Schwarz procedure applied to the discrete HJB system can be interpreted as a block Gauss–Seidel scheme, where the interaction between subdomains is expressed through the off-diagonal blocks.

Subsolutions, supersolutions, and iterative scheme

We introduce the notions of subsolution and supersolution, which provide admissible lower and upper bounds for the iterative process.

- **Subsolution :** A vector $\check{\vartheta}_h \in \mathbb{R}^N$ is a subsolution if :

$$\max_{1\le i\le n}\{\mathscr{A}^i\check{\vartheta}_h - \mathscr{F}^i\} \le 0. \tag{2.11}$$

- **Supersolution :** A vector $\hat{\vartheta}_h \in \mathbb{R}^N$ is a supersolution if :

$$\max_{1\le i\le n}\{\mathscr{A}^i\hat{\vartheta}_h - \mathscr{F}^i\} \ge 0. \tag{2.12}$$

When $\mathscr{F}^i \ge 0$ for all **i**, the zero vector defines an admissible subsolution:

$$\check{\vartheta}_h^0 = (0, 0, \ldots, 0).$$

An admissible supersolution can be computed by solving the linear system:

$$\mathscr{A}^i\hat{\vartheta}_h^0 = \mathscr{F}^i, \quad i = 1, \ldots, n.$$

Algorithm 1: Iterative ODD for Coercive HJB Problems

Initialization: Set $\check{\vartheta}_h^0 = (0, 0, \ldots, 0)$, and let $k = 0$.

Step 1: Update on domain Ω_1:

$$\max_{1\le i\le n}\left\{\mathscr{A}_{1,1}^i\check{\vartheta}_{1h}^{k+1} - \tilde{\mathscr{A}}_{1,2}^i\check{\vartheta}_{2h}^{k} - \mathscr{F}_1^i\right\} = 0.$$

Step 2: Update on domain Ω_2:

$$\max_{1\le i\le n}\left\{-\tilde{\mathscr{A}}_{2,1}^i\check{\vartheta}_{1h}^{k+1} + \mathscr{A}_{2,2}^i\check{\vartheta}_{2h}^{k+1} - \mathscr{F}_2^i\right\} = 0.$$

Step 3: Convergence test: If the criterion is not satisfied, set $k \leftarrow k+1$ and return to Step 1.

2.2.5 Monotonic convergence of lower and upper sequences

This part is devoted to establishing the monotonic behavior and convergence of the iterative sequences defined by the algorithm. The construction involves two sequences: the lower approximations, which increase step by step, and the upper approximations, which decrease iteratively. Both are shown to be bounded and to converge toward the unique discrete solution.

Theorem 2.2.1

Let $(\check{\vartheta}_h^k)$ and $(\hat{\vartheta}_h^k)$ be the sequences generated by Algorithm 1. Then $(\check{\vartheta}_h^k)$ is monotone non-decreasing, $(\hat{\vartheta}_h^k)$ is monotone non-increasing, and both converge to the same limit ϑ_h, which is the unique solution of the discrete HJB system (2.8).

Proof

The argument proceeds in three stages.

- **Step 1.** The sequence of lower approximations $(\check{\vartheta}_h^k)$ is shown to increase monotonically. Moreover, it remains bounded from above, which prevents divergence.
- **Step 2.** The sequence of upper approximations $(\hat{\vartheta}_h^k)$ decreases monotonically, while

being bounded from below, ensuring stability of the iteration.

- **Step 3.** Since the lower sequence is bounded above and the upper sequence is bounded below, and both are monotone, their limits must coincide. The common limit is precisely the unique discrete solution of (2.8), which concludes the proof.

The sequence of lower approximations :

We begin with the sequence of lower solutions $(\check{\vartheta}_h^k)$. The aim here is to establish that this sequence grows monotonically with respect to the iteration index, while remaining a valid subsolution at every step. More precisely, we prove that:

$$\check{\vartheta}_h^{k+1} \geq \check{\vartheta}_h^k,$$

which ensures that the sequence is non-decreasing and bounded from above by the discrete solution.

- **Step 1: Monotonicity of the sequence**
  We begin by showing that the discrete sequence $\left(\check{\vartheta}_h^k\right)_{k\geq 0}$ is non-decreasing. This property will be established through induction on the iteration index k.

  ❖ **Base case:** At the first iteration ($k=0$), we verify the monotonicity separately in each subdomain.

  1. **First subdomain.** The discrete problem in the first region is solved as :
  $$\max_{1\leq i\leq n}\left\{\mathscr{A}_{1,1}^i\check{\vartheta}_{1h}^1 - \tilde{\mathscr{A}}_{1,2}^i\check{\vartheta}_{2h}^0 - \mathscr{F}_1^i\right\} = 0.$$
  Since $\check{\vartheta}_h^0$ is a subsolution, it satisfies:
  $$\max_{1\leq i\leq n}\left\{\mathscr{A}_{1,1}^i\check{\vartheta}_{1h}^0 - \tilde{\mathscr{A}}_{1,2}^i\check{\vartheta}_{2h}^0 - \mathscr{F}_1^i\right\} \leq 0.$$
  A direct comparison of the two relations yields :
  $$\max_{1\leq i\leq n}\left\{\mathscr{A}_{1,1}^i\check{\vartheta}_{1h}^0 - \tilde{\mathscr{A}}_{1,2}^i\check{\vartheta}_{2h}^0 - \mathscr{F}_1^i\right\} \leq \max_{1\leq i\leq n}\left\{\mathscr{A}_{1,1}^i\check{\vartheta}_{1h}^1 - \tilde{\mathscr{A}}_{1,2}^i\check{\vartheta}_{2h}^0 - \mathscr{F}_1^i\right\},$$
  thus, we conclude:
  $$\check{\vartheta}_{1h}^0 \leq \check{\vartheta}_{1h}^1.$$
  2. **Second subdomain.** In the second region, the discrete problem reads :
  $$\max_{1\leq i\leq n}\left\{-\tilde{\mathscr{A}}_{2,1}^i\check{\vartheta}_{1h}^1 + \mathscr{A}_{2,2}^i\check{\vartheta}_{2h}^1 - \mathscr{F}_2^i\right\} = 0. \tag{2.13}$$
  On the other hand, the subsolution property of $\check{\vartheta}_h^0$ ensures :
  $$\max_{1\leq i\leq n}\left\{-\tilde{\mathscr{A}}_{2,1}^i\check{\vartheta}_{1h}^0 + \mathscr{A}_{2,2}^i\check{\vartheta}_{2h}^0 - \mathscr{F}_2^i\right\} \leq 0. \tag{2.14}$$
  Since the result from the first subdomain ensures ($\check{\vartheta}_{1h}^0 \leq \check{\vartheta}_{1h}^1$), it can be shown that:
  $$\max_{1\leq i\leq n}\left\{-\tilde{\mathscr{A}}_{2,1}^i\check{\vartheta}_{1h}^0 + \mathscr{A}_{2,2}^i\check{\vartheta}_{2h}^1 - \mathscr{F}_2^i\right\} \geq \max_{1\leq i\leq n}\left\{-\tilde{\mathscr{A}}_{2,1}^i\check{\vartheta}_{1h}^1 + \mathscr{A}_{2,2}^i\check{\vartheta}_{2h}^1 - \mathscr{F}_2^i\right\}. \tag{2.15}$$

By substituting Equations (2.13) and (2.14), we obtain:

$$\max_{1\le i\le n}\left\{-\tilde{\mathscr{A}}^i_{2,1}\check{\vartheta}^1_{1h}+\mathscr{A}^i_{2,2}\check{\vartheta}^1_{2h}-\mathscr{F}^i_2\right\}\ge\max_{1\le i\le n}\left\{-\tilde{\mathscr{A}}^i_{2,1}\check{\vartheta}^0_{1h}+\mathscr{A}^i_{2,2}\check{\vartheta}^0_{2h}-\mathscr{F}^i_2\right\}.$$

Thus, combining this result with Equation (2.15), we conclude:

$$\check{\vartheta}^0_{2h}\le\check{\vartheta}^1_{2h}.$$

3. **Combined conclusion.** By combining the inequalities obtained in the first and second subdomains, we conclude that:

$$\check{\vartheta}^0_h\le\check{\vartheta}^1_h.$$

Hence, the first iterate $\check{\vartheta}^1_h$ still satisfies the subsolution property, which confirms that the sequence is non-decreasing at the initial step.

❖ **Inductive step.** Assume by induction that the inequality

$$\check{\vartheta}^{k-1}_h\le\check{\vartheta}^k_h$$

holds, and that $\check{\vartheta}^k_h$ satisfies the subsolution conditions. Our goal is now to establish that:

* the monotonicity is preserved, i.e. $\check{\vartheta}^k_h\le\check{\vartheta}^{k+1}_h$,
* and that the iterate $\check{\vartheta}^{k+1}_h$ remains a subsolution.

1. **Analysis in the first subdomain.** In this region, the problem is written as:

$$\max_{1\le i\le n}\left\{\mathscr{A}^i_{1,1}\check{\vartheta}^{k+1}_{1h}-\tilde{\mathscr{A}}^i_{1,2}\check{\vartheta}^k_{2h}-\mathscr{F}^i_1\right\}=0.$$

Since $\check{\vartheta}^k_h$ is a subsolution, we also have:

$$\max_{1\le i\le n}\left\{\mathscr{A}^i_{1,1}\check{\vartheta}^k_{1h}-\tilde{\mathscr{A}}^i_{1,2}\check{\vartheta}^k_{2h}-\mathscr{F}^i_1\right\}\le 0.$$

By comparing the two relations, it follows that:

$$\check{\vartheta}^k_{1h}\le\check{\vartheta}^{k+1}_{1h}.$$

2. **Analysis in the second subdomain.** Here, the corresponding formulation is:

$$\max_{1\le i\le n}\left\{-\tilde{\mathscr{A}}^i_{2,1}\check{\vartheta}^{k+1}_{1h}+\mathscr{A}^i_{2,2}\check{\vartheta}^{k+1}_{2h}-\mathscr{F}^i_2\right\}=0. \tag{2.16}$$

From the induction hypothesis that $\check{\vartheta}^k_h$ is a lower solution, we know:

$$\max_{1\le i\le n}\left\{-\tilde{\mathscr{A}}^i_{2,1}\check{\vartheta}^k_{1h}+\mathscr{A}^i_{2,2}\check{\vartheta}^k_{2h}-\mathscr{F}^i_2\right\}\le 0. \tag{2.17}$$

Since we already established $\check{\vartheta}^k_{1h}\le\check{\vartheta}^{k+1}_{1h}$, we deduce:

$$\max_{1\le i\le n}\left\{-\tilde{\mathscr{A}}^i_{2,1}\check{\vartheta}^k_{1h}+\mathscr{A}^i_{2,2}\check{\vartheta}^{k+1}_{2h}-\mathscr{F}^i_2\right\}\ge\max_{1\le i\le n}\left\{-\tilde{\mathscr{A}}^i_{2,1}\check{\vartheta}^{k+1}_{1h}+\mathscr{A}^i_{2,2}\check{\vartheta}^{k+1}_{2h}-\mathscr{F}^i_2\right\}. \tag{2.18}$$

Moreover, combining (2.16) and (2.17) gives:

$$\max_{1\le i\le n}\left\{-\tilde{\mathscr{A}}^i_{2,1}\check{\vartheta}^{k+1}_{1h}+\mathscr{A}^i_{2,2}\check{\vartheta}^{k+1}_{2h}-\mathscr{F}^i_2\right\}\ge\max_{1\le i\le n}\left\{-\tilde{\mathscr{A}}^i_{2,1}\check{\vartheta}^k_{1h}+\mathscr{A}^i_{2,2}\check{\vartheta}^k_{2h}-\mathscr{F}^i_2\right\}. \tag{2.19}$$

From (2.18) and (2.19), we finally deduce:

$$\check{\vartheta}^k_{2h}\le\check{\vartheta}^{k+1}_{2h}.$$

3. **Combined conclusion.** By combining the inequalities obtained in the first and second subdomains for k, we conclude that
$$\check{\vartheta}_h^k \le \check{\vartheta}_h^{k+1}.$$
Consequently, $\check{\vartheta}_h^{k+1}$ preserves the subsolution property. Iterating this argument yields:
$$\check{\vartheta}_h^0 \le \check{\vartheta}_h^1 \le \cdots \le \check{\vartheta}_h^k \le \check{\vartheta}_h^{k+1}$$
which proves that the sequence is increasing.

- **Step 2: Convergence of the sequence to the discrete solution.**

We now establish that the sequence $(\check{\vartheta}_h^k)$ converges to the solution of the discrete system (2.8).

Since each iterate $\check{\vartheta}_h^k$ is a subsolution, it satisfies the inequality:
$$\max_{1\le i\le n} \left\{\mathscr{A}^i \check{\vartheta}_h^k - \mathscr{F}^i\right\} \le 0. \tag{2.20}$$
For a more precise analysis, we rewrite this condition in the equivalent form:
$$\mathscr{A}^i \check{\vartheta}_h^k - \mathscr{F}^i \le 0, \quad \text{for all } 1 \le i \le n. \tag{2.21}$$
Moreover, we assume the existence of an element $\check{\vartheta}_h^*$ that solves the discrete system, namely it satisfies :
$$\mathscr{A}^i \check{\vartheta}_h^* - \mathscr{F}^i = 0, \quad \text{for all } 1 \le i \le n. \tag{2.22}$$
By comparing (2.21) with (2.22), we directly obtain :
$$\mathscr{A}^i \left(\check{\vartheta}_h^k - \check{\vartheta}_h^*\right) \le 0.$$
Since the matrices $\mathscr{A}^i$ are M-matrices, it follows that :
$$\check{\vartheta}_h^k \le \check{\vartheta}_h^*.$$
This shows that the sequence $(\check{\vartheta}_h^k)$ is bounded above by $\check{\vartheta}_h^*$. Combining this boundedness with the monotonicity already proved, we conclude that the sequence is convergent. More precisely, the limit is given by :
$$\lim_{k\to\infty} \check{\vartheta}_h^k = \check{\vartheta}_h^*. \tag{2.23}$$

- **Step 3: Identification of the limit as the discrete solution.**

We now show that the limit previously obtained, $\check{\vartheta}_h^* = (\check{\vartheta}_{1h}^*, \check{\vartheta}_{2h}^*)$, coincides with the solution of the system (2.8).

According to the iterative scheme described in (2.2.4), we have for each iteration:
$$\max_{1\le i\le n} \left\{\mathscr{A}_{1,1}^i \check{\vartheta}_{1h}^{k+1} - \tilde{\mathscr{A}}_{1,2}^i \check{\vartheta}_{2h}^k - \mathscr{F}_1^i\right\} = 0, \tag{2.24}$$
$$\max_{1\le i\le \mathfrak{n}} \left\{-\tilde{\mathscr{A}}_{2,1}^i \check{\vartheta}_{1h}^{k+1} + \mathscr{A}_{2,2}^i \check{\vartheta}_{2h}^{k+1} - \mathscr{F}_2^i\right\} = 0. \tag{2.25}$$
Passing to the limit as $k \to \infty$ in (2.24)–(2.25), and recalling the convergence result in (2.23), we obtain:
$$\max_{1\le i\le n} \left\{\mathscr{A}_{1,1}^i \check{\vartheta}_{1h}^* - \tilde{\mathscr{A}}_{1,2}^i \check{\vartheta}_{2h}^* - \mathscr{F}_1^i\right\} = 0,$$
$$\max_{1\le i\le \mathfrak{n}} \left\{-\tilde{\mathscr{A}}_{2,1}^i \check{\vartheta}_{1h}^* + \mathscr{A}_{2,2}^i \check{\vartheta}_{2h}^* - \mathscr{F}_2^i\right\} = 0.$$

This block formulation is equivalent to the compact system :

$$\max_{1\leq i\leq \mathfrak{n}} \left\{\mathscr{A}^i\check{\vartheta}_h^* - \mathscr{F}^i\right\} = 0,$$

which shows that $\check{\vartheta}_h^*$ indeed satisfies the original system (2.8). Hence, the limit of the sequence coincides with the discrete solution of the problem.

- **Step 4: Establishing the uniqueness of the discrete solution (2.8).**
  To complete the analysis, it remains to show that the discrete system (2.8) admits a unique solution.

  Assume, by contradiction, that there exist two distinct solutions, denoted by ϑ_h^- and ϑ_h^+. By definition, each of them satisfies:

  $$\max_{1\leq i\leq \mathfrak{n}} \left\{\mathscr{A}^i\vartheta_h^- - \mathscr{F}^i\right\} = 0,$$

  and

  $$\max_{1\leq i\leq n} \left\{\mathscr{A}^i\vartheta_h^+ - \mathscr{F}^i\right\} = 0.$$

  Hence, for every i, we have:

  $$\mathscr{A}^i\vartheta_h^+ - \mathscr{F}^i \leq 0, \qquad \mathscr{A}^i\vartheta_h^- - \mathscr{F}^i \leq 0.$$

  By the definition of the maximum, there exist indices p and p^* such that:

  $$\mathscr{A}^{p^*}\vartheta_h^- - \mathscr{F}^{p^*} = 0, \qquad \mathscr{A}^p\vartheta_h^+ - \mathscr{F}^p = 0.$$

  Subtracting the corresponding relations yields:

  $$\mathscr{A}^{p^*}\left(\vartheta_h^- - \vartheta_h^+\right) \geq 0, \qquad \mathscr{A}^p\left(\vartheta_h^+ - \vartheta_h^-\right) \geq 0.$$

  Since the matrices $\mathscr{A}^i$ are M-matrices, it follows that:

  $$\vartheta_h^- \geq \vartheta_h^+ \quad \text{and} \quad \vartheta_h^+ \geq \vartheta_h^-,$$

  which implies:

  $$\vartheta_h^- = \vartheta_h^+.$$

  Therefore, the discrete system (2.8) admits a unique solution.

The sequence of upper approximations :

We now turn to the analysis of the sequence of upper solutions $(\hat{\vartheta}_h^k)$. The objective of this stage is to prove that the sequence decreases monotonically with the iteration index while remaining a valid supersolution. In particular, we show that each update preserves the inequality

$$\hat{\vartheta}_h^{k+1} \leq \hat{\vartheta}_h^k,$$

so that the sequence is non-increasing and bounded from below by the discrete solution.

- **Step 1: Monotonicity of the sequence**
  We aim to prove that the sequence $\left(\hat{\vartheta}_h^k\right)_{k\geq 0}$ is non-increasing. The proof is carried out by induction on the index k.

❖ **Base case:** For the initial step ($k = 0$), the monotonicity is established in both subdomains separately.

1. **First subdomain.** The discrete problem in the first region reads:

$$\max_{1\le i\le n}\left\{\mathscr{A}^i_{1,1}\hat{\vartheta}^1_{1h}-\tilde{\mathscr{A}}^i_{1,2}\hat{\vartheta}^0_{2h}-\mathscr{F}^i_1\right\}=0.$$

Since $\hat{\vartheta}^0_h$ is assumed to be a supersolution, it satisfies:

$$\max_{1\le i\le n}\left\{\mathscr{A}^i_{1,1}\hat{\vartheta}^0_{1h}-\tilde{\mathscr{A}}^i_{1,2}\hat{\vartheta}^0_{2h}-\mathscr{F}^i_1\right\}\ge 0.$$

Comparing both relations, we deduce:

$$\max_{1\le i\le n}\left\{\mathscr{A}^i_{1,1}\hat{\vartheta}^0_{1h}-\tilde{\mathscr{A}}^i_{1,2}\hat{\vartheta}^0_{2h}-\mathscr{F}^i_1\right\}\ge\max_{1\le i\le n}\left\{\mathscr{A}^i_{1,1}\hat{\vartheta}^1_{1h}-\tilde{\mathscr{A}}^i_{1,2}\hat{\vartheta}^0_{2h}-\mathscr{F}^i_1\right\}.$$

Therefore, the inequality:

$$\hat{\vartheta}^0_{1h}\ge\hat{\vartheta}^1_{1h}$$

holds true.

2. **Second subdomain.** The discrete problem in the second region is given by:

$$\max_{1\le i\le n}\left\{-\tilde{\mathscr{A}}^i_{2,1}\hat{\vartheta}^1_{1h}+\mathscr{A}^i_{2,2}\hat{\vartheta}^1_{2h}-\mathscr{F}^i_2\right\}=0. \tag{2.26}$$

On the other hand, since $\hat{\vartheta}^0_h$ is a supersolution, one has:

$$\max_{1\le i\le n}\left\{-\tilde{\mathscr{A}}^i_{2,1}\hat{\vartheta}^0_{1h}+\mathscr{A}^i_{2,2}\hat{\vartheta}^0_{2h}-\mathscr{F}^i_2\right\}\ge 0. \tag{2.27}$$

Using the inequality $\hat{\vartheta}^0_{1h}\ge\hat{\vartheta}^1_{1h}$, it follows that:

$$\max_{1\le i\le n}\left\{-\tilde{\mathscr{A}}^i_{2,1}\hat{\vartheta}^0_{1h}+\mathscr{A}^i_{2,2}\hat{\vartheta}^1_{2h}-\mathscr{F}^i_2\right\}\le\max_{1\le i\le n}\left\{-\tilde{\mathscr{A}}^i_{2,1}\hat{\vartheta}^1_{1h}+\mathscr{A}^i_{2,2}\hat{\vartheta}^1_{2h}-\mathscr{F}^i_2\right\}. \tag{2.28}$$

By combining (2.26) and (2.27), we get:

$$\max_{1\le i\le n}\left\{-\tilde{\mathscr{A}}^i_{2,1}\hat{\vartheta}^1_{1h}+\mathscr{A}^i_{2,2}\hat{\vartheta}^1_{2h}-\mathscr{F}^i_2\right\}\le\max_{1\le i\le n}\left\{-\tilde{\mathscr{A}}^i_{2,1}\hat{\vartheta}^0_{1h}+\mathscr{A}^i_{2,2}\hat{\vartheta}^0_{2h}-\mathscr{F}^i_2\right\}.$$

Finally, together with (2.28), we conclude that:

$$\hat{\vartheta}^0_{2h}\ge\hat{\vartheta}^1_{2h}.$$

3. **Combined conclusion.** By combining the inequalities obtained in the first and second subdomains, we conclude that:

$$\hat{\vartheta}^0_h\ge\hat{\vartheta}^1_h.$$

Hence, the first iterate $\hat{\vartheta}^1_h$ is still a supersolution, which confirms that the sequence is non-increasing at the initial step.

❖ **Inductive step.** Assume by induction that the inequality

$$\hat{\vartheta}^{k-1}_h\ge\hat{\vartheta}^k_h$$

holds, and that $\hat{\vartheta}^k_h$ satisfies the supersolution conditions. Our goal is now to establish that:

* the monotonicity is preserved, i.e. $\hat{\vartheta}_h^k \geq \hat{\vartheta}_h^{k+1}$,
* and that the iterate $\hat{\vartheta}_h^{k+1}$ remains a supersolution.

1. **Analysis in the first subdomain.** In this region, the problem is written as:

$$\max_{1\leq i\leq n}\left\{\mathscr{A}_{1,1}^i\hat{\vartheta}_{1h}^{k+1} - \tilde{\mathscr{A}}_{1,2}^i\hat{\vartheta}_{2h}^k - \mathscr{F}_1^i\right\} = 0.$$

Since $\hat{\vartheta}_h^k$ is a supersolution, we also have:

$$\max_{1\leq i\leq n}\left\{\mathscr{A}_{1,1}^i\hat{\vartheta}_{1h}^{k} - \tilde{\mathscr{A}}_{1,2}^i\hat{\vartheta}_{2h}^k - \mathscr{F}_1^i\right\} \geq 0.$$

By comparing the two relations, it follows that:

$$\hat{\vartheta}_{1h}^k \geq \hat{\vartheta}_{1h}^{k+1}.$$

2. **Analysis in the second subdomain.** Here, the corresponding formulation is:

$$\max_{1\leq i\leq n}\left\{-\tilde{\mathscr{A}}_{2,1}^i\hat{\vartheta}_{1h}^{k+1} + \mathscr{A}_{2,2}^i\hat{\vartheta}_{2h}^{k+1} - \mathscr{F}_2^i\right\} = 0. \tag{2.29}$$

From the induction hypothesis that $\hat{\vartheta}_h^k$ is a supersolution, we know:

$$\max_{1\leq i\leq n}\left\{-\tilde{\mathscr{A}}_{2,1}^i\hat{\vartheta}_{1h}^{k} + \mathscr{A}_{2,2}^i\hat{\vartheta}_{2h}^{k} - \mathscr{F}_2^i\right\} \geq 0. \tag{2.30}$$

Since we already established $\hat{\vartheta}_{1h}^k \geq \hat{\vartheta}_{1h}^{k+1}$, we deduce:

$$\max_{1\leq i\leq n}\left\{-\tilde{\mathscr{A}}_{2,1}^i\hat{\vartheta}_{1h}^{k} + \mathscr{A}_{2,2}^i\hat{\vartheta}_{2h}^{k+1} - \mathscr{F}_2^i\right\} \leq \max_{1\leq i\leq n}\left\{-\tilde{\mathscr{A}}_{2,1}^i\hat{\vartheta}_{1h}^{k+1} + \mathscr{A}_{2,2}^i\hat{\vartheta}_{2h}^{k+1} - \mathscr{F}_2^i\right\}. \tag{2.31}$$

Moreover, combining (2.29) and (2.30) gives:

$$\max_{1\leq i\leq n}\left\{-\tilde{\mathscr{A}}_{2,1}^i\hat{\vartheta}_{1h}^{k+1} + \mathscr{A}_{2,2}^i\hat{\vartheta}_{2h}^{k+1} - \mathscr{F}_2^i\right\} \leq \max_{1\leq i\leq n}\left\{-\tilde{\mathscr{A}}_{2,1}^i\hat{\vartheta}_{1h}^{k} + \mathscr{A}_{2,2}^i\hat{\vartheta}_{2h}^{k} - \mathscr{F}_2^i\right\}. \tag{2.32}$$

From (2.31) and (2.32), we finally deduce:

$$\hat{\vartheta}_{2h}^k \geq \hat{\vartheta}_{2h}^{k+1}.$$

3. **Combined conclusion.** By combining the inequalities obtained in the first and second subdomains for k, we conclude that:

$$\hat{\vartheta}_h^k \geq \hat{\vartheta}_h^{k+1}.$$

Consequently, $\hat{\vartheta}_h^{k+1}$ preserves the supersolution property. Iterating this argument shows that:

$$\hat{\vartheta}_h^0 \geq \hat{\vartheta}_h^1 \geq \cdots \geq \hat{\vartheta}_h^k \geq \hat{\vartheta}_h^{k+1}$$

which proves the monotonicity of the whole sequence.

- **Step 2: Convergence and lower bound of the sequence**
We now show that the sequence $(\hat{\vartheta}_h^k)$ is bounded from below and convergent to a limit $\hat{\vartheta}_h^*$.

Since $\hat{\vartheta}_h^k$ is a supersolution, we have for all $1 \le i \le n$:

$$\max_{1\le i\le n}\left\{\mathscr{A}^i\hat{\vartheta}_h^k - \mathscr{F}^i\right\} \ge 0 \implies \mathscr{A}^i\hat{\vartheta}_h^k - \mathscr{F}^i \ge 0. \tag{2.33}$$

Assume that there exists $\hat{\vartheta}_h^*$ satisfying:

$$\mathscr{A}^i\hat{\vartheta}_h^* - \mathscr{F}^i = 0. \tag{2.34}$$

Combining (2.33) and (2.34), we obtain:

$$\mathscr{A}^i(\hat{\vartheta}_h^k - \hat{\vartheta}_h^*) \ge 0.$$

Since each matrix $\mathscr{A}^{\mathrm{i}}$ is an M-matrix, it follows that:

$$\hat{\vartheta}_h^k \ge \hat{\vartheta}_h^*.$$

This shows that the sequence $(\hat{\vartheta}_h^k)$ has a lower bound, namely $\hat{\vartheta}_h^*$. Because the sequence is monotonically decreasing and bounded from below, it must converge. In particular, we have:

$$\lim_{k\to\infty}\hat{\vartheta}_h^k = \hat{\vartheta}_h^*.$$

Adjacency between the sequences $(\hat{\vartheta}_{\mathfrak{h}}^k)$ and $(\check{\vartheta}_{\mathfrak{h}}^k)$:

We aim to show that the sequences $(\hat{\vartheta}_h^k)$ and $(\check{\vartheta}_h^k)$ are adjacent on each subdomain. Specifically, we will demonstrate that:

$$\check{\vartheta}_h^k \le \hat{\vartheta}_h^k, \quad k \in \mathbb{N}.$$

❖ **Base case:** At the initial iteration ($k = 0$), assume that $\check{\vartheta}_h^0 \le \hat{\vartheta}_h^0$.

1. **Analysis in the first subdomain.** In the first region, the sequence $\check{\vartheta}_h^1$ is a subsolution, satisfying:

$$\max_{1\le i\le n}\left\{\mathscr{A}_{1,1}^i\check{\vartheta}_{1h}^1 - \tilde{\mathscr{A}}_{1,2}^i\check{\vartheta}_{2h}^0 - \mathscr{F}_1^i\right\} \le 0. \tag{2.35}$$

   Meanwhile, $\hat{\vartheta}_h^1$ being a supersolution implies:

$$\max_{1\le i\le n}\left\{\mathscr{A}_{1,1}^i\hat{\vartheta}_{1h}^1 - \tilde{\mathscr{A}}_{1,2}^i\hat{\vartheta}_{2h}^0 - \mathscr{F}_1^i\right\} \ge 0. \tag{2.36}$$

   By comparing (2.35) and (2.36), we immediately deduce:

$$\max_{1\le i\le n}\left\{\mathscr{A}_{1,1}^i\check{\vartheta}_{1h}^1 - \tilde{\mathscr{A}}_{1,2}^i\check{\vartheta}_{2h}^0 - \mathscr{F}_1^i\right\} \le \max_{1\le i\le n}\left\{\mathscr{A}_{1,1}^i\hat{\vartheta}_{1h}^1 - \tilde{\mathscr{A}}_{1,2}^i\hat{\vartheta}_{2h}^0 - \mathscr{F}_1^i\right\}.$$

   Therefore, $\check{\vartheta}_{2h}^0 \le \hat{\vartheta}_{2h}^0$, and we deduce:

$$\check{\vartheta}_{1h}^1 \le \hat{\vartheta}_{1h}^1.$$

2. **Analysis in the second subdomain.** In the second region, the sequences satisfy:

$$\max_{1\le i\le n}\left\{-\tilde{\mathscr{A}}_{2,1}^i\check{\vartheta}_{1h}^1 + \mathscr{A}_{2,2}^i\check{\vartheta}_{2h}^1 - \mathscr{F}_2^i\right\} \le 0, \tag{2.37}$$

   and

$$\max_{1\le i\le n}\left\{-\tilde{\mathscr{A}}_{2,1}^i\hat{\vartheta}_{1h}^1 + \mathscr{A}_{2,2}^i\hat{\vartheta}_{2h}^1 - \mathscr{F}_2^i\right\} \ge 0. \tag{2.38}$$

Comparing (2.37) and (2.38) gives:

$$\max_{1\leq i\leq n}\left\{-\tilde{\mathscr{A}}^i_{2,1}\check{\vartheta}^1_{1h}+\mathscr{A}^i_{2,2}\check{\vartheta}^1_{2h}-\mathscr{F}^i_2\right\}\leq\max_{1\leq i\leq n}\left\{-\tilde{\mathscr{A}}^i_{2,1}\hat{\vartheta}^1_{1h}+\mathscr{A}^i_{2,2}\hat{\vartheta}^1_{2h}-\mathscr{F}^i_2\right\}.$$

Using the result from the first subdomain ($\check{\vartheta}^1_{1h}\leq\hat{\vartheta}^1_{1h}$), we conclude:

$$\check{\vartheta}^1_{2h}\leq\hat{\vartheta}^1_{2h}.$$

3. **Combined conclusion.** By combining the inequalities obtained in the first and second subdomains, we finally obtain:

$$\check{\vartheta}^1_h\leq\hat{\vartheta}^1_h.$$

This confirms that the inequality is preserved at the first iteration across the whole domain.

❖ **Inductive step:** Assume by induction that the inequality:

$$\check{\vartheta}^k_h\leq\hat{\vartheta}^k_h$$

holds for a given iteration k. We aim to prove that it also holds at the next iteration, i.e.,

$$\check{\vartheta}^{k+1}_h\leq\hat{\vartheta}^{k+1}_h.$$

1. **Analysis in the first subdomain.** In the first subdomain, $\check{\vartheta}^{k+1}_h$ satisfies the subsolution condition:

$$\max_{1\leq i\leq n}\left\{\mathscr{A}^i_{1,1}\check{\vartheta}^{k+1}_{1h}-\tilde{\mathscr{A}}^i_{1,2}\check{\vartheta}^k_{2h}-\mathscr{F}^i_1\right\}\leq 0.$$

Simultaneously, $\hat{\vartheta}^{k+1}_h$ is a supersolution, so we have:

$$\max_{1\leq i\leq n}\left\{\mathscr{A}^i_{1,1}\hat{\vartheta}^{k+1}_{1h}-\tilde{\mathscr{A}}^i_{1,2}\hat{\vartheta}^k_{2h}-\mathscr{F}^i_1\right\}\geq 0.$$

By directly comparing the above relations, we obtain:

$$\max_{1\leq i\leq n}\left\{\mathscr{A}^i_{1,1}\check{\vartheta}^{k+1}_{1h}-\tilde{\mathscr{A}}^i_{1,2}\check{\vartheta}^k_{2h}-\mathscr{F}^i_1\right\}\leq\max_{1\leq i\leq n}\left\{\mathscr{A}^i_{1,1}\hat{\vartheta}^{k+1}_{1h}-\tilde{\mathscr{A}}^i_{1,2}\hat{\vartheta}^k_{2h}-\mathscr{F}^i_1\right\}.$$

Because we assumed $\check{\vartheta}^k_{2h}\leq\hat{\vartheta}^k_{2h}$, it follows that:

$$\check{\vartheta}^{k+1}_{1h}\leq\hat{\vartheta}^{k+1}_{1h}.$$

2. **Analysis in the second subdomain.** In the second subdomain, the corresponding problem reads:

$$\max_{1\leq i\leq n}\left\{-\tilde{\mathscr{A}}^i_{2,1}\check{\vartheta}^{k+1}_{1h}+\mathscr{A}^i_{2,2}\check{\vartheta}^{k+1}_{2h}-\mathscr{F}^i_2\right\}\leq\max_{1\leq i\leq n}\left\{-\tilde{\mathscr{A}}^i_{2,1}\hat{\vartheta}^{k+1}_{1h}+\mathscr{A}^i_{2,2}\hat{\vartheta}^{k+1}_{2h}-\mathscr{F}^i_2\right\}.$$

Using the result from the first subdomain, $\check{\vartheta}^{k+1}_{1h}\leq\hat{\vartheta}^{k+1}_{1h}$, we immediately deduce that:

$$\check{\vartheta}^{k+1}_{2h}\leq\hat{\vartheta}^{k+1}_{2h}.$$

3. **Combined conclusion.** By combining the inequalities obtained in the first and second subdomains for k, we have:

$$\check{\vartheta}^{k+1}_h\leq\hat{\vartheta}^{k+1}_h.$$

Both sequences, $(\check{\vartheta}^k_h)$ and $(\hat{\vartheta}^k_h)$, are monotone—one increasing and the other decreasing—while remaining confined within their respective bounds. Since the sequences are adjacent, their limits coincide, ensuring convergence to the same discrete solution. Therefore, the iterative process produces:

$$\lim_{k\to\infty}\hat{\vartheta}^k_h=\lim_{k\to\infty}\check{\vartheta}^k_h=\vartheta_h,$$

which represents the unique solution of the discrete problem (2.8).

2.2.6 Geometric convergence of lower and upper iterates

In this subsection, we establish the geometric convergence of the lower and upper sequences generated by the iterative algorithm. We show that the lower iterates form a non-decreasing sequence, while the upper iterates form a non-increasing one, and both converge geometrically to the unique solution of the discrete system.

Theorem 2.2.2

Let ϑ_h^0 be an arbitrary initial guess. Then, the sequence (ϑ_h^k) produced by the iterative scheme defined in algorithme 1 converges geometrically to the unique solution of the discrete system (2.8). More precisely, there exists a constant $0 < \rho < 1$ such that:

$$\|\vartheta_h^{k+1} - \vartheta_h^k\|_{L^\infty(\Omega)} \leq \rho^k \|\vartheta^1 - \vartheta^0\|_{L^\infty(\Omega)}, \quad \forall k \in \mathbb{N}.$$

Proof

We now present the proof of convergence by decomposing the argument into three main stages.

- **Step 1: Analysis in the first subdomain.**

  Let us start from the discrete formulation restricted to the first subdomain. At two successive iterations, the scheme satisfies:

$$\max_{1\leq i\leq n} \left\{ \mathscr{A}_{1,1}^i \vartheta_{1h}^{k+1} - \tilde{\mathscr{A}}_{1,2}^i \vartheta_{2h}^k - \mathscr{F}_1^i \right\} = 0,$$

  and

$$\max_{1\leq i\leq n} \left\{ \mathscr{A}_{1,1}^i \vartheta_{1h}^{k} - \tilde{\mathscr{A}}_{1,2}^i \vartheta_{2h}^{k-1} - \mathscr{F}_1^i \right\} = 0.$$

  This corresponds to solving the problems:

$$\begin{cases} \max\limits_{1\leq i\leq n} \left(\mathscr{A}_{1,1}^i \vartheta_{1h}^{k+1} - \mathscr{F}_1^i \right) = 0, & \text{in } \Omega_1, \\ \left(\vartheta_{1h}^{k+1}\right)_\beta = \left(\vartheta_{2h}^{k}\right)_\beta, & \text{on } \Sigma_1, \end{cases}$$

  and

$$\begin{cases} \max\limits_{1\leq i\leq n} \left(\mathscr{A}_{1,1}^i \vartheta_{1h}^{k} - \mathscr{F}_1^i \right) = 0, & \text{in } \Omega_1, \\ \left(\vartheta_{1h}^{k}\right)_\beta = \left(\vartheta_{2h}^{k-1}\right)_\beta, & \text{on } \Sigma_1. \end{cases}$$

  By comparing the boundary conditions of these two problems and adapting the results of [38] to the HJB setting, one obtains the existence of a contraction factor $\omega_1 \in (0, 1)$ such that:

$$\omega_1 = \sup\{v(x) : x \in \Sigma_1\}.$$

  This leads to the conclusion that:

$$\|\vartheta_{1h}^{k+1} - \vartheta_{1h}^k\|_{L^\infty(\Sigma_1)} \leq \omega_1 \|\vartheta_{2h}^k - \vartheta_{2h}^{k-1}\|_{L^\infty(\Omega_2)}.$$

- **Step 2: Analysis in the second subdomain**

  We now turn to the second part of the coupled system, where the scheme reads:

$$\max_{1\leq i\leq n} \left\{ -\tilde{\mathscr{A}}_{2,1}^i \vartheta_{1h}^{k+1} + \mathscr{A}_{2,2}^i \vartheta_{2h}^{k+1} - \mathscr{F}_2^i \right\} = 0,$$

and

$$\max_{1\leq i\leq n}\left\{-\tilde{\mathscr{A}}_{2,1}^{i}\vartheta_{1h}^{k}+\mathscr{A}_{2,2}^{i}\vartheta_{2h}^{k}-\mathscr{F}_{2}^{i}\right\}=0.$$

This is equivalent to solving:

$$\begin{cases}\max\limits_{1\leq i\leq n}\left(\mathscr{A}_{2,2}^{i}\vartheta_{2h}^{k+1}-\mathscr{F}_{2}^{i}\right)=0, & \text{in } \Omega_2,\\ \left(\vartheta_{2h}^{k+1}\right)_{\alpha}=\left(\vartheta_{1h}^{k+1}\right)_{\alpha}, & \text{on } \Sigma_2,\end{cases}$$

and

$$\begin{cases}\max\limits_{1\leq i\leq n}\left(\mathscr{A}_{2,2}^{i}\vartheta_{2h}^{k}-\mathscr{F}_{2}^{i}\right)=0, & \text{in } \Omega_2,\\ \left(\vartheta_{2h}^{k}\right)_{\alpha}=\left(\vartheta_{1h}^{k}\right)_{\alpha}, & \text{on } \Sigma_2.\end{cases}$$

Adapting again the methodology of [38], we deduce the existence of another contraction factor $\omega_2\in(0,1)$ such that:

$$\omega_2=\sup\{v(x): x\in\Sigma_2\}.$$

This implies the following relationship:

$$\|\vartheta_{2h}^{k+1}-\vartheta_{2h}^{k}\|_{L^\infty(\Sigma_2)}\leq\omega_2\|\vartheta_{1h}^{k+1}-\vartheta_{1h}^{k}\|_{L^\infty(\Omega_1)}.$$

- **Step 3: Global contraction and convergence** By combining the two inequalities derived in the previous steps and applying the discrete maximum principle, we obtain:

$$\|\vartheta_{h}^{k+1}-\vartheta_{h}^{k}\|_{L^\infty(\Omega)}\leq\omega_1\omega_2\|\vartheta_{h}^{k}-\vartheta_{h}^{k-1}\|_{L^\infty(\Omega)}.$$

Letting $\rho=\omega_1\omega_2\in(0,1)$, induction yields:

$$\|\vartheta_{h}^{k+1}-\vartheta_{h}^{k}\|_{L^\infty(\Omega)}\leq\rho^k\|\vartheta_{h}^{1}-\vartheta_{h}^{0}\|_{L^\infty(\Omega)},\quad k\in\mathbb{N}.$$

which proves the geometric convergence of the sequence (ϑ_h^k) to the unique solution of system (2.8).

Remark 2.2.1

The factor ρ represents the global contraction coefficient of the Schwarz iteration. Since $0<\rho<1$, the associated iteration mapping satisfies the assumptions of the Banach fixed-point theorem. Consequently, the existence and uniqueness of the fixed point, and hence of the discrete solution of (2.8), follow immediately. Moreover, the geometric decay induced by ρ provides a powerful tool for the quantitative analysis of the method. In particular, it will be used in the sequel to derive $L^\infty(\Omega)$-error estimates and to establish rigorous convergence bounds for the numerical approximation.

2.3 Numerical study of the coercive HJB problem

In this section, we perform a numerical investigation to validate the theoretical results and examine the performance of the proposed method. The problem is discretized using two-dimensional finite elements on a uniform mesh and solved using a domain decomposition approach with overlapping subdomains. The overlap is incorporated to improve convergence of the iterative scheme.

2.3.1 Example setup and problem formulation

We consider the domain

$$\Omega = [0,1] \times [0,1],$$

discretized with uniform finite elements of size h. The stopping criterion of the iterative procedure is set as $\varepsilon = 10^{-6}$. The continuous problem is defined by [40]:

$$\begin{cases} \max\limits_{1\leq i\leq 2} \left\{\mathbb{A}^i\vartheta - \mathbb{F}^i\right\} = 0, & \text{in } \Omega, \\ \vartheta = 0, & \text{on } \partial\Omega. \end{cases}$$

The operators $\mathbb{A}^i$ are:

$$\mathbb{A}^1 = -\left(\frac{\partial^2}{\partial x^2} + \frac{\partial^2}{\partial y^2} + \frac{1}{2}\frac{\partial^2}{\partial y \partial x}\right), \quad \mathbb{A}^2 = -\left(\frac{1}{2}\frac{\partial^2}{\partial x^2} + \frac{\partial^2}{\partial y^2} + \frac{1}{10}\frac{\partial^2}{\partial y \partial x}\right).$$

The exact solution is :

$$\vartheta^*(x,y) = xy(1-x)(1-y),$$

and the source terms $\mathbb{F}^i$ are :

$$\mathbb{F}^1 = \mathbb{F}^2 = \max(\mathbb{A}^1\vartheta^*, \mathbb{A}^2\vartheta^*).$$

The variational form is obtained by multiplying each equation with a test function $u \in H_0^1(\Omega)$ and integrating over Ω:

$$\int\int_\Omega \mathbb{A}^1\vartheta\, u\, dx\, dy = \int\int_\Omega \Big(-\frac{\partial^2\vartheta}{\partial x^2} - \frac{\partial^2\vartheta}{\partial y^2} - \frac{1}{2}\frac{\partial^2\vartheta}{\partial y\partial x}\Big) u\, dx\, dy,$$

$$\int\int_\Omega \mathbb{A}^2\vartheta\, u\, dx\, dy = \int\int_\Omega \Big(-\frac{1}{2}\frac{\partial^2\vartheta}{\partial x^2} - \frac{\partial^2\vartheta}{\partial y^2} - \frac{1}{10}\frac{\partial^2\vartheta}{\partial y\partial x}\Big) u\, dx\, dy.$$

After integration by parts, the corresponding bilinear forms are:

$$a^1\langle\vartheta, u\rangle = \int\int_\Omega \Big(\frac{\partial\vartheta}{\partial x}\frac{\partial u}{\partial x} + \frac{\partial\vartheta}{\partial y}\frac{\partial u}{\partial y} + \frac{1}{2}\frac{\partial\vartheta}{\partial y}\frac{\partial u}{\partial x}\Big) dx\, dy,$$

$$a^2\langle\vartheta, u\rangle = \int\int_\Omega \Big(\frac{1}{2}\frac{\partial\vartheta}{\partial x}\frac{\partial u}{\partial x} + \frac{\partial\vartheta}{\partial y}\frac{\partial u}{\partial y} + \frac{1}{10}\frac{\partial\vartheta}{\partial y}\frac{\partial u}{\partial x}\Big) dx\, dy.$$

The linear functionals corresponding to the source terms are:

$$\langle\mathbb{F}^1, u\rangle = \int\int_\Omega \mathbb{F}^1(x,y)\, u(x,y)\, dx\, dy, \quad \langle\mathbb{F}^2, u\rangle = \int\int_\Omega \mathbb{F}^2(x,y)\, u(x,y)\, dx\, dy.$$

These bilinear and linear forms are used in the finite element method to compute the discrete approximation ϑ_h of the solution to problem (2.8).

2.3.2 Finite element discretization of the HJB problem

Finite element space

We consider the finite element space P_1 consisting of linear polynomials:

$$P_1 = \{p; p(x,y) = a + bx + cy\}.$$

Let τ^h be a regular quasi-uniform triangulation of Ω:

$$\Omega = \bigcup_{K \in \tau^h} K.$$

The associated finite element space is defined by:

$$V_h = \left\{u \in C(\Omega) \cap H_0^1(\Omega) \mid u_{|K} \in P_1,\ \forall K \in \tau^h\right\}.$$

Each function u is continuous over Ω and linear on each triangle K.

Vertices and basis functions

Let A_s, for $s = 1, \ldots, N$, denote the interior vertices of τ^h. The standard nodal basis functions φ_z are defined by:

$$\varphi_z(x,y) \in P_1(K) \quad \forall K, \quad \varphi_z(A_s) = \begin{cases} 1, & \text{if } z = s, \\ 0, & \text{if } z \neq s. \end{cases}$$

Discrete variational formulation

The variational problem in V_h leads to the linear system:

$$\mathscr{A}^i \vartheta_h = \mathscr{F}^i, \quad i = 1, \ldots, n,$$

where $\mathscr{A}^i$ is the stiffness matrix and $\mathscr{F}^i$ is the load vector:

$$\mathscr{A}^i_{zs} = a^i\langle \varphi_z, \varphi_s\rangle, \quad \mathscr{F}^i_z = \langle \mathscr{F}^i, \varphi_z\rangle, \quad 1 \leq z, s \leq N, \quad 1 \leq i \leq n.$$

Explicit form of the matrices

For the example problem, the entries are:

$$\mathscr{A}^1_{zs} = \int\int_\Omega \left(\frac{\partial \varphi_z}{\partial x}\frac{\partial \varphi_s}{\partial x} + \frac{\partial \varphi_z}{\partial y}\frac{\partial \varphi_s}{\partial y} + \frac{1}{2}\frac{\partial \varphi_z}{\partial y}\frac{\partial \varphi_s}{\partial x} \right) dx\, dy,$$

$$\mathscr{A}^2_{zs} = \int\int_\Omega \left(\frac{1}{2}\frac{\partial \varphi_z}{\partial x}\frac{\partial \varphi_s}{\partial x} + \frac{\partial \varphi_z}{\partial y}\frac{\partial \varphi_s}{\partial y} + \frac{1}{10}\frac{\partial \varphi_z}{\partial y}\frac{\partial \varphi_s}{\partial x} \right) dx\, dy.$$

The right-hand side is:

$$\mathscr{F}^1_z = \langle \mathscr{F}^1, \varphi_z\rangle = \int\int_\Omega \mathscr{F}^1 \varphi_z\, dx\, dy, \quad \mathscr{F}^2_z = \langle \mathscr{F}^2, \varphi_z\rangle = \int\int_\Omega \mathscr{F}^2 \varphi_z\, dx\, dy,$$

$$z, s = \overline{1, N}, \quad i = \overline{1, n}.$$

Triangular mesh and node coordinates

To simplify the problem, let us assume that $\Omega =]0,1[\times]0,1[$ and consider the triangulation of Ω illustrated in Fig (2.2) , which is divided using a uniform triangular mesh.

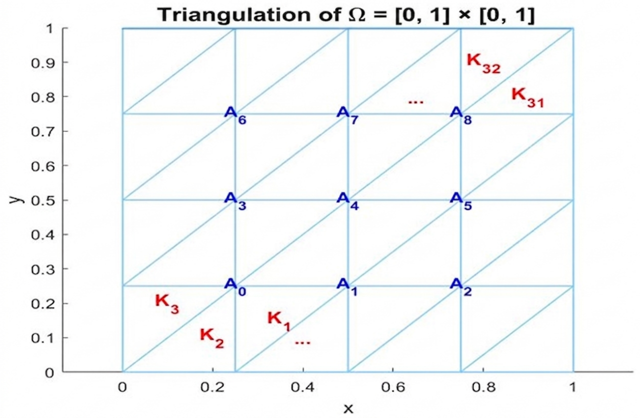

Figure 2.2: **Uniform triangular mesh of a square domain.**

The step size between adjacent points is denoted by h, with the basis function φ_z associated with the interior node. The grid steps in the x and y directions are equal, given by:

$$0 = x_1 < x_2 < \cdots < x_z < x_{z+1} < \cdots < x_N = 1.$$

$$0 = y_1 < y_2 < \cdots < y_s < y_{s+1} < \cdots < y_N = 1.$$

$$x_z = zh_x, \quad y_s = sh_y, \quad h_x = h_y = h = \frac{1}{N+1}, \quad z, s = \overline{1, N},$$

where x_z and y_s represent the coordinates of each node in the mesh, and z and s are the indices of the nodes in the x and y directions, respectively.

Support of basis functions

Consider node A_0 with coordinates $(\mathrm{x}_0, \mathrm{y}_0)$. The neighboring nodes A_1, A_2, A_4, A_5 are positioned in cardinal directions around A_0 where $K_1, K_2, \ldots, K_6$ represent the triangles surrounding the node (x_0, y_0) (see Fig (2.3)). These nodes are interconnected to form the grid structure. The basis function $\varphi_0(x, y)$ is associated with node A_0.

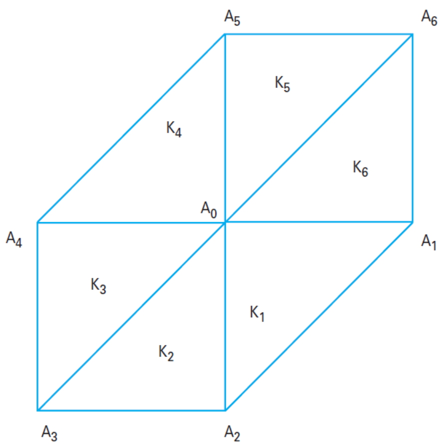

Figure 2.3: **Triangles surrounding node** $(\mathrm{x}_0, \mathrm{y}_0)$**.**

The piecewise linear basis function φ_0 associated with A_0 has support :

$$\operatorname{supp}(\varphi_0) = \bigcup_{z=1}^{6} K_z.$$

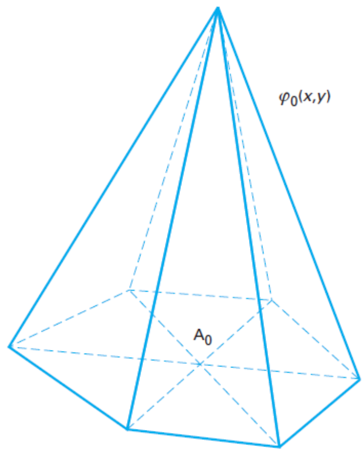

Figure 2.4: **Support of a basis function P_1.**

The intersection of the supports of φ_z and φ_s (see Fig.(2.4)) is often empty, making $\mathscr{A}^i$ a sparse matrix (most of its coefficients are zero), such that:

$$\mathscr{A}^i_{zs} = \begin{cases} a^i\langle\varphi_z, \varphi_s\rangle & \text{if } \operatorname{supp}(\varphi_z) \cap \operatorname{supp}(\varphi_s) \neq \emptyset, \\ 0, & \text{otherwise.} \end{cases}$$

Piecewise definition and gradients

For each triangle K_z,

$$\varphi_0|_{K_z} = a_z x + b_z y + c_z, \quad \varphi_z(A_s) = \delta_{z,s}.$$

The basis function $\varphi_0(x, y)$ is defined piecewise over the triangular elements surrounding the node (x_0, y_0) as follows:

$$\varphi_0(x,y) = \begin{cases} 1 + \dfrac{x_0 - x}{h} + \dfrac{y - y_0}{h}, & \text{if } (x,y) \in K_1, \\ \dfrac{y - y_0}{h}, & \text{if } (x,y) \in K_2, \\ \dfrac{x - x_0}{h}, & \text{if } (x,y) \in K_3, \\ 1 + \dfrac{x - x_0}{h} + \dfrac{y_0 - y}{h}, & \text{if } (x,y) \in K_4, \\ \dfrac{y_0 - y}{h} + 2, & \text{if } (x,y) \in K_5, \\ \dfrac{x_0 - x}{h} + 2, & \text{if } (x,y) \in K_6, \\ 0, & \text{otherwise.} \end{cases}$$

The partial derivatives of φ_0 are:

$$\frac{\partial\varphi_0}{\partial x}=\begin{cases}-\dfrac{1}{h}, & (x,y)\in K_1,\\ 0, & (x,y)\in K_2,\\ \dfrac{1}{h}, & (x,y)\in K_3,\\ \dfrac{1}{h}, & (x,y)\in K_4,\\ 0, & (x,y)\in K_5,\\ -\dfrac{1}{h}, & (x,y)\in K_6,\\ 0, & \text{otherwise,}\end{cases}\qquad \frac{\partial\varphi_0}{\partial y}=\begin{cases}\dfrac{1}{h}, & (x,y)\in K_1,\\ \dfrac{1}{h}, & (x,y)\in K_2,\\ 0, & (x,y)\in K_3,\\ -\dfrac{1}{h}, & (x,y)\in K_4,\\ -\dfrac{1}{h}, & (x,y)\in K_5,\\ 0, & (x,y)\in K_6,\\ 0, & \text{otherwise.}\end{cases}$$

Similarly, the gradients of other basis functions are:

$$\nabla\varphi_1|_{K_1}=\left(\frac{1}{h},0\right),\quad \nabla\varphi_1|_{K_6}=\left(\frac{1}{h},-\frac{1}{h}\right),$$

$$\nabla\varphi_3|_{K_4}=\left(0,\frac{1}{h}\right),\quad \nabla\varphi_3|_{K_5}=\left(-\frac{1}{h},\frac{1}{h}\right),$$

$$\nabla\varphi_4|_{K_5}=\left(\frac{1}{h},0\right),\quad \nabla\varphi_4|_{K_6}=\left(0,\frac{1}{h}\right).$$

2.3.3 Computation of the stiffness matrix using the finite element method

In this section, we present the step-by-step computation of the stiffness matrix coefficients $\mathscr{A}^1$ using the finite element method. Each entry is computed by evaluating the relevant double integrals over the domain, taking into account the support of each basis function.

Computation of the stiffness matrix $\mathscr{A}^1$:

We denote by $a^1\langle\varphi_z,\varphi_s\rangle$ the (z,s)-th entry of the stiffness matrix $\mathscr{A}^1$. The computation involves checking the intersection of supports:

$$\operatorname{supp}(\varphi_z)\cap\operatorname{supp}(\varphi_s)\neq\emptyset$$

and evaluating the integrals over the triangles where this intersection is non-empty.

1. Diagonal term: The diagonal entry $\mathfrak{a}^1\langle\varphi_0,\varphi_0\rangle$, corresponding to the basis function φ_0, is given by:

$$a^1\langle\varphi_0,\varphi_0\rangle=\iint_\Omega\left(|\nabla\varphi_0|^2+\frac{1}{2}\frac{\partial\varphi_0}{\partial y}\frac{\partial\varphi_0}{\partial x}\right)dx\,dy=\sum_{z=1}^{6}\iint_{K_z}\left(|\nabla\varphi_0|^2+\frac{1}{2}\frac{\partial\varphi_0}{\partial y}\frac{\partial\varphi_0}{\partial x}\right)dx\,dy.$$

Each triangle contributes because φ_0 is supported over all six triangles. Since the gradient of φ_0 is constant on each triangle and the area of each triangle is $\text{area}(K_z)=\frac{h^2}{2}$, we obtain:

$$a^1\langle\varphi_0,\varphi_0\rangle=\sum_{z=1}^{6}\left(|\nabla\varphi_0|^2_{K_z}\ \text{area}(K_z)+\iint_{K_z}\frac{1}{2}\frac{\partial\varphi_0}{\partial y}\frac{\partial\varphi_0}{\partial x}\,dx\,dy\right).$$

Substituting the corresponding gradient values on each triangle yields:

$$a^1\langle\varphi_0,\varphi_0\rangle=\left[\frac{2}{h^2}+\frac{2}{h^2}+\frac{1}{h^2}+\frac{1}{h^2}+\frac{1}{h^2}+\frac{1}{h^2}\right]\frac{h^2}{2}-\frac{1}{2h^2}(h^2+h^2)=3.$$

2. Off-diagonal terms:

- $a^1\langle\varphi_0,\varphi_1\rangle$: Since $\mathrm{supp}(\varphi_0)\cap\mathrm{supp}(\varphi_1)\neq\emptyset$ only on triangles K_1 and K_6, we have:

$$a^1\langle\varphi_0,\varphi_1\rangle = \iint_{K_1}\left(\nabla\varphi_0\cdot\nabla\varphi_1+\frac{1}{2}\frac{\partial\varphi_0}{\partial y}\frac{\partial\varphi_1}{\partial x}\right)dx\,dy+\iint_{K_6}\left(\nabla\varphi_0\cdot\nabla\varphi_1+\frac{1}{2}\frac{\partial\varphi_0}{\partial y}\frac{\partial\varphi_1}{\partial x}\right)dx\,dy.$$

$$=\left[-\frac{1}{h^2}-\frac{1}{h^2}\right]\frac{h^2}{2}+\frac{1}{2h^2}(h^2)=-\frac{1}{2}.$$

- $a^1\langle\varphi_0,\varphi_3\rangle$: Since $\mathrm{supp}(\varphi_0)\cap\mathrm{supp}(\varphi_3)\neq\emptyset$ only on triangles K_4 and K_5, we compute:

$$a^1\langle\varphi_0,\varphi_3\rangle = \iint_{K_4}\left(\nabla\varphi_0\cdot\nabla\varphi_3+\frac{1}{2}\frac{\partial\varphi_0}{\partial y}\frac{\partial\varphi_3}{\partial x}\right)dx\,dy+\iint_{K_5}\left(\nabla\varphi_0\cdot\nabla\varphi_3+\frac{1}{2}\frac{\partial\varphi_0}{\partial y}\frac{\partial\varphi_3}{\partial x}\right)dx\,dy.$$

Therefore,

$$=\left[-\frac{1}{h^2}-\frac{1}{h^2}\right]\frac{h^2}{2}+\frac{1}{2h^2}(h^2)=-\frac{1}{2}.$$

- $a^1\langle\varphi_0,\varphi_4\rangle$: Since $\mathrm{supp}(\varphi_0)\cap\mathrm{supp}(\varphi_4)\neq\emptyset$ only on triangles K_5 and K_6, we obtain:

$$a^1\langle\varphi_0,\varphi_4\rangle = \iint_{K_5}\left(\nabla\varphi_0\cdot\nabla\varphi_4+\frac{1}{2}\frac{\partial\varphi_0}{\partial y}\frac{\partial\varphi_4}{\partial x}\right)dx\,dy+\iint_{K_6}\left(\nabla\varphi_0\cdot\nabla\varphi_4+\frac{1}{2}\frac{\partial\varphi_0}{\partial y}\frac{\partial\varphi_4}{\partial x}\right)dx\,dy.$$

Thus,

$$=0-\frac{1}{2h^2}(h^2)=-\frac{1}{2}.$$

- Remaining off-diagonal terms:

$$a^1\langle\varphi_0,\varphi_2\rangle=0,\quad a^1\langle\varphi_0,\varphi_5\rangle=0,\quad a^1\langle\varphi_0,\varphi_6\rangle=0.$$

Finally, the coefficients associated with φ_0 are summarized as follows:

$$a^1\langle\varphi_0,\varphi_1\rangle=a^1\langle\varphi_0,\varphi_3\rangle=a^1\langle\varphi_0,\varphi_4\rangle=-\frac{1}{2},$$

$$a^1\langle\varphi_0,\varphi_2\rangle=a^1\langle\varphi_0,\varphi_5\rangle=a^1\langle\varphi_0,\varphi_6\rangle=0.$$

Computation of the stiffness matrix $\mathscr{A}^2$:

We denote by $a^2\langle\varphi_z,\varphi_s\rangle$ the (z,s)-th entry of the stiffness matrix $\mathscr{A}^2$. The computation relies on the intersection of supports:

$$\mathrm{supp}(\varphi_z)\cap\mathrm{supp}(\varphi_s)\neq\emptyset$$

and evaluating the integrals only over the triangles where this intersection is non-empty.

1. Diagonal term. The diagonal entry corresponding to φ_0 is given by:

$$a^2\langle\varphi_0,\varphi_0\rangle=\sum_{z=1}^{6}\iint_{K_z}\left(\frac{1}{2}\frac{\partial\varphi_0}{\partial x}\frac{\partial\varphi_0}{\partial x}+\frac{\partial\varphi_0}{\partial y}\frac{\partial\varphi_0}{\partial y}+\frac{1}{10}\frac{\partial\varphi_0}{\partial y}\frac{\partial\varphi_0}{\partial x}\right)dx\,dy.$$

$$=\left[\frac{2}{h^2}+\frac{4}{h^2}\right]\frac{h^2}{2}-\frac{2}{10h^2}h^2=\frac{14}{5}=2.8.$$

2. Off-diagonal terms.

- $a^2\langle\varphi_0,\varphi_1\rangle$.

  Since
  $$\operatorname{supp}(\varphi_0)\cap\operatorname{supp}(\varphi_1)\neq\emptyset$$
  only on triangles K_1 and K_6, we compute:
  $$\begin{aligned}
  a^2\langle\varphi_0,\varphi_1\rangle &= \iint_{K_1}\left(\frac{1}{2}\frac{\partial\varphi_0}{\partial x}\frac{\partial\varphi_1}{\partial x}+\frac{\partial\varphi_0}{\partial y}\frac{\partial\varphi_1}{\partial y}+\frac{1}{10}\frac{\partial\varphi_0}{\partial y}\frac{\partial\varphi_1}{\partial x}\right)dx\,dy\\
  &\quad+\iint_{K_6}\left(\frac{1}{2}\frac{\partial\varphi_0}{\partial x}\frac{\partial\varphi_1}{\partial x}+\frac{\partial\varphi_0}{\partial y}\frac{\partial\varphi_1}{\partial y}+\frac{1}{10}\frac{\partial\varphi_0}{\partial y}\frac{\partial\varphi_1}{\partial x}\right)dx\,dy\\
  &=\left(-\frac{2}{2h^2}\cdot\frac{h^2}{2}\right)+\frac{1}{10h^2}h^2\\
  &=-0.4.
  \end{aligned}$$

- $a^2\langle\varphi_0,\varphi_3\rangle$.

  Since
  $$\operatorname{supp}(\varphi_0)\cap\operatorname{supp}(\varphi_3)\neq\emptyset$$
  only on triangles K_4 and K_5, we compute:
  $$\begin{aligned}
  a^2\langle\varphi_0,\varphi_3\rangle &= \iint_{K_4}\left(\frac{1}{2}\frac{\partial\varphi_0}{\partial x}\frac{\partial\varphi_3}{\partial x}+\frac{\partial\varphi_0}{\partial y}\frac{\partial\varphi_3}{\partial y}+\frac{1}{10}\frac{\partial\varphi_0}{\partial y}\frac{\partial\varphi_3}{\partial x}\right)dx\,dy\\
  &\quad+\iint_{K_5}\left(\frac{1}{2}\frac{\partial\varphi_0}{\partial x}\frac{\partial\varphi_3}{\partial x}+\frac{\partial\varphi_0}{\partial y}\frac{\partial\varphi_3}{\partial y}+\frac{1}{10}\frac{\partial\varphi_0}{\partial y}\frac{\partial\varphi_3}{\partial x}\right)dx\,dy\\
  &=\left(-\frac{2}{h^2}\cdot\frac{h^2}{2}\right)+\frac{1}{10h^2}h^2\\
  &=-0.9.
  \end{aligned}$$

- $a^2\langle\varphi_0,\varphi_4\rangle$.

  Since
  $$\operatorname{supp}(\varphi_0)\cap\operatorname{supp}(\varphi_4)\neq\emptyset$$
  only on triangles K_5 and K_6, we obtain:
  $$\begin{aligned}
  a^2\langle\varphi_0,\varphi_4\rangle &= \iint_{K_5}\left(\frac{1}{2}\frac{\partial\varphi_0}{\partial x}\frac{\partial\varphi_4}{\partial x}+\frac{\partial\varphi_0}{\partial y}\frac{\partial\varphi_4}{\partial y}+\frac{1}{10}\frac{\partial\varphi_0}{\partial y}\frac{\partial\varphi_4}{\partial x}\right)dx\,dy\\
  &\quad+\iint_{K_6}\left(\frac{1}{2}\frac{\partial\varphi_0}{\partial x}\frac{\partial\varphi_4}{\partial x}+\frac{\partial\varphi_0}{\partial y}\frac{\partial\varphi_4}{\partial y}+\frac{1}{10}\frac{\partial\varphi_0}{\partial y}\frac{\partial\varphi_4}{\partial x}\right)dx\,dy\\
  &=-\frac{1}{10}=-0.1.
  \end{aligned}$$

- Remaining off-diagonal terms.
  $$a^2\langle\varphi_0,\varphi_2\rangle=a^2\langle\varphi_0,\varphi_5\rangle=a^2\langle\varphi_0,\varphi_6\rangle=0.$$

Finally, the coefficients associated with φ_0 are summarized as follows:

$$\begin{array}{lll} a^2\langle\varphi_0,\varphi_0\rangle = 2.8, & a^2\langle\varphi_0,\varphi_1\rangle = -0.4, & \\ a^2\langle\varphi_0,\varphi_3\rangle = -0.9, & a^2\langle\varphi_0,\varphi_4\rangle = -0.1, & \\ a^2\langle\varphi_0,\varphi_2\rangle = 0, & a^2\langle\varphi_0,\varphi_5\rangle = 0, & a^2\langle\varphi_0,\varphi_6\rangle = 0. \end{array}$$

Right-hand side.

Using the trapezoidal rule,

$$\begin{aligned} \iint_{\Omega} \mathscr{F}^i(x,y)\varphi_0(x,y)\,dx\,dy &= \sum_{z=1}^{6} \iint_{K_z} \mathscr{F}^i(x,y)\varphi_0(x,y)\,dx\,dy \\ &\approx \sum_{z=1}^{6} \frac{h^2}{6}\mathscr{F}^i(A_0) = h^2\mathscr{F}^i(A_0). \end{aligned}$$

Block tridiagonal structure of the stiffness matrix $\mathscr{A}^i$.

As a result, the stiffness matrix $\mathscr{A}^i$ exhibits a block tridiagonal structure:

$$\mathscr{A}^i = \begin{pmatrix} \mathscr{E}^i & \mathscr{C}^i & & \\ \mathscr{C}^{iT} & \mathscr{E}^i & \ddots & \\ & \ddots & \ddots & \mathscr{C}^i \\ & & \mathscr{C}^{iT} & \mathscr{E}^i \end{pmatrix}, \quad i = 1, 2.$$

where $\mathscr{E}^i$ and $\mathscr{C}^i$ are defined for $i = 1, 2$ as follows.

	Diagonal bloc	Sub co-diagonal bloc
$\mathscr{A}^1$	$\mathscr{E}^1 = \begin{bmatrix} a & b & & \\ b & \ddots & \ddots & \\ & \ddots & \ddots & b \\ & & b & a \end{bmatrix}$	$\mathscr{C}^1 = \begin{bmatrix} b & b & & \\ & b & \ddots & \\ & & \ddots & b \\ & & & b \end{bmatrix}$
$\mathscr{A}^2$	$\mathscr{E}^2 = \begin{bmatrix} a' & b' & & \\ b' & \ddots & \ddots & \\ & \ddots & \ddots & b' \\ & & b' & a' \end{bmatrix}$	$\mathscr{C}^2 = \begin{bmatrix} c & c' & & \\ & c & \ddots & \\ & & \ddots & c' \\ & & & c \end{bmatrix}$

Table 2.1: **Elements of matrix.**

Such that :

$$\begin{array}{ll} a = 3, & b = -0.5, \\ a' = 2.8, & b' = -0.4, \\ c = -0.9, & c' = -0.1. \end{array}$$

2.3.4 Numerical results and graphical interpretation

This section presents the numerical performance of the proposed overlapping domain decomposition method in comparison with the non-overlapping variant. The objective is to assess the quality of the approximation, the convergence behavior, and the computational efficiency through representative indicators such as residual norms, iteration counts, CPU time, and error evolution in the L^∞-norm. The discussion is complemented by graphical results illustrating the behavior of the iterative sequences and the accuracy of the numerical solution with respect to the exact one.

Residual and convergence indicators

The convergence of the iterative process is first evaluated through the residual quantity:

$$R = \max_{1 \leq i \leq 2} \left\{ \mathscr{A}^i \check{\vartheta}_h^k - \mathscr{F}^i \right\},$$

which measures the imbalance of the discrete system at each iteration. The results reported in Table (2.2) show that both approaches rapidly drive the residual to very small values, confirming the consistency of the discretization. However, the overlapping strategy systematically attains smaller residuals at earlier iterations, indicating a more effective stabilization of the iterative process.

Table 2.2: **Maximum norm of the residual R for $h = 1/20$.**

Iteration	DDM ($d > 1$)	DDM ($d = 1$)
1	7.25×10^{-10}	1.10×10^{-9}
4	4.92×10^{-10}	8.97×10^{-10}
8	3.01×10^{-10}	6.13×10^{-10}
Last	1.47×10^{-10}	3.76×10^{-10}

A complementary measure of performance is given by the number of iterations required to reach convergence. As shown in Table (2.3), the refinement of the mesh naturally increases the computational effort. Nevertheless, the overlapping decomposition consistently reduces the iteration count, confirming its role in accelerating convergence.

Table 2.3: **Number of iterations required for convergence.**

h	DDM ($d > 1$)	DDM ($d = 1$)
1/20	10	22
1/30	18	28
1/40	23	35
1/50	27	38

The computational cost follows the same tendency, as illustrated in Table (2.4). Although refinement increases the CPU time in both cases, the overlapping strategy remains consistently more efficient due to its faster convergence.

Table 2.4: **Computation time for different h.**

h	DDM ($d > 1$)	DDM ($d = 1$)
1/20	0.364	0.553
1/30	0.593	0.836
1/40	0.976	1.408
1/50	1.478	1.879

Behavior of solution sequences

To better illustrate the convergence mechanism of the iterative process, we analyze the evolution of both lower and upper solution sequences at a representative point.

Table 2.5: **Values of the lower solution $\check{\vartheta}_h^k$ at $(0.5, 0.5)$ for $h = 1/20$.**

Iteration	DDM : $d > 1$	DDM : $d = 1$
1	0.054302234247351	0.052610948825456
4	0.062313579024814	0.060034282247694
8	0.062498815627914	0.062117196798672
Last iteration	0.062499960405392	0.062499948402463

Table 2.6: **Values of the upper solution $\hat{\vartheta}_h^k$ at $(0.5, 0.5)$ for $h = 1/20$.**

Iteration	DDM : $d > 1$	DDM : $d = 1$
1	0.065103443280430	0.065410001781282
4	0.062560430873437	0.063243722960188
8	0.062500382778641	0.062617429458465
Last iteration	0.062500006101231	0.062500066203848

- The lower sequence $(\check{\vartheta}_h^k)$ is monotone increasing and converges from below to the exact value $\vartheta^* = 0.0625$.
- The upper sequence $(\hat{\vartheta}_h^k)$ is monotone decreasing and converges from above to the same limit.
- The overlapping strategy ($d > 1$) accelerates the contraction of both sequences and reduces the gap between them.
- The combination of both sequences provides a natural and reliable enclosure of the exact solution.

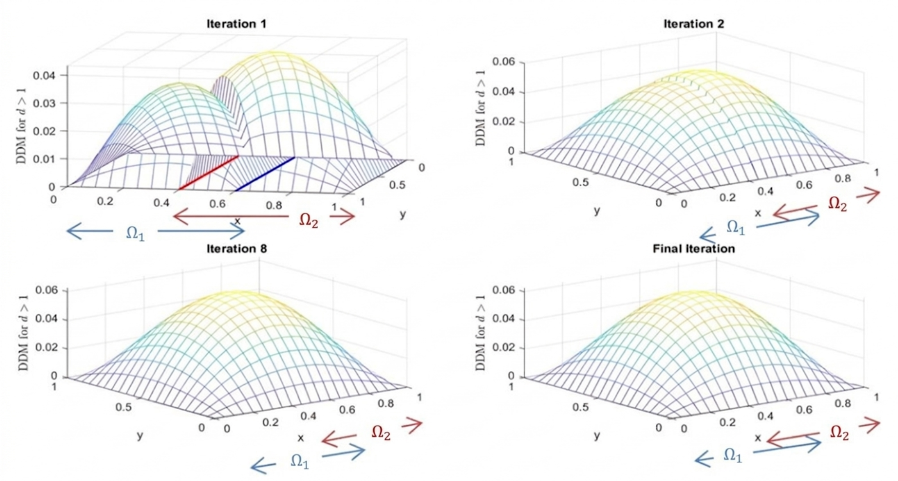

Figure 2.5: **Iteration evolution with overlap ($d > 1$).**

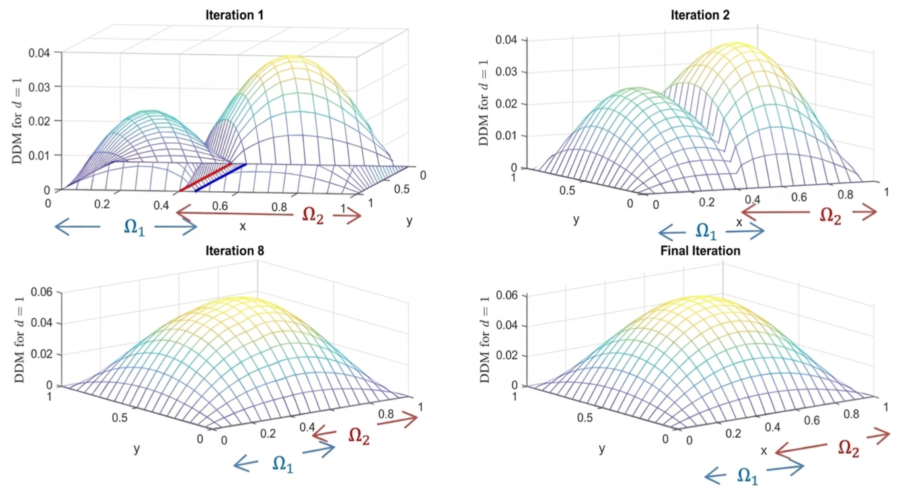

Figure 2.6: **Convergence with minimal overlap ($d = 1$).**

Figures (2.5) and (2.6) show that increasing the overlap significantly improves convergence speed by reducing the number of required iterations. In contrast, the minimal overlap case exhibits slower stabilization, which is consistent with the theoretical analysis of domain decomposition methods.

Error analysis and convergence verification

To assess the accuracy of the proposed numerical scheme and confirm its convergence behavior, we present a detailed error analysis in both the discrete and continuous settings.

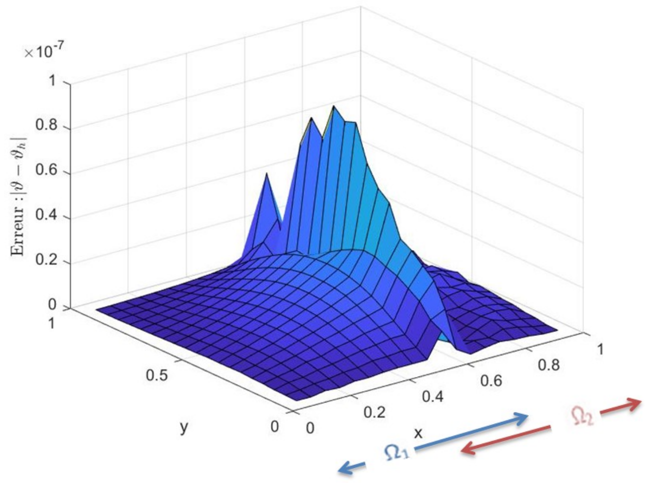

Figure 2.7: **Infinity norm error: exact vs. approximate solutions.**

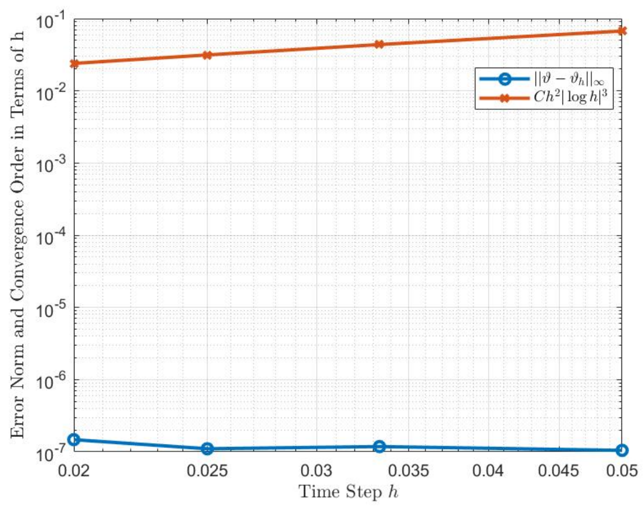

Figure 2.8: **Error estimate in the L^∞-norm.**

The numerical results confirm that:

- The error remains extremely small, indicating high accuracy of the approximation.
- The observed convergence rate is consistent with the theoretical estimate

$$\|\vartheta - \vartheta_h\|_{L^\infty(\Omega)} \leq Ch^2|\log h|^3,$$

- The overlapping domain decomposition method preserves stability and accuracy even in two-dimensional settings.
- The numerical solution is practically indistinguishable from the exact solution.

Chapter three :

Overlapping domain decomposition methods for non-coercive HJB equations

In this chapter, we establish the monotone and geometric convergence of the discrete non-coercive HJB equation within a finite difference framework. The analysis relies on an overlapping domain decomposition method together with iterative sous-solution and sur-solution sequences, which play a central role in the convergence proof. Numerical experiments are also presented to confirm the theoretical results and illustrate the efficiency of the proposed approach.

Contents

3.1 The noncoercive HJB problem

In this section, we address HJB equations in the noncoercive framework, and construct numerical techniques adapted to this setting. The main elements are organized as follows:

3.1.1 The continuous noncoercive HJB equation

- We consider the noncoercive HJB problem with homogeneous Dirichlet boundary condition:

$$\begin{cases} \max\limits_{1\le i\le n}(\mathbb{A}^i\vartheta - \mathbb{F}^i) = 0, & \text{in } \Omega, \\ \vartheta = 0, & \text{on } \partial\Omega. \end{cases} \tag{3.1}$$

- The operators $\mathbb{A}^i$ are assumed to be uniformly elliptic but not coercive (2.2).
- The coefficients satisfy the structural hypotheses (2.6), (2.4), and (2.5).
- The forcing terms $\mathbb{F}^i$ are smooth, with $\mathbb{F}^i \in C^2(\overline{\Omega})$.
- Following the approach of the coercive case, the problem (3.1) can be reformulated as a system of noncoercive variational inequalities of quasi-type (IQV) given in (1.24).
- Under these assumptions, well-posedness is preserved and the system admits a unique solution (see [35, 42]).

3.1.2 Reformulation into a coercive HJB

For non-coercive Hamilton-Jacobi-Bellman (HJB) systems, the bilinear forms $a^i\langle u, v\rangle$ do not satisfy the coercivity property. To overcome this limitation, we introduce a modified formulation based on the following steps:

- The original quasi-variational inequality system (1.24) is replaced by a coercive counterpart obtained by adding a stabilization term.
- The new problem consists in finding $\vartheta = (\vartheta^1, \ldots, \vartheta^n) \in (H_0^1(\Omega))^n$ such that:

$$\begin{cases} b^i\langle\vartheta^i, u-\vartheta^i\rangle \ge \langle\mathbb{F}^i + \mu\vartheta^i, u-\vartheta^i\rangle, & \forall u \in H_0^1(\Omega), \\ \vartheta^i \le \kappa + \vartheta^{i+1}, \quad u \le \kappa + \vartheta^{i+1}, \\ \vartheta^{n+1} = \vartheta^1, \quad i = \overline{1,n}, \quad \kappa \ge 0. \end{cases} \tag{3.2}$$

- In the modeling of control problems, the dynamics may be dominated by deterministic terms associated with the coefficients a_i^s, and the strong coercivity assumption is not always satisfied, which complicates the analysis. To ensure the stability of the problem, a regularization is introduced through a sufficiently large parameter $\mu > 0$ satisfying [32]:

$$b^i\langle u, v\rangle = a^i\langle u, v\rangle + \mu\langle u, v\rangle, \tag{3.3}$$

  where $\mu > 0$ is a parameter that enforces strong coercivity.

- The coercivity condition takes the form:

$$b^i\langle u, u\rangle \ge \lambda\|u\|^2_{H^1(\Omega)}, \quad \forall u \in H_0^1(\Omega), \quad \lambda > 0. \tag{3.4}$$

- To guarantee (3.4), one determines a suitable parameter μ according to the construction given in [32]. Specifically, the bound

$$a = \sup_{\substack{s \\ x\in\Omega}} |a_s(x)|. \tag{3.5}$$

is introduced to control the contribution of the non-coercive part.

Then, the coercive bilinear form $b^i\langle .,. \rangle$ takes the following explicit representation:

$$b^i\langle u,u\rangle = \int_\Omega \left(\sum_{z,s=1}^{N} a_{zs}(x) \frac{\partial u}{\partial x_z}\frac{\partial u}{\partial x_s} + \sum_{s=1}^{N} a_s(x)\frac{\partial u}{\partial x_s} u + a_0(x)u^2 + \mu u^2 \right) dx.$$

Using the ellipticity condition (2.6), assumption (2.4), Hölder's inequality in theorem 1.1.1, together with the bound (3.5), one derives the estimate:

$$b^i\langle u,u\rangle \geq \delta \int_\Omega \sum_{z=1}^{N} \left(\frac{\partial u}{\partial x_z}\right)^2 dx - \frac{a\epsilon}{2}\int_\Omega \sum_{z=1}^{N}\left(\frac{\partial u}{\partial x_z}\right)^2 dx - \frac{a}{2\epsilon}\int_\Omega u^2 dx + (\gamma+\mu)\int_\Omega u^2 dx.$$

By reorganizing the terms, we obtain:

$$b^i\langle u,u\rangle \geq \delta \int_\Omega \sum_{z=1}^{N}\left(\frac{\partial u}{\partial x_z}\right)^2 dx - a\sqrt{\epsilon}\left(\int_\Omega \sum_{z=1}^{N}\left(\frac{\partial u}{\partial x_z}\right)^2 dx\right)^{\frac{1}{2}} \frac{1}{\sqrt{\epsilon}}\left(\int_\Omega u^2 dx\right)^{\frac{1}{2}} + (\mu+\gamma)\int_\Omega u^2 dx.$$

This leads to the inequality:

$$b^i\langle u,u\rangle \geq \left(\delta - \epsilon\frac{a}{2}\right)\int_\Omega \sum_{z=1}^{N}\left(\frac{\partial u}{\partial x_z}\right)^2 dx + \left(\mu+\gamma-\frac{a}{2\epsilon}\right)\int_\Omega u^2 dx.$$

- The coercivity condition is guaranteed if:

$$\epsilon < \frac{2\delta}{a}, \quad \mu > \frac{a}{2\epsilon} - \gamma.$$

- Provided that $b \neq 0$, the bilinear form $b^i\langle\cdot,\cdot\rangle$ becomes coercive.

Following this procedure, which goes back to [32], the non-coercive HJB problem (3.1) is transformed into an equivalent coercive problem. The resulting formulation is:

$$\begin{cases} \max\limits_{1\leq i\leq n} (\mathbb{B}^i\vartheta - \mathbb{G}^i(\vartheta)) = 0, & \text{in } \Omega, \\ \vartheta = 0, & \text{on } \partial\Omega. \end{cases} \tag{3.6}$$

The new operators are defined as:

$$\mathbb{B}^i = \sum_{z,s=1}^{N} a^i_{zs}(x)\frac{\partial^2}{\partial x_z \partial x_s} + \sum_{s=1}^{N} a^i_s(x)\frac{\partial}{\partial x_s} + (a^i_0(x)+\mu), \tag{3.7}$$

with the relations:

$$\mathbb{B}^i = \mathbb{A}^i + \mu I, \quad \mathbb{G}^i(\vartheta) = \mathbb{F}^i + \mu\vartheta, \quad i = \overline{1,n}. \tag{3.8}$$

3.1.3 The discrete coercive HJB equations

In order to obtain a computable approximation of the coercive Hamilton–Jacobi–Bellman problem (3.6), we discretize the domain Ω using a finite difference mesh of size h, and denote by ϑ_h the discrete approximation of the continuous solution ϑ. The discrete counterpart of problem (3.6) is then formulated as:

$$\begin{cases} \text{Find} \quad \vartheta_h \in V_h \quad \text{solution to :} \\ \max\limits_{1\leq i\leq n} \left(\mathscr{B}^i \vartheta_h - \mathscr{G}^i(\vartheta_h)\right) = 0. \end{cases} \tag{3.9}$$

The discrete operators $\mathscr{B}^i$ are defined by:

$$\mathscr{B}^i = \mathscr{A}^i + \mu I,$$

where $\mathscr{A}^i$ denotes the finite difference approximation of the continuous operator $\mathbb{A}^i$, and the additional term μI guarantees the coercivity at the discrete level.

In parallel, the nonlinear functions $\mathscr{G}^i(\vartheta_h)$ are given by

$$\mathscr{G}^i(\vartheta_h) = \mathscr{F}^i + \mu\vartheta_h, \qquad i = 1, ..., n,$$

where $\mathscr{F}^i$ represents the discretization of the source terms $\mathbb{F}^i$ arising in the continuous formulation.

The discrete matrices $\mathscr{B}^i$ are constructed so as to satisfy the discrete maximum principle and to belong to the class of M-matrices.This structural property plays a central role in ensuring the stability of the approximation and the monotone convergence of the numerical scheme, as established in [35, 42].

3.2 Overlapping domain decomposition method

In this part, the overlapping domain decomposition strategy developed earlier is adapted to the coercive discrete Hamilton-Jacobi-Bellman (HJB) setting. The transition from the non-coercive to the coercive formulation induces a change of notation: the matrices previously written as $\mathscr{A}^i$ are now denoted $\mathscr{B}^i$, and the source terms $\mathscr{F}^i$ are replaced by the nonlinear expressions $\mathscr{G}^i(\vartheta_h)$. Apart from this modification, the iterative algorithm retains the same structure as in the non-coercive case, ensuring the consistency of the overall numerical procedure [27].

3.2.1 Discrete block domain decomposition method

Let $\Omega \subset \mathbb{R}^2$ be a bounded and regular computational domain. For the discrete HJB equations, the domain is partitioned into two overlapping regions Ω_1 and Ω_2, each subject to the same type of boundary conditions as in the continuous setting. The essential modifications with respect to the previous chapter lie in the operators involved, while the decomposition principle itself remains unchanged.

The bilinear form associated with the discretized system, denoted by $b^i(u, v)$, now relies on the matrices $\mathscr{B}^i$ and their nonlinear counterparts. The unknowns are split according to the subdomain structure:

$$\vartheta_h = \begin{pmatrix} \vartheta_{1h} \\ \vartheta_{2h} \end{pmatrix}, \qquad \mathscr{G}^i(\vartheta_h) = \begin{pmatrix} \mathscr{G}^i(\vartheta_{1h}) \\ \mathscr{G}^i(\vartheta_{2h}) \end{pmatrix},$$

with a block decomposition of the discrete operator given by:

$$\mathscr{B}^i = \begin{pmatrix} \mathscr{B}^i_{1,1} & -\tilde{\mathscr{B}}^i_{1,2} \\ -\tilde{\mathscr{B}}^i_{2,1} & \mathscr{B}^i_{2,2} \end{pmatrix}.$$

Here, ϑ_{1h} and ϑ_{2h} correspond to the discrete solutions restricted to each subdomain. The block structure of $\tilde{\mathscr{B}}^i$ preserves the coupling across interfaces, which is essential for the convergence of the Schwarz iterations.

The discrete HJB problem introduced in (3.9) can thus be rewritten in this partitioned form as:

$$\begin{cases} \max\limits_{1\le i\le n} \left(\tilde{\mathscr{B}}^i \vartheta_h - \mathscr{G}^i(\vartheta_h)\right) = 0, & \text{in } \Omega, \\ \vartheta_h = 0, & \text{on } \partial\Omega. \end{cases}$$

This formulation will serve as the basis for the overlapping Schwarz algorithm in the discrete coercive case.

3.2.2 Iterative solution strategy on subdomains

To facilitate the solution process, the discrete system is reformulated within each subdomain independently, following an overlapping domain decomposition strategy.

- **Update in Subdomain Ω_1:** The unknown ϑ_{1h}^{k+1} is computed by solving:

$$\begin{cases} \max\limits_{1\le i\le n} \left(\mathscr{B}^i_{1,1}\vartheta_{1h}^{k+1} - \mathscr{G}^i(\vartheta_{1h}^k)\right) = 0, & \text{in } \Omega_1, \\ \left(\vartheta_{1h}^{k+1}\right)_\beta = \left(\vartheta_{2h}^{k}\right)_\beta, & \text{on } \Sigma_1 = \partial\Omega_1 \cap \Omega_2. \end{cases}$$

- **Update in Subdomain Ω_2:** Similarly, the updated solution ϑ_{2h}^{k+1} is obtained by solving:

$$\begin{cases} \max\limits_{1\le i\le n} \left(\mathscr{B}^i_{2,2}\vartheta_{2h}^{k+1} - \mathscr{G}^i(\vartheta_{2h}^k)\right) = 0, & \text{in } \Omega_2, \\ \left(\vartheta_{2h}^{k+1}\right)_\alpha = \left(\vartheta_{1h}^{k+1}\right)_\alpha, & \text{on } \Sigma_2 = \partial\Omega_2 \cap \Omega_1. \end{cases}$$

Bringing together the discrete systems of both subdomains, we arrive at the following block-structured iteration:

$$\begin{cases} \max\limits_{1\le i\le n} \left\{\mathscr{B}^i_{1,1}\vartheta_{1h}^{k+1} - \tilde{\mathscr{B}}^i_{1,2}\vartheta_{2h}^{k} - \mathscr{G}^i(\vartheta_{1h}^k)\right\} = 0, & \text{in } \Omega_1, \\ \max\limits_{1\le i\le n} \left\{\mathscr{B}^i_{2,2}\vartheta_{2h}^{k+1} - \tilde{\mathscr{B}}^i_{2,1}\vartheta_{1h}^{k+1} - \mathscr{G}^i(\vartheta_{2h}^k)\right\} = 0, & \text{in } \Omega_2. \end{cases}$$

We begin by stating the definitions, followed by the presentation of the algorithm.

$\check{\vartheta}_h \in \mathbb{R}^N$ is called a subsolution if it satisfies:

$$\max_{1\le i\le n} \left(\mathscr{B}^i\check{\vartheta}_h - \mathscr{G}^i(\check{\vartheta}_h)\right) \le 0,$$

while $\hat{\vartheta}_h \in \mathbb{R}^N$ is called a supersolution if:

$$\max_{1\le i\le n} \left(\mathscr{B}^i\hat{\vartheta}_h - \mathscr{G}^i(\hat{\vartheta}_h)\right) \ge 0.$$

For the initialization, following the convention of [22], if all components of $\mathscr{G}^i$ are nonnegative, then the zero vector provides an admissible starting subsolution:

$$\check{\vartheta}_h^0 = (0, 0, \ldots, 0).$$

The initial supersolution $\hat{\vartheta}_h^0$ is obtained by solving the system:

$$\mathscr{B}^i \hat{\vartheta}_h^0 = \mathscr{G}^i(\hat{\vartheta}_h^0), \quad i = 1, \ldots, n.$$

Based on these initial bounds, the overlapping iterative procedure can be formulated as follows.

Algorithm 2: Iterative ODD for non-coercive HJB problems

Initialization: Set the initial subsolution $\check{\vartheta}_h^0 = (0, 0, \ldots, 0)$, and let $k = 0$.

Step 1: Update on domain Ω_1:

$$\max_{1 \le i \le n} \left\{ \mathscr{B}_{1,1}^i \check{\vartheta}_{1h}^{k+1} - \tilde{\mathscr{B}}_{1,2}^i \check{\vartheta}_{2h}^k - \mathscr{G}^i(\check{\vartheta}_{1h}^k) \right\} = 0.$$

Step 2: Update on domain Ω_2:

$$\max_{1 \le i \le n} \left\{ -\tilde{\mathscr{B}}_{2,1}^i \check{\vartheta}_{1h}^{k+1} + \mathscr{B}_{2,2}^i \check{\vartheta}_{2h}^{k+1} - \mathscr{G}^i(\check{\vartheta}_{2h}^k) \right\} = 0.$$

Step 3: Convergence test: If the criterion is not satisfied, set $k \leftarrow k + 1$ and return to Step 1.

3.2.3 Monotone and geometric convergence

In this subsection, we study the convergence properties of the overlapping domain decomposition method introduced in Algorithm 2.

Theorem 3.2.1: [27]

The iteration defined by Algorithm 2 generates two sequences $(\check{\vartheta}_h^k)$ and $(\hat{\vartheta}_h^k)$ which evolve monotonically. More precisely, $(\check{\vartheta}_h^k)$ is non-decreasing and $(\hat{\vartheta}_h^k)$ is non-increasing. Moreover, both sequences converge to the same limit, which coincides with the unique discrete solution ϑ_h of system (3.9).

Theorem 3.2.2: [27]

Let ϑ_h^0 be an arbitrary initial guess. Then the sequence (ϑ_h^k) generated by Algorithm 2 converges to the unique solution of system (3.9) at a geometric rate. More precisely, there exists a constant $0 < \rho < 1$ such that:

$$\|\vartheta_h^{k+1} - \vartheta_h^k\|_{L^\infty(\Omega)} \le \rho^k \, \|\vartheta_h^1 - \vartheta_h^0\|_{L^\infty(\Omega)}, \quad \forall k \in \mathbb{N}.$$

3.3 Computational study and numerical implementation

This section presents the numerical investigation of a Hamilton-Jacobi-Bellman (HJB) type problem derived from an obstacle formulation. The focus is on evaluating the efficiency of numerical schemes based on overlapping domain decomposition.

3.3.1 Problem setup and transformation

The obstacle problem is reformulated in a Hamilton–Jacobi–Bellman framework in order to enable the use of efficient numerical schemes [1]. The computational domain is defined by:

$$\Omega = [0,1] \times [0,1],$$

with homogeneous boundary conditions imposed on $\partial\Omega$.

The continuous obstacle formulation is written in variational inequality form as:

$$\begin{cases} \mathscr{B}\vartheta_h \geq \mathscr{G}, & \text{in } \Omega, \\ \langle \mathscr{B}\vartheta_h - \mathscr{G}, \vartheta_h - \Psi \rangle = 0, & \text{in } \Omega, \\ \vartheta_h \leq \Psi, & \text{in } \Omega, \\ \vartheta_h = 0, & \text{on } \partial\Omega. \end{cases}$$

The differential operator is defined by:

$$\mathscr{B} = -\frac{\partial^2}{\partial x^2} - \frac{\partial^2}{\partial y^2} + 0.5x\frac{\partial}{\partial x} + 0.5y\frac{\partial}{\partial y} + 0.045,$$

while the source term and obstacle function are given by:

$$\mathscr{G} = \sin(2\pi x)\sin(2\pi y), \quad \Psi = 0.$$

For the purpose of applying iterative solvers, the problem is equivalently reformulated as a nonlinear system of Hamilton–Jacobi–Bellman type:

$$\begin{cases} \max\{\mathscr{B}^1\vartheta_h - \mathscr{G}^1,\ \mathscr{B}^2\vartheta_h - \mathscr{G}^2\} = 0, & \text{in } \Omega, \\ \vartheta_h = 0, & \text{on } \partial\Omega. \end{cases}$$

The operators are defined as follows:

- ❖ $\mathscr{B}^1 = \mathscr{B} + \mu I$, $\mathscr{G}^1 = \mathscr{G} + \mu\vartheta_h$, with $\mu = 1$,
- ❖ $\mathscr{B}^2 = I$, $\mathscr{G}^2 = \Psi$.

3.3.2 Discretization via finite differences

The numerical approximation is constructed using the finite difference method, where the continuous derivatives are replaced by discrete operators on a uniform grid with mesh size h. This approach leads to an algebraic system that approximates the original differential problem at the grid level.

The computational procedure can be summarized as follows:

- The domain Ω is discretized into a regular mesh, and the unknown solution is represented at the grid nodes.
- The second-order derivatives and first-order terms in the operator $\mathscr{B}$ are approximated using standard finite difference formulas.
- An iterative scheme based on overlapping subdomains is applied to solve the resulting nonlinear discrete system, improving convergence efficiency.

- The iteration is stopped when the stopping criterion

$$\|\vartheta_h^{k+1} - \vartheta_h^k\|_\infty < \varepsilon, \quad \varepsilon = 10^{-6},$$

  is satisfied.

- The implementation is carried out using MATLAB R20218a, ensuring efficient handling of matrix assembly and iterative computations.

This discretization framework provides the basis for the numerical experiments and convergence analysis presented in the next sections.

MATLAB implementation

This subsection details the matlab implementation of the finite difference (FD) scheme for solving the discretized Hamilton-Jacobi-Bellman (HJB) equation. The emphasis is on structuring the computational algorithm efficiently while preserving the mathematical operations.

The procedure is organized as follows:

- **Grid and step sizes:** define a uniform grid over the spatial domain with step sizes h_x and h_y for the x and y directions, respectively. The solution values at grid points are denoted by $\vartheta_{z,s}$.

- **Finite difference approximations:** Derivatives are approximated using standard FD formulas:

  - **Central difference (first-order)**:

$$\frac{\partial \vartheta}{\partial x}(x_z, y_s) \approx \frac{\vartheta_{z+1,s} - \vartheta_{z-1,s}}{2h_x}, \quad \frac{\partial \vartheta}{\partial y}(x_z, y_s) \approx \frac{\vartheta_{z,s+1} - \vartheta_{z,s-1}}{2h_y}$$

  - **Central difference (second-order):**

$$\frac{\partial^2 \vartheta}{\partial x^2} \approx \frac{\vartheta_{z+1,s} - 2\vartheta_{z,s} + \vartheta_{z-1,s}}{h_x^2}, \quad \frac{\partial^2 \vartheta}{\partial y^2} \approx \frac{\vartheta_{z,s+1} - 2\vartheta_{z,s} + \vartheta_{z,s-1}}{h_y^2}$$

  - **Finite difference operators:** Let $D_{h,x}^{\pm}$ and $D_{h,y}^{\pm}$ denote the forward/backward difference operators in x and y, respectively. The corresponding matrix forms for the second-order derivatives are:

$$D_{xx} = \frac{1}{h_x^2}\begin{bmatrix} -2 & 1 & 0 & \cdots & 0 \\ 1 & -2 & 1 & \cdots & 0 \\ 0 & 1 & -2 & \ddots & \vdots \\ \vdots & \ddots & \ddots & \ddots & 1 \\ 0 & \cdots & 0 & 1 & -2 \end{bmatrix}, \quad D_{yy} = \frac{1}{h_y^2}\begin{bmatrix} -2 & 1 & 0 & \cdots & 0 \\ 1 & -2 & 1 & \cdots & 0 \\ 0 & 1 & -2 & \ddots & \vdots \\ \vdots & \ddots & \ddots & \ddots & 1 \\ 0 & \cdots & 0 & 1 & -2 \end{bmatrix}$$

  - **First-order terms:** The first-order derivatives weighted by coordinates are discretized as:

$$0.5\, x_z \frac{\partial \vartheta}{\partial x} \approx 0.5\, x_z \frac{\vartheta_{z+1,s} - \vartheta_{z-1,s}}{2h_x}, \quad 0.5\, y_s \frac{\partial \vartheta}{\partial y} \approx 0.5\, y_s \frac{\vartheta_{z,s+1} - \vartheta_{z,s-1}}{2h_y}.$$

We obtain:

$$D_x = \frac{1}{2h_x}\begin{bmatrix} 0 & 0.5x_1 & 0 & \cdots & 0 \\ -0.5x_2 & 0 & 0.5x_2 & \cdots & 0 \\ 0 & -0.5x_3 & 0 & \ddots & \vdots \\ \vdots & \ddots & \ddots & \ddots & 0.5x_{N-1} \\ 0 & \cdots & 0 & -0.5x_N & 0 \end{bmatrix},$$

$$D_y = \frac{1}{2h_y}\begin{bmatrix} 0 & 0.5y_1 & 0 & \cdots & 0 \\ -0.5y_2 & 0 & 0.5y_2 & \cdots & 0 \\ 0 & -0.5y_3 & 0 & \ddots & \vdots \\ \vdots & \ddots & \ddots & \ddots & 0.5y_{N-1} \\ 0 & \cdots & 0 & -0.5y_N & 0 \end{bmatrix}.$$

- **Constant term:** The additive constant $0.045\vartheta_{z,s}$ is represented as a scaled identity matrix:

$$0.045I = 0.045\begin{bmatrix} 1 & 0 & \cdots & 0 \\ 0 & 1 & \cdots & 0 \\ \vdots & \vdots & \ddots & \vdots \\ 0 & 0 & \cdots & 1 \end{bmatrix}$$

This formulation provides a clear and structured translation of the continuous derivatives into matlab compatible matrix operations while preserving the full generality of the discretized HJB problem.

- **Computational domain and grid definition:** Consider the domain $\Omega = [0,1] \times [0,1]$ with homogeneous Dirichlet boundary conditions. We introduce a uniform grid with N interior points in both the x and y directions. The grid points are defined as:

$$x_z = zh, \quad y_s = sh, \quad 0 \leq z, s \leq N+1, \quad h_x = h_y = h = \frac{1}{N+1}, \quad N \in \mathbb{N}.$$

- **Example:** 3×3 **grid** For illustration, let $N = 3$ with $z, s = 1, 2, 3$. The uniform mesh spacing is:

$$h_x = h_y = h = \frac{1}{4}.$$

- **Second-order derivative matrices:**
  - In the x-direction:

$$D_{xx} = \frac{1}{h^2}\begin{bmatrix} -2 & 1 & 0 \\ 1 & -2 & 1 \\ 0 & 1 & -2 \end{bmatrix} = \begin{bmatrix} -32 & 16 & 0 \\ 16 & -32 & 16 \\ 0 & 16 & -32 \end{bmatrix}.$$

  - In the y-direction:

$$D_{yy} = D_{xx}.$$

- **First-order derivative matrices:**
  - In the x-direction, substituting $x_1 = h, x_2 = 2h, x_3 = 3h$:

$$D_x = \frac{1}{2h}\begin{bmatrix} 0 & 0.5x_1 & 0 \\ -0.5x_2 & 0 & 0.5x_2 \\ 0 & -0.5x_3 & 0 \end{bmatrix} = \begin{bmatrix} 0 & 0.25 & 0 \\ -0.5 & 0 & 0.5 \\ 0 & -0.75 & 0 \end{bmatrix}.$$

  - In the y-direction:

$$D_y = D_x.$$

- **Discrete system matrix assembly:** The final system matrix for the 2D HJB problem can be constructed efficiently in MATLAB using the Kronecker product:

$$\mathscr{B}^1 = -I_N \otimes D_{xx} - D_{yy} \otimes I_N + (I_N \otimes D_x) + (D_y \otimes I_N) + 0.045I.$$

  This assembly guarantees that each directional derivative is accurately incorporated, preserving sparsity and compatibility with vectorized matlab operations.

Manual computations

In this subsection, we present the manual derivation of the finite difference scheme. Our aim is to provide a detailed understanding of the discretization process by approximating the first- and second-order derivatives using standard finite difference formulas.

- **Finite difference approximation of the operator $\mathscr{B}^1$:** For $z, s = \overline{1, N}$, the discrete approximation reads:

$$\mathscr{B}^1\vartheta(x_z, y_s) = -\frac{\vartheta_{z+1,s} - 2\vartheta_{z,s} + \vartheta_{z-1,s}}{h^2} - \frac{\vartheta_{z,s+1} - 2\vartheta_{z,s} + \vartheta_{z,s-1}}{h^2} + 0.5x_z\frac{\vartheta_{z+1,s} - \vartheta_{z-1,s}}{2h}$$
$$+0.5y_s\frac{\vartheta_{z,s+1} - \vartheta_{z,s-1}}{2h} + (0.045 + \mu)\vartheta_{z,s}.$$

- **Matrix representation of the discrete system:**

$$\left[\frac{4}{h^2} + (0.045 + \mu)\right]\vartheta_{z,s} + \left[-\frac{1}{h^2} + \frac{0.5x_z}{2h}\right]\vartheta_{z+1,s} + \left[-\frac{1}{h^2} - \frac{0.5x_z}{2h}\right]\vartheta_{z-1,s}$$
$$+\left[-\frac{1}{h^2} + \frac{0.5y_s}{2h}\right]\vartheta_{z,s+1} + \left[-\frac{1}{h^2} - \frac{0.5y_s}{2h}\right]\vartheta_{z,s-1}.$$

- **Vectorization for matrix form:** To express the system in matrix form $\mathscr{B}^1\vartheta_h$, the grid matrix $(\vartheta_{z,s})$ is reshaped into a vector ϑ_h of size $N \times N$. Numbering the points (x_z, y_s) row-wise (or column-wise) results in a sparse matrix structure. Each point is indexed as:

$$L = z + (s-1)N.$$

- **Grid organization and boundary conditions:** The vector is organized in blocks:

$$\vartheta = [(\vartheta_{1,1}, \ldots, \vartheta_{N,1}), (\vartheta_{1,2}, \ldots, \vartheta_{N,2}), \ldots, (\vartheta_{1,N}, \ldots, \vartheta_{N,N})].$$

  Boundary conditions:

$$\vartheta_{0,s} = \vartheta_{N+1,s} = 0, \quad \vartheta_{z,0} = \vartheta_{z,N+1} = 0.$$

- **Example:** 5×5 **grid** Here, $N = 3$, $z, s = 1, 2, 3$, and mesh size:

$$h_x = h_y = h = \frac{1}{4}.$$

  Discretization points:

$$x_z = z \cdot h, \quad y_s = s \cdot h.$$

  Structured grid:

$$\begin{bmatrix} (h,h) & (2h,h) & (3h,h) \\ (h,2h) & (2h,2h) & (3h,2h) \\ (h,3h) & (2h,3h) & (3h,3h) \end{bmatrix}.$$

- **Coefficients for $N = 3$ and $\mu = 1$:**

$$a = \frac{4}{h^2} + 0.045 + \mu = 65.045, \quad b = -16 + 0.25z, \quad c = -16 - 0.25z,$$

$$d = -16 + 0.25s, \quad e = -16 - 0.25s.$$

- **Vectorized grid mapping:**

$$(z, s) \to L = z + (s-1)N.$$

The general finite difference equation at each grid point:

$$a\vartheta_L + b\vartheta_{L+1} + c\vartheta_{L-1} + d\vartheta_{L+N} + e\vartheta_{L-N}, \quad L = \overline{1,9}.$$

- **Index mapping for 3×3 grid:**

$$\begin{array}{lll} L = 1 \to (1,1), & L = 2 \to (2,1), & L = 3 \to (3,1), \\ L = 4 \to (1,2), & L = 5 \to (2,2), & L = 6 \to (3,2), \\ L = 7 \to (1,3), & L = 8 \to (2,3), & L = 9 \to (3,3). \end{array}$$

- **Structured unknowns vector:**

$$\begin{bmatrix} \vartheta_1 & \vartheta_2 & \vartheta_3 \\ \vartheta_4 & \vartheta_5 & \vartheta_6 \\ \vartheta_7 & \vartheta_8 & \vartheta_9 \end{bmatrix} \to \begin{bmatrix} \vartheta_1 \\ \vartheta_2 \\ \vartheta_3 \\ \vartheta_4 \\ \vartheta_5 \\ \vartheta_6 \\ \vartheta_7 \\ \vartheta_8 \\ \vartheta_9 \end{bmatrix}.$$

- **Correspondence of vector components:**

$$\begin{array}{lll} \vartheta_1 = \vartheta(x_1, y_1), & \vartheta_2 = \vartheta(x_2, y_1), & \vartheta_3 = \vartheta(x_3, y_1), \\ \vartheta_4 = \vartheta(x_1, y_2), & \vartheta_5 = \vartheta(x_2, y_2), & \vartheta_6 = \vartheta(x_3, y_2), \\ \vartheta_7 = \vartheta(x_1, y_3), & \vartheta_8 = \vartheta(x_2, y_3), & \vartheta_9 = \vartheta(x_3, y_3). \end{array}$$

3.3.3 Final matrix representation

Following the manual derivation of the finite difference discretization, we proceed to assemble the corresponding matrix system for the 2D HJB problem. This system is formulated as a sparse matrix, where each entry directly corresponds to the coefficients obtained from the discrete approximation of the differential operator. The explicit construction of this matrix allows for an efficient and structured numerical solution of the problem.

To illustrate this construction, we enumerate the individual grid points and their corresponding contributions to the system.

1. Point (x_1, y_1), **with** $L = 1$:

$$x_1 = 1 \cdot h, \quad y_1 = 1 \cdot h.$$

Neighbors: Right ($L = 2$), Up ($L = 4$):

$$\mathbf{65.045}\vartheta_1 - \mathbf{15.75}\vartheta_2 - \mathbf{15.75}\vartheta_4.$$

2. Point (x_2, y_1), **with** $L = 2$:

$$x_2 = 2 \cdot h, \quad y_1 = 1 \cdot h.$$

Neighbors: Left ($L = 1$), Right ($L = 3$), Up ($L = 5$):

$$\mathbf{65.045}\vartheta_2 - \mathbf{16.5}\vartheta_1 - \mathbf{15.5}\vartheta_3 - \mathbf{15.75}\vartheta_5.$$

3. Point (x_3, y_1), **with** $L = 3$:

$$x_3 = 3 \cdot h, \quad y_1 = 1 \cdot h.$$

Neighbors: Left ($L = 2$), Up ($L = 6$):

$$\mathbf{65.045}\vartheta_3 - \mathbf{15.75}\vartheta_2 - \mathbf{15.75}\vartheta_6.$$

4. Point (x_1, y_2), **with** $L = 4$:

$$x_1 = 1 \cdot h, \quad y_2 = 2 \cdot h.$$

Neighbors: Down ($L = 1$), Right ($L = 5$), Up ($L = 7$):

$$\mathbf{65.045}\vartheta_4 - \mathbf{16.5}\vartheta_1 - \mathbf{15.75}\vartheta_5 - \mathbf{15.5}\vartheta_7.$$

5. Point (x_2, y_2), **with** $L = 5$:

$$x_2 = 2 \cdot h, \quad y_2 = 2 \cdot h.$$

Neighbors: Left ($L = 4$), Right ($L = 6$), Down ($L = 2$), Up ($L = 8$):

$$\mathbf{65.045}\vartheta_5 - \mathbf{16.5}\vartheta_2 - \mathbf{16.5}\vartheta_4 - \mathbf{15.5}\vartheta_6 - \mathbf{15.5}\vartheta_8.$$

6. Point (x_3, y_2), **with** $L = 6$:

$$x_3 = 3 \cdot h, \quad y_2 = 2 \cdot h.$$

Neighbors: Left ($L = 5$), Down ($L = 3$), Up ($L = 9$):

$$\mathbf{65.045}\vartheta_6 - \mathbf{16.5}\vartheta_3 - \mathbf{16.75}\vartheta_5 - \mathbf{15.5}\vartheta_9.$$

7. Point (x_1, y_3), **with** $L = 7$:

$$x_1 = 1 \cdot h, \quad y_3 = 3 \cdot h.$$

Neighbors: Down ($L = 4$), Right ($L = 8$):

$$\mathbf{65.045}\vartheta_7 - \mathbf{16.75}\vartheta_4 - \mathbf{15.75}\vartheta_8.$$

8. Point (x_2, y_3), **with** $L = 8$:

$$x_2 = 2 \cdot h, \quad y_3 = 3 \cdot h.$$

Neighbors: Left ($L = 7$), Right ($L = 9$), Down ($L = 5$):

$$\mathbf{65.045}\vartheta_8 - \mathbf{16.75}\vartheta_5 - \mathbf{16.5}\vartheta_7 - \mathbf{15.5}\vartheta_9.$$

9. Point (x_3, y_3), **with** $L = 9$:

$$x_3 = 3 \cdot h, \quad y_3 = 3 \cdot h.$$

Neighbors: Left ($L = 8$), Down ($L = 6$):

$$\mathbf{65.045}\vartheta_9 - \mathbf{16.75}\vartheta_6 - \mathbf{16.75}\vartheta_8.$$

Finally, the complete system can be assembled into matrix form as:

$$\mathscr{B}^1\vartheta = \begin{pmatrix} a & b & 0 & d & 0 & 0 & 0 & 0 & 0 \\ c & a & b & 0 & d & 0 & 0 & 0 & 0 \\ 0 & c & a & 0 & 0 & d & 0 & 0 & 0 \\ e & 0 & 0 & a & b & 0 & d & 0 & 0 \\ 0 & e & 0 & c & a & b & 0 & d & 0 \\ 0 & 0 & e & 0 & c & a & 0 & 0 & d \\ 0 & 0 & 0 & e & 0 & 0 & a & b & 0 \\ 0 & 0 & 0 & 0 & e & 0 & c & a & b \\ 0 & 0 & 0 & 0 & 0 & e & 0 & c & a \end{pmatrix} \begin{pmatrix} \vartheta_1 \\ \vartheta_2 \\ \vartheta_3 \\ \vartheta_4 \\ \vartheta_5 \\ \vartheta_6 \\ \vartheta_7 \\ \vartheta_8 \\ \vartheta_9 \end{pmatrix}.$$

The corresponding numerical matrix for $N = 3$ reads:

$$\begin{pmatrix} 65.0450 & -15.7500 & 0 & -15.7500 & 0 & 0 & 0 & 0 & 0 \\ -16.5000 & 65.0450 & -15.5000 & 0 & -15.7500 & 0 & 0 & 0 & 0 \\ 0 & -16.7500 & 65.0450 & 0 & 0 & -15.7500 & 0 & 0 & 0 \\ -16.5000 & 0 & 0 & 65.0450 & -15.7500 & 0 & -15.5000 & 0 & 0 \\ 0 & -16.5000 & 0 & -16.5000 & 65.0450 & -15.5000 & 0 & -15.5000 & 0 \\ 0 & 0 & -16.5000 & 0 & -16.7500 & 65.0450 & 0 & 0 & -15.5000 \\ 0 & 0 & 0 & -16.7500 & 0 & 0 & 65.0450 & -15.7500 & 0 \\ 0 & 0 & 0 & 0 & -16.7500 & 0 & -16.5000 & 65.0450 & -15.5000 \\ 0 & 0 & 0 & 0 & 0 & -16.7500 & 0 & -16.7500 & 65.0450 \end{pmatrix}.$$

This construction can be generalized to the block-tridiagonal structure of order $N \times N$:

$$\mathfrak{B}^1 = \begin{pmatrix} \mathscr{D}^1 & \mathscr{C}^1 & & \\ \mathscr{E}^1 & \ddots & \ddots & \\ & \ddots & \ddots & \mathscr{C}^1 \\ & & \mathscr{E}^1 & \mathscr{D}^1 \end{pmatrix},$$

where the blocks are defined as follows:

	Diagonal block $\mathscr{D}^1$	**Upper block** $\mathscr{C}^1$	**Lower block** $\mathscr{E}^1$
$\mathscr{B}^1$	$\mathscr{D}^1 = \begin{bmatrix} a & b & & \\ c & a & \ddots & \\ & \ddots & \ddots & b \\ & & c & a \end{bmatrix}$	$\mathscr{C}^1 = \begin{bmatrix} d_1 & & & \\ & d_1 & & \\ & & \ddots & \\ & & & d_1 \end{bmatrix}$	$\mathscr{E}^1 = \begin{bmatrix} e & & & \\ & e & & \\ & & \ddots & \\ & & & e \end{bmatrix}$,

Table 3.1: **Block Structure of Matrix** $\mathfrak{B}^1$

The coefficients are explicitly given by:

$$
\begin{aligned}
a &= \frac{4}{h^2} + 0.045 + \mu, & b &= \frac{-1}{h^2} + \frac{0.25x_z}{h},\\
c &= \frac{-1}{h^2} - \frac{0.25x_z}{h}, & d_1 &= \frac{-1}{h^2} + \frac{0.25y_s}{h},\\
e &= \frac{-1}{h^2} - \frac{0.25y_s}{h}, & z, s &= \overline{1, N}.
\end{aligned}
$$

3.3.4 Numerical results and analytical discussion

In this section, we provide a detailed presentation of the numerical simulations for the non-coercive Hamilton-Jacobi-Bellman (HJB) equation, solved via the finite difference method. The results are analyzed in terms of accuracy, convergence, and efficiency, and are compared with the corresponding analytical solutions to assess the performance of the method.

Furthermore, we investigate the influence of domain decomposition strategies by comparing the classical non-overlapping method ($d = 1$) with the newly proposed overlapping domain decomposition method ($d > 1$). The numerical outcomes are summarized in tables and visualized in figures, generated through matlab.

Residual analysis :

- Table (3.2) reports the infinity norm of the residual error $\|R\|_\infty$ for each iteration, where the residual is defined by:

$$R = \max_{1\leq i\leq 2} \left\{ \mathscr{B}^i \check{\vartheta}_h^k - \mathscr{G}^i\left(\check{\vartheta}_h^{k-1}\right)\right\}.$$

- The results indicate that the residual decreases steadily with each iteration, reflecting the stability and accuracy of the finite difference discretization.
- Configurations with overlap ($d > 1$) exhibit a faster decline in residuals, confirming that overlapping subdomains enhance the convergence speed and improve numerical precision.

Table 3.2: **Infinity norm of the residual error.**

Iteration	DDM: $d > 1$	DDM: $d = 1$
1	7.3910e-04	9.5913e-04
4	1.6080e-04	2.3635e-04
8	3.6307e-05	5.8367e-05
Last iteration	2.1623e-05	3.6670e-05

Evolution of solution sequences :

The convergence of the lower and upper solution sequences at the grid point $(x, y)^\top = (0.5, 0.25)^\top$ with $h = 1/20$ is illustrated in Tables (3.3) and (3.4).

- Table (3.3) shows the progression of the upper solution $\hat{\vartheta}_h^k$, which decreases monotonically with iterations, gradually approaching the target value.
- Table (3.4) displays the evolution of the lower solution $\check{\vartheta}_h^k$, exhibiting increasing monotonic convergence.

- In both sequences, increasing the overlap parameter ($d > 1$) accelerates convergence, requiring fewer iterations to reach high-accuracy approximations.

Table 3.3: **Upper solution $\hat{\vartheta}_h^k$ at $(0.5, 0.25)$ for $h = 1/20$.**

Iteration	DDM: $d > 1$	DDM: $d = 1$
1	-0.00418351	-0.00380439
4	-0.00560505	-0.00519486
8	-0.00561998	-0.00555738
Last iteration	-0.00561999	-0.00561992

Table 3.4: **Lower solution $\check{\vartheta}_h^k$ at $(0.5, 0.25)$ for $h = 1/20$.**

Iteration	DDM: $d > 1$	DDM: $d = 1$
1	-0.38797945	-0.63728425
4	-0.04825616	-0.17337723
8	-0.00575788	-0.04453074
Last iteration	-0.00562000	-0.00562008

Graphical representation of the Schwarz iterative reconstruction

The following figures (3.1) illustrate the progressive construction of the approximate solution obtained by the overlapping domain decomposition method.

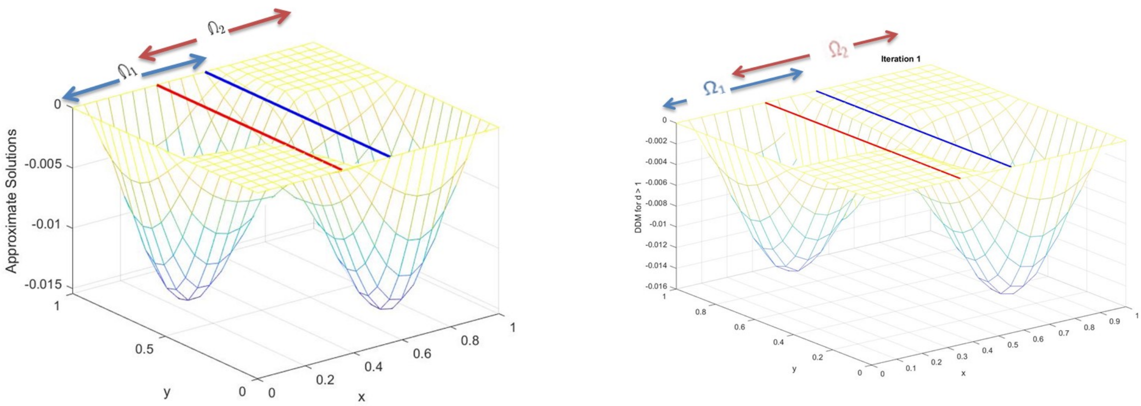

Figure 3.1: **Schwarz iterations for the approximate solution.**

- The first graphical representation corresponds to the initial Schwarz iteration, where the approximation is still strongly influenced by the decomposition of the computational domain.
- The second representation illustrates the final converged iteration obtained after the stabilization of the iterative process.
- The evolution from the initial approximation toward the final state clearly shows how the global solution is progressively reconstructed through information exchange between overlapping subdomains.

- The overlap region plays a fundamental role in transmitting interface information and reducing discontinuities between neighboring subdomains.
- The smooth matching observed near the interfaces confirms the efficiency of the overlap transmission conditions and the stability of the proposed decomposition strategy.

Convergence analysis and residual behavior

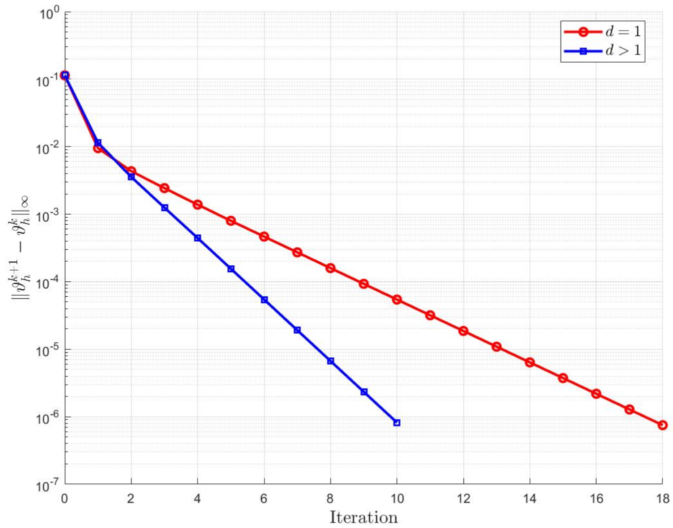

Figure 3.2: **Convergence behavior of the iterative scheme.**

- Figure (3.2) presents the evolution of the error measured in the L^∞-norm between successive iterations.
- The observed decay confirms the expected geometric convergence of the iterative scheme.
- Notably, increasing the overlap accelerates convergence, reducing both the total number of iterations and the computational time, which aligns with theoretical predictions.

Maximum residual across the domain

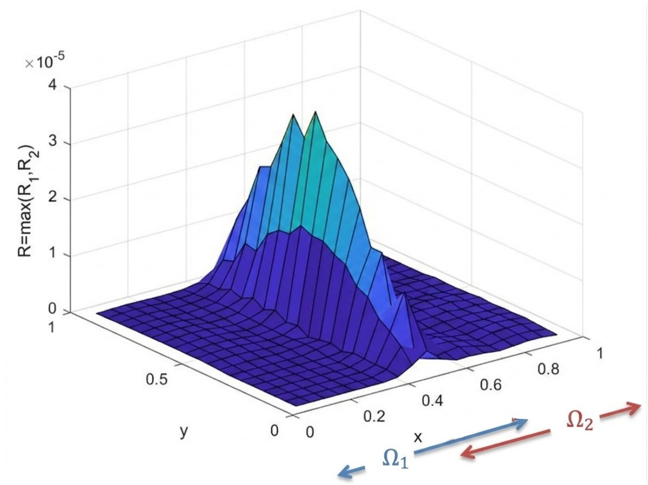

Figure 3.3: **Maximum residual over the computational domain.**

- Figure (3.3) displays the maximum residual, defined as

$$R = \max_{1 \leq i \leq 2} \left\{ \mathscr{B}^i \check{\vartheta}_h^k - \mathscr{G}^i(\check{\vartheta}_h^{k-1}) \right\},$$

  which quickly attains very small values ($\sim 10^{-5}$) in the overlap region between subdomains.

- This observation emphasizes the rapid stabilization of the scheme and confirms its efficiency in converging towards the numerical solution.

Chapter four :

Computational approaches to asymptotic behavior for QVI systems related to the HJB evolutionary equation

The numerical treatment of stationary HJB equations has witnessed significant progress over the years, with several effective methods proposed in the literature; see, for instance, [31,33,44] and references therein. Among the notable contributions, Lions and Mercier [43] introduced two iterative algorithms for solving elliptique HJB equations, where each iteration involves solving either a linear complementarity problem or a linear system of equations. Later, Boulbrachene and Haiour [22] conducted a finite element approximation study for the stationary version of problem (4.1), using the subsolution method and relying on the Bensoussan-Lions algorithm [7]. They successfully derived a quasi-optimal error estimate in the L^∞-norm, stated as follows:

$$\|\vartheta^\infty - \vartheta_h^m\|_{L^\infty} \leq Ch^2 \,|\log h|^2,$$

In a recent work (see [5]), exploiting the above arguments, where we have analyzed the semi-implicit time scheme combined with a finite-element spatial approximation for the system of parabolic quasi-variational inequalities, we derived the following error estimate:

$$\|\vartheta^\infty - \vartheta_h^m\|_{L^\infty} \leq C \left(h^2 \,|\log h|^4 + \left(\frac{1}{1+\gamma\Delta t} \right)^m \right),$$

where C is a constant independent of both h and Δt, and γ denotes the coercivity constant associated with the bilinear forms. The discrete solution ϑ_h^k is computed at each time level $t_k = k\Delta t$, $k = 1, \ldots, m$, with final time $T = m\Delta t$. In particular, ϑ_h^m denotes the solution at the final time. Moreover, ϑ^∞ is the asymptotic solution of the corresponding stationary problem.

Building on these theoretical and numerical foundations, this work focuses on the numerical solution of a non-coercive parabolic quasi-variational inequality (QVI) system associated with Hamilton–Jacobi–Bellman (HJB) equations arising in deterministic optimal control problems.

To treat this problem, a backward Euler time discretization is first applied, which transforms the original parabolic QVI system into a sequence of elliptic QVI problems linked to a coercive HJB formulation. This reformulation provides a suitable framework for the subsequent analysis.

A fully discrete scheme is then constructed using finite element discretization in space. To efficiently solve the resulting algebraic problems, an overlapping Schwarz domain decomposition method is developed in two settings. For two subdomains, the method is applied directly to the HJB formulation, which is equivalent to the original QVI system, while for a general decomposition into q subdomains, it is applied directly to the QVI system. In both cases, the iterative process is built using sub- and super-solutions to ensure convergence. This framework allows us to establish monotonicity and geometric convergence of the algorithm.

Moreover, the analysis leads to a quasi-optimal error estimate in the L^∞-norm of the form:

$$\|\vartheta^\infty - \vartheta_h^m\|_{L^\infty} \leq Ch^2|\log h|^3.$$

Finally, numerical experiments based on finite element discretization confirm the theoretical results and illustrate the accuracy and efficiency of the proposed method for this class of problems.

Contents

4.1 Continuous non-coercive QVI system related to HJB equations

4.1.1 Mathematical description of the non-coercive QVI system

In this section, we examine the continuous representation of an evolutionary QVI system that arises in connection with HJB equations and is subject to homogeneous Dirichlet boundary conditions. The system under consideration characterizes a class of fully nonlinear, non-coercive, time-dependent problems, where the dynamics are governed by a supremum over a finite set of second-order elliptic operators. The system can be stated as follows:

$$\text{find } \left(\vartheta^1, \vartheta^2, \ldots, \vartheta^n\right) \in \left[L^2\left(0, T; H_0^1(\Omega)\right)\right]^n,$$

such that for each $i = 1, \ldots, n$:

$$\begin{cases} \left\langle \dfrac{\partial \vartheta^i}{\partial t}, u - \vartheta^i \right\rangle + a^i\langle \vartheta^i, u - \vartheta^i\rangle \geq \langle \mathbb{F}^i, u - \vartheta^i\rangle, & \forall u \in H_0^1(\Omega), \\ \vartheta^i \leq \kappa + \vartheta^{i+1}, \quad u \leq \kappa + \vartheta^{i+1}, & \text{in } Q, \\ \vartheta^i(x, 0) = \vartheta_0^i(x), & \text{in } \Omega. \end{cases} \tag{4.1}$$

The main elements of this framework include:

- The spatial domain $\Omega \subset \mathbb{R}^N$ is bounded with a sufficiently smooth boundary $\partial\Omega$, and the spatial dimension satisfies $N \geq 1$.
- The temporal interval is $[0, T]$ for a fixed $T < \infty$, and the corresponding space-time domain is $Q = \Omega \times [0, T] \subset \mathbb{R}^N \times \mathbb{R}$.
- The operators $\mathbb{A}^i$, $i = 1, \ldots, n$, are uniformly elliptic second-order differential operators with variable coefficients, as defined in (2.2).
- Each $\mathbb{A}^i$ corresponds to a bilinear form $a^i\langle\cdot,\cdot\rangle$, described in (2.3), which may not satisfy a coercivity condition.
- The coefficient functions $a_{zs}^i(x), a_s^i(x), a_0^i(x)$ belong to $(L^\infty(\Omega) \cap C^2(\overline{\Omega}))^n$ for all $x \in \overline{\Omega}$ and $1 \leq z, s \leq N$, satisfying the regularity and boundedness conditions in (2.4), (2.5), and (2.6).
- The source terms $\mathbb{F}^i$ are non-negative and sufficiently smooth:

$$\mathbb{F}^i \in \left(L^2(0, T; L^\infty(\Omega)) \cap C^2(0, T; H^{-1}(\Omega))\right)^n, \quad \mathbb{F}^i \geq 0.$$

For analytical purposes, it is often useful to consider a family of parabolic inequalities that approximate the solution. Specifically, we seek $(\vartheta^1, \ldots, \vartheta^n) \in [L^2(0, T; H_0^1(\Omega))]^n$ satisfying, for $i = 1, \ldots, n$:

$$\begin{cases} \dfrac{\partial \vartheta^i}{\partial t} + \mathbb{A}^i\vartheta^i \leq \mathbb{F}^i, & \text{in } Q, \\ \vartheta^i \leq \kappa + \vartheta^{i+1}, \quad \vartheta^{n+1} = \vartheta^1, & \text{in } Q, \\ \left\langle \frac{\partial \vartheta^i}{\partial t} + \mathbb{A}^i\vartheta^i - \mathbb{F}^i \right\rangle \cdot \left\langle \vartheta^i - (\kappa + \vartheta^{i+1}) \right\rangle = 0, & \text{in } Q, \\ \vartheta^i(x, 0) = \vartheta_0^i(x), & \text{in } \Omega, \\ \vartheta^i = 0, & \text{on } \partial\Omega. \end{cases} \tag{4.2}$$

This formulation represents an equivalent version of the original variational inequality with a max-structure and is closely related to approaches used for stationary HJB problems (see, e.g., [2, 35]).

From an abstract variational perspective, system (4.2) can be interpreted as a continuous, non-coercive parabolic HJB problem:

$$\begin{cases} \max\limits_{1\leq i\leq n}\left(\dfrac{\partial\vartheta}{\partial t}+\mathbb{A}^i\vartheta-\mathbb{F}^i\right)=0, & \text{in } Q,\\ \vartheta=0, & \text{on } \partial\Omega,\\ \vartheta(x,0)=\vartheta_0(x), & \text{in } \Omega. \end{cases} \tag{4.3}$$

Previous studies [13, 15] confirm the existence, uniqueness, of the parabolic QVI (4.1).

4.1.2 Transformation into elliptic coercive QVI system related to HJB

Following the approach in [13], a semi-implicit time discretization together with a finite element spatial discretization is applied to reformulate the original parabolic Hamilton–Jacobi–Bellman (HJB) problem as an elliptic coercive system. The method starts with a backward scheme in time while preserving the variational inequality structure.

For each time level $k=1,\ldots,m$ and each index $i=1,\ldots,n$, one seeks $\vartheta^{i,k}\in H_0^1(\Omega)$ such that:

$$\begin{cases} \left\langle\dfrac{\vartheta^{i,k}-\vartheta^{i,k-1}}{\Delta t},u-\vartheta^{i,k}\right\rangle+a^i\langle\vartheta^{i,k},u-\vartheta^{i,k}\rangle\geq\langle\mathbb{F}^i,u-\vartheta^{i,k}\rangle,\\ \vartheta^{i,k}\leq\kappa+\vartheta^{i+1,k},\quad u\leq\kappa+\vartheta^{i+1,k},\quad \forall u\in H_0^1(\Omega),\\ \vartheta^{i,0}(x)=\vartheta_0^i,\quad \text{in } \Omega. \end{cases} \tag{4.4}$$

where the time step is:

$$\Delta t=\frac{T}{m}. \tag{4.5}$$

This system can be rewritten as a coercive elliptic QVI:

$$\begin{cases} \dfrac{1}{\Delta t}\langle\vartheta^{i,k},u-\vartheta^{i,k}\rangle+b^i\langle\vartheta^{i,k},u-\vartheta^{i,k}\rangle\geq\langle\mathbb{F}^i+(\mu+\dfrac{1}{\Delta t})\vartheta^{i,k-1},u-\vartheta^{i,k}\rangle,\\ \vartheta^{i,k}\leq\kappa+\vartheta^{i+1,k},\quad u\leq\kappa+\vartheta^{i+1,k},\quad \forall u\in H_0^1(\Omega),\\ \vartheta^{n+1,k}=\vartheta^{1,k},\quad \kappa>0,\quad i=1,\ldots,n,\\ \vartheta^{i,0}(x)=\vartheta_0^i. \end{cases} \tag{4.6}$$

We introduce the following notation for clarity:

$$\theta=\frac{1}{\Delta t}=\frac{m}{T}.$$

Moreover, the bilinear form $b^i\langle,.\rangle$ is decomposed as:

$$b^i\langle\vartheta^{i,k},u-\vartheta^{i,k}\rangle=\mu\langle\vartheta^{i,k},u-\vartheta^{i,k}\rangle+a^i\langle\vartheta^{i,k},u-\vartheta^{i,k}\rangle.$$

Thus, system (4.6) can be compactly rewritten as:

$$\begin{cases} c^i\langle\vartheta^{i,k},u-\vartheta^{i,k}\rangle\geq\langle\mathbb{F}^i+\eta\vartheta^{i,k-1},u-\vartheta^{i,k}\rangle,\\ \vartheta^{i,k}\leq\kappa+\vartheta^{i+1,k},\quad u\leq\kappa+\vartheta^{i+1,k},\quad \forall u\in H_0^1(\Omega),\\ \vartheta^{n+1,k}=\vartheta^{1,k},\quad \kappa>0,\quad i=1,\ldots,n,\\ \vartheta^{i,0}(x)=\vartheta_0^i. \end{cases} \tag{4.7}$$

where:

$$c^i\langle\vartheta^{i,k}, u-\vartheta^{i,k}\rangle = \theta\langle\vartheta^{i,k}, u-\vartheta^{i,k}\rangle + b^i\langle\vartheta^{i,k}, u-\vartheta^{i,k}\rangle,$$

or equivalently:

$$c^i\langle\vartheta^{i,k}, u-\vartheta^{i,k}\rangle = \eta\langle\vartheta^{i,k}, u-\vartheta^{i,k}\rangle + a^i\langle\vartheta^{i,k}, u-\vartheta^{i,k}\rangle, \quad \eta = \mu+\theta.$$

The coercivity property holds:

$$c^i\langle u, u\rangle \geq \lambda\|u\|^2_{H^1(\Omega)}.$$

Hence, the sequence of coercive elliptic quasi-variational inequalities (4.7) corresponds to the fully continuous coercive HJB formulation:

$$\text{find } \vartheta^k = (\vartheta^{1,k}, \ldots, \vartheta^{n,k}) \in (H^1_0(\Omega))^n :$$

$$\begin{cases} \max\limits_{1\leq i\leq n} \left(\mathbb{C}^i\vartheta^k - \mathbb{Z}^i(\vartheta^{k-1})\right) = 0, & \text{in } \Omega, \\ \vartheta^k = 0, & \text{on } \partial\Omega, \\ \vartheta^k(x,0) = \vartheta^k_0, & \text{in } \Omega. \end{cases} \tag{4.8}$$

where the operators are given by:

$$\mathbb{C}^i = \mathbb{A}^i + \mu I, \quad \mathbb{Z}^i(\vartheta^{k-1}) = \mathbb{F}^i + \eta\vartheta^{k-1},$$

or equivalently,

$$\mathbb{C}^i = \mathbb{B}^i + \theta I, \quad \mathbb{Z}^i(\vartheta^{k-1}) = G^i(\vartheta^{k-1}) + \theta\vartheta^{k-1}, \quad G^i(\vartheta^{k-1}) = \mathbb{F}^i + \mu\vartheta^{k-1}.$$

Here, $\mathbb{C}^i$ denotes the coercive operator associated with the bilinear form:

$$c^i\langle u, u\rangle = \int_\Omega \sum_{z,s=1}^{N} a_{zs}(x)\frac{\partial u}{\partial x_z}\frac{\partial u}{\partial x_s} + \sum_{s=1}^{N} a_s(x)\frac{\partial u}{\partial x_s}u + (a_0(x)+\eta)u^2\,dx.$$

Here:

- μ is the coercivity constant introduced in Chapter 3.
- θ represents the inverse of the time step, defined by $\theta = m/T$.

4.1.3 Existence and uniqueness of the continuous problem

To prove the existence and uniqueness of solutions for the continuous quasi-variational inequality system, we proceed following an approach inspired by the iterative techniques used for elliptic problems in Chapter 1. The main steps are outlined as follows.

We introduce a fixed-point mapping [21] defined by:

$$\begin{aligned} T : H^+ &\longrightarrow \left(L^\infty_+(\Omega)\right)^n, \\ V &\longmapsto TV = \left(\vartheta^{1,k}, \ldots, \vartheta^{n,k}\right). \end{aligned}$$

where each component $\vartheta^{i,k}$ is the solution of a coercive quasi-variational inequality depending on the previous iterate $V = (v^1, \ldots, v^n)$. For each $i = 1, \ldots, n$ and time level $k = 1, \ldots, m$, satisfies:

$$\begin{cases} c^i\langle\vartheta^{i,k}, u-\vartheta^{i,k}\rangle \geq \langle\mathbb{F}^i, u-\vartheta^{i,k}\rangle + \eta\langle v^i, u-\vartheta^{i,k}\rangle, \quad \forall u \in H^1_0(\Omega), \\ \vartheta^{i,k} \leq \kappa + v^{i+1}, \quad u \leq \kappa + v^{i+1}, \\ \vartheta^{n,k} = \vartheta^{1,k}. \end{cases} \tag{4.9}$$

Theorem 4.1.1: [21]

Under the previous hypotheses and notations, the mapping T is a contraction in $(L^\infty_+(\Omega))^n$ with a rate of contraction $\frac{1}{1+\Delta t\gamma}$. Therefore, T admits a unique fixed point which coincides with the solution of problem (4.1) or (4.9).

4.2 The discrete non-coercive QVI system related to HJB

This section develops the fully discrete formulation of the non-coercive QVI system associated with HJB equations using a finite element spatial discretization.

4.2.1 Finite element discretization

The spatial domain Ω is subdivided into triangular elements, generating a mesh τ^h with mesh size $h > 0$. The mesh family is assumed to be regular and quasi-uniform.

Let $\{\varphi_z\}_{z=1}^{N(h)}$ denote the standard continuous piecewise affine basis functions associated with τ^h, satisfying the nodal property:

$$\varphi_z(A_s) = \delta_{zs},$$

where A_s are the mesh vertices. The corresponding finite element space is defined by:

$$V_h = \Big\{u \in (L^2(0,T;H_0^1(\Omega))\cap C(0,T;H_0^1(\overline{\Omega})))^n : u|_K \in P_1\ \forall K \in \tau^h,\ \vartheta(\cdot,0) = \vartheta_0 \text{ in } \Omega,\ \vartheta = 0 \text{ on } \partial\Omega\Big\},$$

where P_1 is the space of polynomials of degree one. Let r_h denote the nodal interpolation operator:

$$r_h u = \sum_{z=1}^{N(h)} u(A_z)\,\varphi_z(x), \qquad \forall u \in L^2(0,T;H_0^1(\Omega)) \cap C(0,T;H_0^1(\overline{\Omega})). \tag{4.10}$$

To ensure stability and monotonicity of the discrete system, we assume that the stiffness matrices $\mathscr{A}^i = (a^i\langle\varphi_z,\varphi_s\rangle)_{zs}$ satisfy the M-matrix property for all $1 \le i \le n$. This is essential to preserve the qualitative behavior of the solution and to guarantee convergence.

4.2.2 Discrete quasi-variational inequality system formulation

In this section, we present the discrete formulation of the time-dependent QVI system. For each i, the discrete QVI system reads:

$$\begin{cases} \left\langle \dfrac{\partial \vartheta_h^i}{\partial t}, u_h - \vartheta_h^i \right\rangle + a^i\langle\vartheta_h^i, u_h - \vartheta_h^i\rangle \ge \left\langle \mathscr{F}^i, u_h - \vartheta_h^i\right\rangle, \quad \forall u_h \in V_h, \\ \vartheta_h^i \le r_h(\kappa + \vartheta_h^{i+1}), \quad u_h \le r_h(\kappa + \vartheta_h^{i+1}), \\ \vartheta_h^i(x,0) = \vartheta_{h,0}^i(x). \end{cases} \tag{4.11}$$

In algebraic form, the discrete variational inequality is expressed as:

$$\frac{\partial \vartheta_h^i}{\partial t} + \mathscr{A}^i\vartheta_h^i \le \mathscr{F}^i, \quad \vartheta_h^i \le r_h(\kappa + \vartheta_h^{i+1}), \quad \vartheta_h^{n+1} = \vartheta_h^1,$$

with complementarity condition:

$$\left(\frac{\partial \vartheta_h^i}{\partial t} + \mathscr{A}^i\vartheta_h^i - \mathscr{F}^i\right)\left(\vartheta_h^i - r_h(\kappa + \vartheta_h^{i+1})\right) = 0.$$

Combining the above, the non-coercive, time-dependent HJB problem in discrete form is:

$$\max_{1\le i\le n}\Big(\frac{\partial\vartheta_h}{\partial t}+\mathscr{A}^i\vartheta_h-\mathscr{F}^i\Big)=0,\quad \forall\vartheta_h\in V_h. \tag{4.12}$$

4.2.3 Reformulation as a discrete elliptic coercive QVI system related to HJB

In this section, we describe the transformation of the discrete non-coercive QVI system into a family of coercive elliptic QVI systems through a combination of spatial discretization and semi-implicit time-stepping.

We consider a finite-dimensional subspace $V_h\subset H_0^1(\Omega)$ to approximate the solution at discrete mesh points.

Let $t_k=k\Delta t$ for $k=0,\dots,m$. At each time level, we seek an approximate solution $\vartheta_h^{i,k}\in(V_h)$ starting from the initial data $\vartheta_h^{i,0}=\vartheta_0^i$. The semi-discrete problem, combining space and time, is: for $k=1,\dots,m$, find $\vartheta_h^{i,k}\in(V_h)$ such that:

$$\begin{cases}\Big\langle\dfrac{\vartheta_h^{i,k}-\vartheta_h^{i,k-1}}{\Delta t},u_h-\vartheta_h^{i,k}\Big\rangle+a^i\langle\vartheta_h^{i,k},u_h-\vartheta_h^{i,k}\rangle\ge\langle\mathscr{F}^i,u_h-\vartheta_h^{i,k}\rangle,\\ \vartheta_h^{i,k}\le r_h(\kappa+\vartheta_h^{i+1,k}),\quad u_h\le r_h(\kappa+\vartheta_h^{i+1,k}),\quad i=1,\dots,n,\\ \vartheta_h^{i,0}(x)=\vartheta_{0,h}^i(x).\end{cases} \tag{4.13}$$

The equivalent formulation is obtained by bringing the previous time level to the right-hand side:

$$\begin{cases}\Big\langle\dfrac{\vartheta_h^{i,k}}{\Delta t},u_h-\vartheta_h^{i,k}\Big\rangle+a^i\langle\vartheta_h^{i,k},u_h-\vartheta_h^{i,k}\rangle\ge\Big\langle\mathscr{F}^i+\dfrac{\vartheta_h^{i,k-1}}{\Delta t},u_h-\vartheta_h^{i,k}\Big\rangle,\\ \vartheta_h^{i,k}\le r_h(\kappa+\vartheta_h^{i+1,k}),\quad u_h\le r_h(\kappa+\vartheta_h^{i+1,k}),\\ \vartheta_h^{i,0}(x)=\vartheta_{0,h}^i(x).\end{cases} \tag{4.14}$$

Introducing the coercive bilinear form:

$$b^i\langle\vartheta_h^{i,k},u_h-\vartheta_h^{i,k}\rangle=\mu\langle\vartheta_h^{i,k},u_h-\vartheta_h^{i,k}\rangle+a^i\langle\vartheta_h^{i,k},u_h-\vartheta_h^{i,k}\rangle,$$

the system (4.14) can be rewritten as a sequence of elliptic coercive QVIs:

$$\begin{cases}c^i\langle\vartheta_h^{i,k},u_h-\vartheta_h^{i,k}\rangle\ge\Big\langle\mathscr{F}^i+\eta\vartheta_h^{i,k-1},u_h-\vartheta_h^{i,k}\Big\rangle,\\ \vartheta_h^{i,k}\le r_h(\kappa+\vartheta_h^{i+1,k}),\quad \vartheta_h^{n+1,k}=\vartheta_h^{1,k},\quad i=1,\dots,n,\\ \vartheta_h^{i,0}(x)=\vartheta_{0,h}^i(x),\end{cases} \tag{4.15}$$

where the coercive form is defined by:

$$c^i\langle\vartheta_h^{i,k},u_h-\vartheta_h^{i,k}\rangle=\theta\langle\vartheta_h^{i,k},u_h-\vartheta_h^{i,k}\rangle+b^i\langle\vartheta_h^{i,k},u_h-\vartheta_h^{i,k}\rangle,\quad \eta=\mu+\theta.$$

This construction ensures that each time-discrete problem is a coercive elliptic quasi-variational inequality, which is suitable for analysis and numerical approximation.

4.2.4 Discrete approximation of the HJB related QVI system

In this section, we describe the approximation of the continuous elliptic quasi-variational inequality (EQVI) system using a discrete Hamilton–Jacobi–Bellman (HJB) formulation. The main idea is to represent the variational inequality problem through finite-dimensional operators in order to construct efficient iterative and numerical solution procedures.

Let $\mathscr{A}^i$ denote the finite element matrices associated with the bilinear forms $a^i\langle .,.\rangle$, defined by:

$$(\mathscr{A}^i)_{zs} = a^i\langle \varphi_z, \varphi_s\rangle, \quad 1 \leq i \leq n, \quad 1 \leq z, s \leq N(h).$$

We also introduce the matrices $\mathscr{B}^i$, associated with the coercive bilinear forms $b^i\langle .,.\rangle$, given by:

$$(\mathscr{B}^i)_{zs} = b^i\langle \varphi_z, \varphi_s\rangle,$$

where:

$$b^i\langle \varphi_z, \varphi_s\rangle = a^i\langle \varphi_z, \varphi_s\rangle + \mu\langle \varphi_z, \varphi_s\rangle.$$

The matrices $\mathcal{C}^i$, corresponding to the fully discretized c^i, are defined by:

$$(\mathcal{C}^i)_{zs} = c^i\langle \varphi_z, \varphi_s\rangle.$$

The bilinear form $c^i\langle .,.\rangle$ admits the equivalent representations:

$$c^i\langle \varphi_z, \varphi_s\rangle = b^i\langle \varphi_z, \varphi_s\rangle + \theta\langle \varphi_z, \varphi_s\rangle = a^i\langle \varphi_z, \varphi_s\rangle + \eta\langle \varphi_z, \varphi_s\rangle.$$

Using these matrices together with the semi-implicit discretization scheme, the EQVI system (4.7) can be approximated by the following discrete HJB problem: find

$$\vartheta^k = (\vartheta^{1,k}, \ldots, \vartheta^{n,k}) \in (H_0^1(\Omega))^n,$$

such that:

$$\max_{1\leq i\leq n} \left(\mathbb{C}^i\vartheta^k - \mathbb{Z}^i(\vartheta^{k-1})\right) = 0.$$

The finite element discretization of system (4.15) takes the form:

$$\vartheta_h^k = (\vartheta_h^{1,k}, \ldots, \vartheta_h^{n,k}) \in (V_h)^n,$$

such that:

$$\max_{1\leq i\leq n} \left(\mathcal{C}^i\vartheta_h^k - \mathcal{Z}^i(\vartheta_h^{k-1})\right) = 0. \tag{4.16}$$

The discrete operators $\mathcal{C}^i$ and $\mathcal{Z}^i$ can be written in the equivalent forms:

$$\mathcal{C}^i = \mathscr{A}^i + \eta I, \quad \mathcal{Z}^i(\vartheta_h^{k-1}) = \mathscr{F}^i + \eta\vartheta_h^{k-1},$$

or alternatively,

$$\mathcal{C}^i = \mathscr{B}^i + \theta I, \quad \mathcal{Z}^i(\vartheta_h^{k-1}) = \mathscr{G}^i(\vartheta_h^{k-1}) + \theta\vartheta_h^{k-1},$$

with:

$$\mathscr{G}^i(\vartheta_h^{k-1}) = \mathscr{F}^i + \mu\vartheta_h^{k-1}.$$

4.2.5 Existence and uniqueness of the discrete QVI system

To establish the well-posedness of the discrete quasi-variational inequality system, we adapt the continuous analysis framework to the discrete setting while taking into account the properties of the finite-dimensional operators and the associated discrete data.

We introduce the mapping T_h defined on the positive cone H^+ by:

$$
\begin{aligned}
T_h : H^+ &\longrightarrow (V_h)^n, \\
V &\longmapsto T_h(V) = \left(\vartheta_h^{1,k}, \ldots, \vartheta_h^{n,k}\right).
\end{aligned}
$$

For each index $i = 1, \ldots, n$, the component $\vartheta_h^{i,k}$ satisfies the following discrete coercive quasi-variational inequality system:

$$
\begin{cases}
c^i \left\langle \vartheta_h^{i,k}, u_h - \vartheta_h^{i,k} \right\rangle \geq \left\langle \mathscr{F}^i, u_h - \vartheta_h^{i,k} \right\rangle + \eta \left\langle v^i, u_h - \vartheta_h^{i,k} \right\rangle, \quad \forall u_h \in V_h, \\
\vartheta_h^{i,k} \leq r_h(\kappa + v^{i+1}), \quad u_h \leq r_h(\kappa + v^{i+1}), \\
\vartheta_h^{n,k} = \vartheta_h^{1,k}.
\end{cases}
\tag{4.17}
$$

The following proposition establishes the existence and uniqueness of the discrete solution.

Proposition 4.2.1: [5]

Under the d.m.p , and the previous hypotheses and notations, the mapping $T_h$is a contraction in H^+ with a rate of contraction: $\frac{1}{1+\Delta t\,\gamma}$. Therefore, T_h admits a unique fixed point which coincides with the solution of problem (4.15) or (4.17).

4.2.6 Error analysis on L^∞

In this section, we derive an estimate of the error between the continuous stationary solution and its discrete approximation. This result provides a quantitative measure of the accuracy of the numerical method and confirms its convergence behavior.

Theorem 4.2.1: [13]

Under the previous assumptions and the maximum principle, there exists a constant C, independent of h, such that:

$$
\|\vartheta_h^\infty - \vartheta^\infty\|_\infty = \max_{1\leq i\leq n} \left\|\vartheta^{i,\infty} - \vartheta_h^{i,\infty}\right\|_\infty \leq Ch^2 |\log h|^3.
$$

Where $\vartheta^{i,\infty}$ is an asymptotic continuous solution and $\vartheta_h^{i,\infty}$ denotes the discrete solution at the final time $T = m\Delta t$, satisfy the stationary forms of the corresponding continuous and discrete variational inequalities: [22]:

$$
c^i \left(\vartheta^{i,\infty}, u - \vartheta^{i,\infty}\right) \geq \left(\mathbb{F}^i + \eta\vartheta^{i,\infty}, u - \vartheta^{i,\infty}\right), \quad \forall u \in H_0^1(\Omega), \tag{4.18}
$$

$$
c^i \left(\vartheta_h^{i,\infty}, u_h - \vartheta_h^{i,\infty}\right) \geq \left(\mathscr{F}^i + \eta\vartheta_h^{i,\infty}, u_h - \vartheta_h^{i,\infty}\right), \quad \forall u_h \in V_h. \tag{4.19}
$$

Remark 4.2.1

Although the discrete problem, such as equation (4.15), is written using the indices k and $k-1$, the convergence analysis of the Schwarz iterative method is naturally formulated through the transition from k to $k+1$. This notation is consistent with the recursive structure of the algorithm and facilitates the treatment of initialization, iterative updates, and convergence proofs.

4.3 Domain decomposition approach for parabolic QVI systems related to HJB

In this section, we investigate the asymptotic behavior of numerical approximations for non-coercive parabolic QVI systems associated with HJB equations. We employ a backward scheme for temporal discretization, which transforms the parabolic problem into a sequence of coercive elliptic QVIs (or equivalently, HJB problems) that can be solved independently at each time step. Building upon the methodology introduced in Chapters 2 and 3, a domain decomposition strategy is applied to ensure stability and facilitate convergence. The approach is further generalized to q overlapping subdomains, allowing for flexible handling of complex geometries. Convergence analysis establishes monotone behavior of the iterative process and provides an L^∞ error bound derived from geometric contraction principles.

4.3.1 Overlapping decomposition with two subdomains

We first consider the classical scenario involving two overlapping subdomains. The global discrete system is decomposed into local subproblems, which are solved iteratively while exchanging boundary information over the overlapping region. This procedure preserves the monotone structure of the discrete operator and guarantees convergence within the QVI framework.

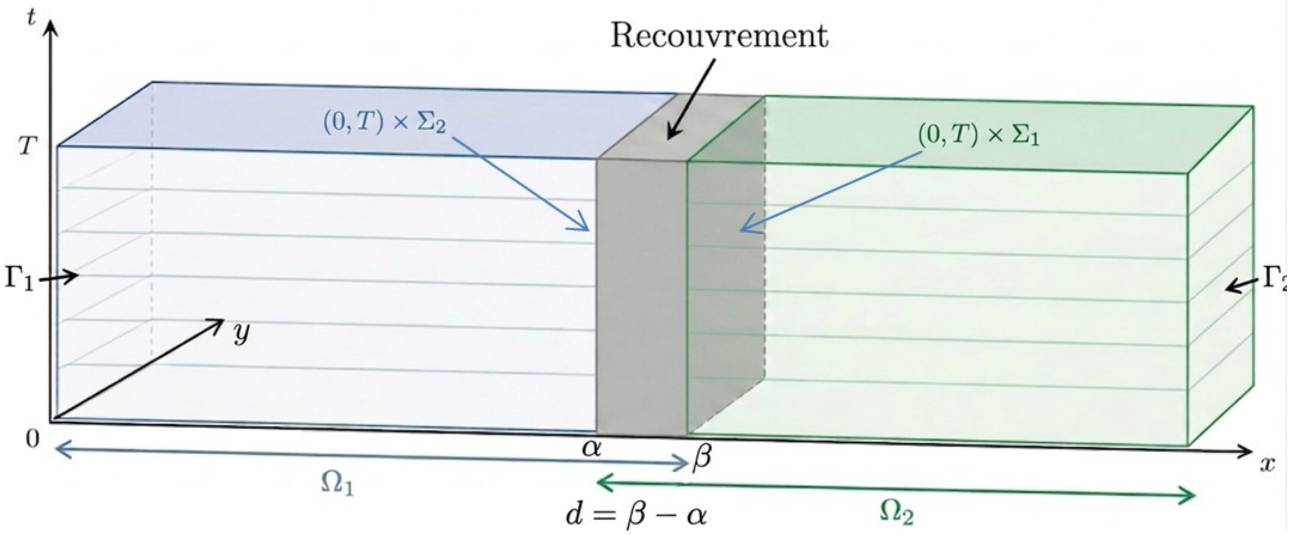

Figure 4.1: **Domain decomposition into 2 overlapping subdomains.**

The discrete solution is written in block form as:

$$\vartheta_h^k = \begin{pmatrix} \vartheta_{1h}^k \\ \vartheta_{2h}^k \end{pmatrix}, \qquad \mathcal{Z}^i(\vartheta_h^{k-1}) = \begin{pmatrix} \mathcal{Z}^i(\vartheta_{1h}^{k-1}) \\ \mathcal{Z}^i(\vartheta_{2h}^{k-1}) \end{pmatrix}, \qquad \mathcal{C}^i = \begin{pmatrix} \mathcal{C}_{1,1}^i & -\tilde{\mathcal{C}}_{1,2}^i \\ -\tilde{\mathcal{C}}_{2,1}^i & \mathcal{C}_{2,2}^i \end{pmatrix}.$$

Here $\mathcal{C}^i$ represents the discretized elliptic operator associated with the control index i, while $\mathcal{Z}^i$ denotes the discrete Hamiltonian term.

The discrete HJB equation is formulated as:

$$\max_{1\le i\le n} \left(\tilde{\mathcal{C}}^i \vartheta_h^k - \mathcal{Z}^i(\vartheta_h^{k-1}) \right) = 0, \quad \vartheta_h^k \in (V_h)^n$$

On the first subdomain Ω_1, the iterative problem is:

$$\begin{cases} \max\limits_{1\leq i\leq n} \Big(\mathcal{C}^i_{1,1}\vartheta^k_{1h} - \mathcal{Z}^i(\vartheta^{k-1}_{1h})\Big) = 0, & \\ (\vartheta^k_{1h})_\beta = (\vartheta^{k-1}_{2h})_\beta, & \text{on } \Sigma_1. \end{cases}$$

On the second subdomain Ω_2, we have:

$$\begin{cases} \max\limits_{1\leq i\leq n} \Big(\mathcal{C}^i_{2,2}\vartheta^k_{2h} - \mathcal{Z}^i(\vartheta^{k-1}_{2h})\Big) = 0, & \\ (\vartheta^k_{2h})_\alpha = (\vartheta^k_{1h})_\alpha, & \text{on } \Sigma_2. \end{cases}$$

The iteration can be written in each subdomain as follows:

$$\begin{cases} \max\limits_{1\leq i\leq n} \Big\{\mathcal{C}^i_{1,1}\vartheta^k_{1h} - \tilde{\mathcal{C}}^i_{1,2}\vartheta^{k-1}_{2h} - \mathcal{Z}^i(\vartheta^{k-1}_{1h})\Big\} = 0, \quad \text{in} \quad \Omega_1, \\ \max\limits_{1\leq i\leq n} \Big\{-\tilde{\mathcal{C}}^i_{2,1}\vartheta^k_{1h} + \mathcal{C}^i_{2,2}\vartheta^k_{2h} - \mathcal{Z}^i(\vartheta^{k-1}_{2h})\Big\} = 0, \quad \text{in} \quad \Omega_2. \end{cases}$$

For initialization, we construct a lower and an upper solution $\check{\vartheta}^0_h$ and $\hat{\vartheta}^0_h$ such that:

$$\max_{1\leq i\leq n} \Big\{\mathcal{C}^i\check{\vartheta}^0_h - \mathcal{Z}^i(\check{\vartheta}^0_h)\Big\} \leq 0, \qquad \max_{1\leq i\leq n} \Big\{\mathcal{C}^i\hat{\vartheta}^0_h - \mathcal{Z}^i(\hat{\vartheta}^0_h)\Big\} \geq 0.$$

Typically, one takes $\check{\vartheta}^0_h = (0,\ldots,0)$, while $\hat{\vartheta}^0_h$ is obtained by solving:

$$\mathcal{C}^i\hat{\vartheta}^0_h = \mathcal{Z}^i(\hat{\vartheta}^0_h), \quad i = 1,\ldots,n.$$

Algorithm 3: Iterative ODD for non-coercive parabolic HJB problems

Initialization: choose the initial supersolution $\hat{\vartheta}^0_h$, set $k = 1$.
Step 1: solve on Ω_1:

$$\max_{1\leq i\leq n} \Big\{\mathcal{C}^i_{1,1}\hat{\vartheta}^k_{1h} - \tilde{\mathcal{C}}^i_{1,2}\hat{\vartheta}^{k-1}_{2h} - \mathcal{Z}^i(\hat{\vartheta}^{k-1}_{1h})\Big\} = 0.$$

Step 2: solve on Ω_2:

$$\max_{1\leq i\leq n} \Big\{-\tilde{\mathcal{C}}^i_{2,1}\hat{\vartheta}^k_{1h} + \mathcal{C}^i_{2,2}\hat{\vartheta}^k_{2h} - \mathcal{Z}^i(\hat{\vartheta}^{k-1}_{2h})\Big\} = 0.$$

Step 3: check convergence. If not satisfied, set $k \leftarrow k+1$ and repeat Steps 1–2.

Theorem 4.3.1: [27]

The sequences $(\check{\vartheta}^k_h)$ and $(\hat{\vartheta}^k_h)$ generated by the DDM algorithm 3 are monotone, namely

$$\check{\vartheta}^k_h \leq \check{\vartheta}^{k+1}_h, \qquad \hat{\vartheta}^{k+1}_h \leq \hat{\vartheta}^k_h,$$

and they converge to the unique solution ϑ_h of the discrete HJB equation.

Theorem 4.3.2: [27]

The iterates (ϑ_h^k) generated by the DDM algorithm 3 are converge geometrically to the unique discrete solution of problem (4.11). There exists $0 < \rho < 1$ such that:

$$\|\vartheta_h^k - \vartheta_h^{k-1}\|_{L^\infty(\Omega)} \leq \rho^{k-1}\|\vartheta_h^1 - \vartheta_h^0\|_{L^\infty(\Omega)}, \quad k \in \mathbb{N}^*.$$

4.3.2 Generalized domain decomposition into q overlapping subdomains

To extend the Schwarz alternating strategy to a general setting, we consider the decomposition of the computational domain into q overlapping subdomains. The iterative scheme follows the same principle as the classical two-subdomain method: local problems are solved sequentially on each subdomain while information is exchanged along the overlapping regions. This construction guarantees monotone convergence of the sequence towards the unique discrete solution, and allows for establishing L^∞-error bounds.

Description of the method

Let Ω denote a bounded, connected, open subset of $\mathbb{R}^2$ with smooth boundary. We partition Ω into q overlapping subdomains, labeled $\Omega_1, \ldots, \Omega_q$, satisfying:

$$\Omega = \bigcup_{j=1}^{q} \Omega_j, \quad \Omega_j \cap \Omega_l \neq \emptyset, \quad j, l = \overline{1, q}, \quad j \neq l.$$

We assume that the solution ϑ restricted to each subdomain satisfies:

$$\vartheta_{|\Omega_j} \in W^{2,p}(\Omega_j), \quad j = \overline{1, q}, \quad 2 \leq p < \infty.$$

The boundary of each subdomain is denoted by: $\Gamma_j = \partial\Omega_j$, and the interface is defined as:

$$\Sigma_j = \partial\Omega_j \cap \Omega_l, \quad l \neq j, \quad j, l = \overline{1, q}.$$

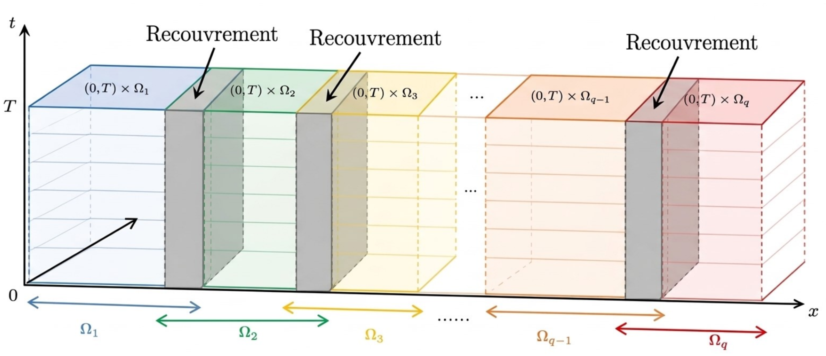

Figure 4.2: **Illustration of the domain Ω decomposed into q overlapping subdomains.**

Continuous domain decomposition algorithm

Building upon the continuous problem introduced in equation (4.7), we construct an iterative Schwarz scheme for q overlapping subdomains. For each subdomain Ω_j, the local sequence

$\vartheta_j^{i,k+1}$ is defined within the convex set $K_j^{i,k+1}$ and satisfies:

$$\begin{cases} c_j^i\langle \vartheta_j^{i,k+1}, u - \vartheta_j^{i,k+1}\rangle \geq \langle \mathbb{F}_j^i + \eta\vartheta_j^{i,k}, u - \vartheta_j^{i,k+1}\rangle, & \forall u \in H_0^1(\Omega), \\ \vartheta_j^{i,k+1} \leq \kappa + \vartheta_j^{i+1,k+1}, \quad i = \overline{1,n}, \\ \vartheta_j^{i,k+1} = \vartheta_l^{i,k+1_{jl}}, \quad u = \vartheta_l^{i,k+1_{jl}}, \quad \text{on } \Sigma_j. \end{cases}$$

The admissible set is:

$$\mathbb{K}_j^{i,k+1} = \{u \in H_0^1(\Omega) \,|\, u \leq \kappa + \vartheta_j^{i+1,k+1},\, u = \vartheta_l^{i,k+1_{jl}} \text{ on } \Sigma_j\}.$$

The interface indicator is:

$$1_{jl} = \begin{cases} 1, & j > l, \\ 0, & j < l. \end{cases}$$

Finally, the restriction of the global forcing term to subdomain Ω_j is expressed as :

$$\mathbb{F}_j^i + \eta\vartheta_j^{i,k} = (\mathbb{F}^i + \eta\vartheta^{i,k})_{|\Omega_j}, \quad \vartheta_j^i = \vartheta_{|\Omega_j}^i.$$

Discrete domain decomposition algorithm

At the discrete level, using the formulation in equation (4.15), the iterative Schwarz sequences $\vartheta_{jh}^{i,k+1}$, for $j = \overline{1,q}$, $i = \overline{1,n}$, and $k \in \mathbb{N}$, are defined on each subdomain Ω_j as follows:

$$\begin{cases} c_j^i\langle \vartheta_{jh}^{i,k+1}, u_h - \vartheta_{jh}^{i,k+1}\rangle \geq \langle \mathscr{F}_j^i + \eta\vartheta_{jh}^{i,k}, u_h - \vartheta_{jh}^{i,k+1}\rangle, & \forall u_h \in V_h, \\ \vartheta_{jh}^{i,k+1} \leq \kappa + \vartheta_{jh}^{i+1,k+1}, \quad u_h \leq \kappa + \vartheta_{jh}^{i+1,k+1}, & i = \overline{1,n}, \\ \vartheta_{jh}^{i,k+1} = \vartheta_{lh}^{i,k+1_{jl}}, \quad u_h = \vartheta_{lh}^{i,k+1_{jl}}, & \text{on } \Sigma_j. \end{cases} \tag{4.20}$$

with the discrete admissible set:

$$\mathbb{K}_{jh}^{i,k+1} = \{u_h \in V_h \,|\, u_h \leq \kappa + \vartheta_{jh}^{i+1,k+1},\, u_h = \vartheta_{lh}^{i,k+1_{jl}} \text{ on } \Sigma_j\}.$$

Schwarz algorithm for iterative domain decomposition

The Schwarz iterative procedure solves partial differential equations by partitioning the computational domain into q overlapping subdomains. The global solution is obtained through repeated updates on each subdomain, exchanging interface values at the overlaps, until convergence is reached. The procedure can be summarized as follows:

- **Lower solution:** Initialize a lower solution $\check{\vartheta}_h$ on each subdomain as:

$$\check{\vartheta}_{jh}^{i,0} = 0, \quad j \in \{1,\dots,q\}, \quad i \in \{1,\dots,n\}. \tag{4.21}$$

- **Upper solution:** For each subdomain Ω_j, compute an upper solution $\hat{\vartheta}_{jh}^{i,0}$ by solving:

$$c_j^i\langle \hat{\vartheta}_{jh}^{i,0}, u_h\rangle = \langle \mathscr{F}_j^i + \eta\hat{\vartheta}_{jh}^{i,0}, u_h\rangle, \quad \forall u_h \in V_h. \tag{4.22}$$

Remark 4.3.1

The sequence $\left(\vartheta_{jh}^{i,k+1}\right)_{j\in\{1,\dots,q\}}^{i\in\{1,\dots,n\},k\geq 0}$ simultaneously functions as a lower and an upper solution, providing a natural bounding framework that ensures stability and convergence.

4.3.3 Monotone convergence in domain decomposition algorithms

In the following theorem, we will establish the monotonicity of the discrete alternating Schwarz sequences $\left(\vartheta_{jh}^{i,k+1}\right)$:

Theorem 4.3.3

The sequence $\left(\vartheta_{jh}^{i,k+1}\right)_{j=\overline{1,q}}^{i=\overline{1,n};k\in\mathbb{N}}$ converges monotonically (either increasing or decreasing) to the unique solution of the discrete problem (4.15), assuming the initial condition is either a subsolution or a supersolution.

We proceed by induction to demonstrate that the sequence of upper solutions is decreasing, while the sequence of lower solutions is increasing. As a result, we obtain:

$$\check{\vartheta}_h^{k+1} \leq \hat{\vartheta}_h^{k+1}, \quad \forall k \in \mathbb{N}.$$

The proof is structured into three main steps.

Monotone convergence of the lower sequence

We establish that the sequence $\left(\check{\vartheta}_{jh}^{i,k+1}\right)_{j=\overline{1,q}}^{i=\overline{1,n};k\in\mathbb{N}}$ is increasing, assuming that the initial value $\check{\vartheta}_h$ is a subsolution.

❖ **Base Cases: for** $k = 0$

1. **Subdomains preceding the interface Ω_j with $j < l$**
   On each subdomain Ω_j for $j < l$, the sequence is initialized as:

   $$\check{\vartheta}_{jh}^{i,0} = 0 \quad \text{for} \quad k = 0.$$

   The first iterate, $\check{\vartheta}_{jh}^{i,1}$, is computed by solving the following variational inequality system:

   $$\begin{cases} c_j^i\langle \check{\vartheta}_{jh}^{i,1}, u_h - \check{\vartheta}_{jh}^{i,1}\rangle \geq \langle \mathscr{F}_j^i + \eta\check{\vartheta}_{jh}^{i,0}, u_h - \check{\vartheta}_{jh}^{i,1}\rangle, & \forall u_h \in V_h, \\ \check{\vartheta}_{jh}^{i,1} \leq \kappa + \check{\vartheta}_{jh}^{i+1,1}, \quad u_h \leq \kappa + \check{\vartheta}_{jh}^{i+1,1}, \\ \check{\vartheta}_{jh}^{i,1} = \check{\vartheta}_{lh}^{i,0} \quad \text{on} \quad \Sigma_j, \quad u_h = \check{\vartheta}_{lh}^{i,0} \quad \text{on} \quad \Sigma_j. \end{cases} \tag{4.23}$$

   Under the positivity assumption $\mathscr{F}_j^i \geq 0$, we immediately have:

   $$\check{\vartheta}_{jh}^{i,1} \geq 0 = \check{\vartheta}_{jh}^{i,0}.$$

   Hence, it follows that:

   $$\check{\vartheta}_{jh}^{i,0} \leq \check{\vartheta}_{jh}^{i,1} \quad \text{and} \quad \check{\vartheta}_{jh}^{i,1} \geq 0 \quad \Rightarrow \quad \check{\vartheta}_{lh}^{i,0} \geq 0.$$

2. **Subdomains following the interface Ω_l with $j > l$.** Similarly, for each subdomain Ω_l with $j > l$, the sequence is initialized as:

   $$\check{\vartheta}_{lh}^{i,0} = 0 \quad \text{for} \quad k = 0.$$

   The next iterate $\check{\vartheta}_{lh}^{i,1}$ is determined by solving:

   $$\begin{cases} c_l^i\langle \check{\vartheta}_{lh}^{i,1}, u_h - \check{\vartheta}_{lh}^{i,1}\rangle \geq \langle \mathscr{F}_l^i + \eta\check{\vartheta}_{lh}^{i,0}, u_h - \check{\vartheta}_{lh}^{i,1}\rangle, & \forall u_h \in V_h, \\ \check{\vartheta}_{lh}^{i,1} \leq \kappa + \check{\vartheta}_{lh}^{i+1,1}, \quad u_h \leq \kappa + \check{\vartheta}_{lh}^{i+1,1}, \\ \check{\vartheta}_{lh}^{i,1} = \check{\vartheta}_{jh}^{i,1} \quad \text{on} \quad \Sigma_l, \quad u_h = \check{\vartheta}_{jh}^{i,1} \quad \text{on} \quad \Sigma_l. \end{cases} \tag{4.24}$$

   Assuming $\mathscr{F}_l^i \geq 0$, it follows that:

   $$\check{\vartheta}_{lh}^{i,1} \geq 0 = \check{\vartheta}_{lh}^{i,0},$$

   which implies:

   $$\check{\vartheta}_{lh}^{i,0} \leq \check{\vartheta}_{lh}^{i,1} \quad \text{and} \quad \check{\vartheta}_{lh}^{i,1} = \check{\vartheta}_{jh}^{i,1}.$$

❖ **Case** $k = 1$

1. **Subdomains preceding the interface Ω_j with** $j < l$ On each subdomain Ω_j with $j < l$, the sequence at $k = 1$ is initialized with $\check{\vartheta}_{jh}^{i,0} = 0$. The subsequent term, $\check{\vartheta}_{jh}^{i,2}$, is then computed as the solution of the following system:

$$\begin{cases} c_j^i \langle \check{\vartheta}_{jh}^{i,2}, u_h - \check{\vartheta}_{jh}^{i,2} \rangle \geq \langle \mathscr{F}_j^i + \eta \check{\vartheta}_{jh}^{i,1}, u_h - \check{\vartheta}_{jh}^{i,2} \rangle \quad \forall u_h \in V_h, \\ \check{\vartheta}_{jh}^{i,2} \leq \kappa + \check{\vartheta}_{jh}^{i+1,2}, \quad u_h \leq \kappa + \check{\vartheta}_{jh}^{i+1,2}, \\ \check{\vartheta}_{jh}^{i,2} = \check{\vartheta}_{lh}^{i,1} \quad \text{on} \quad \Sigma_j, \quad u_h = \check{\vartheta}_{lh}^{i,1} \quad \text{on} \quad \Sigma_j. \end{cases} \tag{4.25}$$

Choosing $u_h = \check{\vartheta}_{jh}^{i,2} - v_h, v_h \geq 0$ in (4.25), we obtain:

$$c_j^i \langle \check{\vartheta}_{jh}^{i,2}, v_h \rangle \leq \langle \mathscr{F}_j^i + \eta \check{\vartheta}_{jh}^{i,1}, v_h \rangle \quad \forall u_h \in V_h. \tag{4.26}$$

For the system (4.23), setting $u_h = \check{\vartheta}_{jh}^{i,1} - v_h, v_h \geq 0$, we get:

$$c_j^i \langle \check{\vartheta}_{jh}^{i,1}, v_h \rangle \leq \langle \mathscr{F}_j^i + \eta \check{\vartheta}_{jh}^{i,0}, v_h \rangle \quad \forall u_h \in V_h \tag{4.27}$$

Subtracting (4.26) from (4.27), we get:

$$c_j^i \langle \check{\vartheta}_{jh}^{i,1} - \check{\vartheta}_{jh}^{i,2}, v_h \rangle \leq \langle \eta (\check{\vartheta}_{jh}^{i,0} - \check{\vartheta}_{jh}^{i,1}), v_h \rangle \leq 0.$$

Since we have:

$$\check{\vartheta}_{jh}^{i,0} \leq \check{\vartheta}_{jh}^{i,1}, \ v_h \geq 0, \ \eta \geq 0$$
$$\Rightarrow \check{\vartheta}_{jh}^{i,1} - \check{\vartheta}_{jh}^{i,2} \leq 0$$
$$\Rightarrow \check{\vartheta}_{jh}^{i,1} \leq \check{\vartheta}_{jh}^{i,2}; \quad \check{\vartheta}_{jh}^{i,2} = \check{\vartheta}_{lh}^{i,1} \text{ on } \Sigma_j; \quad \check{\vartheta}_{jh}^{i,2} \geq 0 \Rightarrow \check{\vartheta}_{lh}^{i,1} \geq 0.$$

2. **Subdomains following the interface Ω_l with** $j > l$ On each subdomain Ω_l with $j > l$, the sequence at $k = 1$ is initialized with $\check{\vartheta}_{lh}^{i,0} = 0$. The next term, $\check{\vartheta}_{lh}^{i,2}$, is then determined as the solution of the following system:

$$\begin{cases} c_l^i \langle \check{\vartheta}_{lh}^{i,2}, u_h - \check{\vartheta}_{lh}^{i,2} \rangle \geq \langle \mathscr{F}_l^i + \eta \check{\vartheta}_{lh}^{i,1}, u_h - \check{\vartheta}_{lh}^{i,2} \rangle \quad \forall u_h \in V_h, \\ \check{\vartheta}_{lh}^{i,2} \leq \kappa + \check{\vartheta}_{lh}^{i+1,2}, \quad u_h \leq \kappa + \check{\vartheta}_{lh}^{i+1,2}, \\ \check{\vartheta}_{lh}^{i,2} = \check{\vartheta}_{jh}^{i,2} \quad \text{on} \quad \Sigma_l, \quad u_h = \check{\vartheta}_{jh}^{i,2} \quad \text{on} \quad \Sigma_l. \end{cases} \tag{4.28}$$

By setting $u_h = \check{\vartheta}_{lh}^{i,2} - v_h$ with $v_h \geq 0$ in (4.28), we obtain:

$$c_l^i \langle \check{\vartheta}_{lh}^{i,2}, v_h \rangle \leq (\mathscr{F}_l^i + \eta \check{\vartheta}_{lh}^{i,1}, v_h). \tag{4.29}$$

In system (4.24), choosing $u_h = \check{\vartheta}_{lh}^{i,1} - v_h$ with $v_h \geq 0$ leads to:

$$c_l^i \langle \check{\vartheta}_{lh}^{i,1}, v_h \rangle \leq \langle \mathscr{F}_l^i + \eta \check{\vartheta}_{lh}^{i,0}, v_h \rangle. \tag{4.30}$$

Subtracting (4.29) from (4.30) yields:

$$c_l^i \langle \check{\vartheta}_{lh}^{i,1} - \check{\vartheta}_{lh}^{i,2}, v_h \rangle \leq \langle \eta (\check{\vartheta}_{lh}^{i,0} - \check{\vartheta}_{lh}^{i,1}), v_h \rangle \leq 0.$$

Since we have:

$$\check{\vartheta}_{lh}^{i,0} \leq \check{\vartheta}_{lh}^{i,1}, \quad v_h \geq 0, \quad \eta \geq 0$$
$$\Rightarrow \check{\vartheta}_{lh}^{i,1} - \check{\vartheta}_{lh}^{i,2} \leq 0$$
$$\Rightarrow \check{\vartheta}_{lh}^{i,1} \leq \check{\vartheta}_{lh}^{i,2}, \quad \check{\vartheta}_{lh}^{i,2} = \check{\vartheta}_{jh}^{i,2} \quad \text{on} \quad \Sigma_l, \quad \check{\vartheta}_{lh}^{i,2} \geq 0 \Rightarrow \check{\vartheta}_{jh}^{i,2} \geq 0.$$

❖ **Induction Step: for general $k \geq 1$**

1. **Subdomains preceding the interface Ω_j with $j < l$:** On each subdomain Ω_j with $j < l$, we verify the property for $k+1$ under the induction hypothesis that it holds for k. Specifically, we assume:

$$\check{\vartheta}_{jh}^{i,k-1} \leq \check{\vartheta}_{jh}^{i,k} \quad \text{and} \quad \check{\vartheta}_{jh}^{i,k} = \check{\vartheta}_{lh}^{i,k-1} \quad \text{on } \Sigma_j.$$

We now consider the function $\check{\vartheta}_{jh}^{i,k}$ as a solution satisfying the system:

$$\begin{cases} c_j^i\langle \check{\vartheta}_{jh}^{i,k}, u_h - \check{\vartheta}_{jh}^{i,k}\rangle \geq \langle \mathscr{F}_j^i + \eta\check{\vartheta}_{jh}^{i,k-1}, u_h - \check{\vartheta}_{jh}^{i,k}\rangle, \quad \forall u_h \in V_h, \\ \check{\vartheta}_{jh}^{i,k} \leq \kappa + \check{\vartheta}_{jh}^{i+1,k}, \quad u_h \leq \kappa + \check{\vartheta}_{jh}^{i+1,k}, \\ \check{\vartheta}_{jh}^{i,k} = \check{\vartheta}_{lh}^{i,k-1} \quad \text{on } \Sigma_j, \quad u_h = \check{\vartheta}_{lh}^{i,k-1} \quad \text{on } \Sigma_j. \end{cases} \tag{4.31}$$

To analyze the sequence behavior, let $u_h = \check{\vartheta}_{jh}^{i,k+1} - v_h$, where $v_h \geq 0$, and substitute it into system (4.31), yielding:

$$c_j^i\langle \check{\vartheta}_{jh}^{i,k+1}, v_h\rangle \leq \langle \mathscr{F}_j^i + \eta\check{\vartheta}_{jh}^{i,k}, v_h\rangle. \tag{4.32}$$

Similarly, substituting $u_h = \check{\vartheta}_{jh}^{i,k} - v_h$ into equation (4.31), we obtain:

$$c_j^i\langle \check{\vartheta}_{jh}^{i,k}, v_h\rangle \leq \langle \mathscr{F}_j^i + \eta\check{\vartheta}_{jh}^{i,k-1}, v_h\rangle. \tag{4.33}$$

Subtracting (4.33) from (4.32), we get:

$$c_j^i\langle \check{\vartheta}_{jh}^{i,k} - \check{\vartheta}_{jh}^{i,k+1}, v_h\rangle \leq \langle \eta(\check{\vartheta}_{jh}^{i,k-1} - \check{\vartheta}_{jh}^{i,k}), v_h\rangle.$$

Since $\check{\vartheta}_{jh}^{i,k} \geq \check{\vartheta}_{jh}^{i,k-1}$, $v_h \geq 0$, and $\eta \geq 0$, the right-hand side is non-positive, leading to:

$$c_j^i\langle \check{\vartheta}_{jh}^{i,k} - \check{\vartheta}_{jh}^{i,k+1}, v_h\rangle \leq 0.$$

This results in:

$$\check{\vartheta}_{jh}^{i,k} - \check{\vartheta}_{jh}^{i,k+1} \leq 0.$$

Thus, we conclude:

$$\check{\vartheta}_{jh}^{i,k+1} \geq \check{\vartheta}_{jh}^{i,k}, \quad \text{and on } \Sigma_j, \quad \check{\vartheta}_{jh}^{i,k+1} = \check{\vartheta}_{lh}^{i,k}, \quad \check{\vartheta}_{jh}^{i,k+1} \geq 0 \Rightarrow \check{\vartheta}_{lh}^{i,k} \geq 0.$$

2. **Subdomains following the interface Ω_l with $j > l$:** On each subdomain Ω_l with $j > l$, we verify the property for $k+1$ under the induction hypothesis that it holds for k, which assumes:

$$\check{\vartheta}_{lh}^{i,k-1} \leq \check{\vartheta}_{lh}^{i,k} \quad \text{and} \quad \check{\vartheta}_{lh}^{i,k} = \check{\vartheta}_{jh}^{i,k} \text{ on } \Sigma_l.$$

Let $\check{\vartheta}_{lh}^{i,k}$ be a solution to the following system:

$$\begin{cases} c_l^i\langle \check{\vartheta}_{lh}^{i,k}, u_h - \check{\vartheta}_{lh}^{i,k}\rangle \geq \langle \mathscr{F}_l^i + \eta\check{\vartheta}_{lh}^{i,k-1}, u_h - \check{\vartheta}_{lh}^{i,k}\rangle \quad \forall u_h \in V_h, \\ \check{\vartheta}_{lh}^{i,k} \leq \kappa + \check{\vartheta}_{lh}^{i+1,k}, \quad u_h \leq \kappa + \check{\vartheta}_{lh}^{i+1,k}, \\ \check{\vartheta}_{lh}^{i,k} = \check{\vartheta}_{jh}^{i,k} \quad \text{on } \Sigma_l, \quad u_h = \check{\vartheta}_{jh}^{i,k} \quad \text{on } \Sigma_l. \end{cases} \tag{4.34}$$

To analyze the behavior of the sequence, let $u_h = \check{\vartheta}_{lh}^{i,k+1} - v_h$ with $v_h \geq 0$, and substitute this expression into system (4.34). This leads to:

$$c_l^i\langle \check{\vartheta}_{lh}^{i,k+1}, v_h\rangle \leq \langle \mathscr{F}_l^i + \eta\check{\vartheta}_{lh}^{i,k}, v_h\rangle. \tag{4.35}$$

Similarly, by substituting $u_h = \check{\vartheta}_{lh}^{i,k} - v_h$ into equation (4.34), we obtain:

$$c_l^i \langle \check{\vartheta}_{lh}^{i,k}, v_h \rangle \leq \langle \mathscr{F}_l^i + \eta \check{\vartheta}_{lh}^{i,k-1}, v_h \rangle. \tag{4.36}$$

Subtracting equation (4.36) from equation (4.35), we obtain:

$$c_l^i \langle \check{\vartheta}_{lh}^{i,k} - \check{\vartheta}_{lh}^{i,k+1}, v_h \rangle \leq \langle \eta(\check{\vartheta}_{lh}^{i,k-1} - \check{\vartheta}_{lh}^{i,k}), v_h \rangle.$$

Since $\check{\vartheta}_{lh}^{i,k} \geq \check{\vartheta}_{lh}^{i,k-1}$, $v_h \geq 0$, and $\eta \geq 0$, the right-hand side is non-positive, leading to:

$$c_l^i \langle \check{\vartheta}_{lh}^{i,k} - \check{\vartheta}_{lh}^{i,k+1}, v_h \rangle \leq 0.$$

This directly implies:

$$\check{\vartheta}_{lh}^{i,k} - \check{\vartheta}_{lh}^{i,k+1} \leq 0.$$

Consequently, we deduce:

$$\check{\vartheta}_{lh}^{i,k+1} \geq \check{\vartheta}_{lh}^{i,k}, \quad \text{and} \quad \check{\vartheta}_{lh}^{i,k+1} = \check{\vartheta}_{jh}^{i,k+1} \text{ on } \Sigma_l,$$

which implies:

$$\check{\vartheta}_{lh}^{i,k+1} \geq 0 \Rightarrow \check{\vartheta}_{jh}^{i,k+1} \geq 0.$$

Monotone convergence of the upper sequence

We now aim to prove that the sequence $\left(\hat{\vartheta}_{jh}^{i,k+1}\right)_{j=\overline{1,q}}^{i=\overline{1,n};k\in\mathbb{N}}$ is monotonically decreasing, assuming that the initial value $\hat{\vartheta}_h$ is a supersolution.

- **Base Cases: for $k = 0$**

1. **Subdomains preceding the interface Ω_j with $j < l$** Specifically, for each $j < l$ and within the subdomain Ω_j, at the base case $k = 0$, we define: $\hat{\vartheta}_{jh}^{i,1}$ as the solution of the following system:

$$\begin{cases} c_j^i \langle \hat{\vartheta}_{jh}^{i,1}, u_h - \hat{\vartheta}_{jh}^{i,1} \rangle \geq \langle \mathscr{F}_j^i + \eta \hat{\vartheta}_{jh}^{i,0}, u_h - \hat{\vartheta}_{jh}^{i,1} \rangle \quad \forall u_h \in V_h, \\ \hat{\vartheta}_{jh}^{i,1} \leq \kappa + \hat{\vartheta}_{jh}^{i+1,1}, \quad u_h \leq \kappa + \hat{\vartheta}_{jh}^{i+1,1}, \\ \hat{\vartheta}_{jh}^{i,1} = \hat{\vartheta}_{lh}^{i,0} \quad \text{on } \Sigma_j, \quad u_h = \hat{\vartheta}_{lh}^{i,0} \quad \text{on } \Sigma_j. \end{cases} \tag{4.37}$$

To proceed, consider a function $\varphi \in H_0^1(\Omega)$ and define $\varphi_+ = \max(\varphi, 0)$. Next, introduce u_h as

$$u_h = \hat{\vartheta}_{jh}^{i,1} - \left(\hat{\vartheta}_{jh}^{i,1} - \hat{\vartheta}_{jh}^{i,0}\right)_+.$$

By substituting this expression for u_h into equation (4.37), we obtain:

$$c_j^i \langle \hat{\vartheta}_{jh}^{i,1}, -\left(\hat{\vartheta}_{jh}^{i,1} - \hat{\vartheta}_{jh}^{i,0}\right)_+ \rangle \geq \langle \mathscr{F}_j^i + \eta \hat{\vartheta}_{jh}^{i,0}, -\left(\hat{\vartheta}_{jh}^{i,1} - \hat{\vartheta}_{jh}^{i,0}\right)_+ \rangle.$$

$$\Rightarrow c_j^i \langle \hat{\vartheta}_{jh}^{i,1}, \left(\hat{\vartheta}_{jh}^{i,1} - \hat{\vartheta}_{jh}^{i,0}\right)_+ \rangle \leq \langle \mathscr{F}_j^i + \eta \hat{\vartheta}_{jh}^{i,0}, \left(\hat{\vartheta}_{jh}^{i,1} - \hat{\vartheta}_{jh}^{i,0}\right)_+ \rangle. \tag{4.38}$$

The term $\hat{\vartheta}_{jh}^{i,0}$ satisfies the following system of equations:

$$c_j^i \langle \hat{\vartheta}_{jh}^{i,0}, u_h \rangle = \langle \mathscr{F}_j^i + \eta \hat{\vartheta}_{jh}^{i,0}, u_h \rangle \quad \forall u_h \in V_h,$$

Now, assume that $u_h = \left(\hat{\vartheta}_{jh}^{i,1} - \hat{\vartheta}_{jh}^{i,0}\right)_+$ is a solution of the system (4.22). As a result, we obtain:

$$c_j^i\langle \hat{\vartheta}_{jh}^{i,0}, \left(\hat{\vartheta}_{jh}^{i,1} - \hat{\vartheta}_{jh}^{i,0}\right)_+\rangle = \langle \mathscr{F}_j^i + \eta\hat{\vartheta}_{jh}^{i,0}, \left(\hat{\vartheta}_{jh}^{i,1} - \hat{\vartheta}_{jh}^{i,0}\right)_+\rangle. \tag{4.39}$$

By integrating equations (4.38) and (4.39), we derive the following result:

$$c_j^i\langle \hat{\vartheta}_{jh}^{i,1}, \left(\hat{\vartheta}_{jh}^{i,1} - \hat{\vartheta}_{jh}^{i,0}\right)_+\rangle \leq c_j^i\langle \hat{\vartheta}_{jh}^{i,0}, \left(\hat{\vartheta}_{jh}^{i,1} - \hat{\vartheta}_{jh}^{i,0}\right)_+\rangle.$$

$$\Rightarrow c_j^i\langle \hat{\vartheta}_{jh}^{i,1} - \hat{\vartheta}_{jh}^{i,0}, \left(\hat{\vartheta}_{jh}^{i,1} - \hat{\vartheta}_{jh}^{i,0}\right)_+\rangle \leq 0, \quad \text{where} \quad \left(\hat{\vartheta}_{jh}^{i,1} - \hat{\vartheta}_{jh}^{i,0}\right)_+ \geq 0.$$

$$\Rightarrow \hat{\vartheta}_{jh}^{i,1} - \hat{\vartheta}_{jh}^{i,0} \leq 0.$$

As a result, we can deduce that:

$$\hat{\vartheta}_{jh}^{i,1} \leq \hat{\vartheta}_{jh}^{i,0}; \quad \text{and} \quad \hat{\vartheta}_{jh}^{i,1} = \hat{\vartheta}_{lh}^{i,0} \quad \text{on } \Sigma_j; \quad \text{then} \quad \hat{\vartheta}_{jh}^{i,1} \geq 0 \quad \text{implies} \quad \hat{\vartheta}_{lh}^{i,0} \geq 0.$$

2. **Subdomains following the interface Ω_l with $j > l$** For each $j > l$ within the subdomain Ω_l, at the base case $k = 0$, we define $\hat{\vartheta}_{lh}^{i,1}$ as the solution of the following system:

$$\begin{cases} c_l^i\langle \hat{\vartheta}_{lh}^{i,1}, u_h - \hat{\vartheta}_{lh}^{i,1}\rangle \geq \langle \mathscr{F}_l^i + \eta\hat{\vartheta}_{lh}^{i,0}, u_h - \hat{\vartheta}_{lh}^{i,1}\rangle \quad \forall u_h \in V_h, \\ \hat{\vartheta}_{lh}^{i,1} \leq \kappa + \hat{\vartheta}_{lh}^{i+1,1}, \quad u_h \leq \kappa + \hat{\vartheta}_{lh}^{i+1,1}, \\ \hat{\vartheta}_{lh}^{i,1} = \hat{\vartheta}_{jh}^{i,1} \quad \text{on } \Sigma_l, \quad u_h = \hat{\vartheta}_{jh}^{i,1} \quad \text{on } \Sigma_l. \end{cases} \tag{4.40}$$

Let u_h be defined as

$$u_h = \hat{\vartheta}_{lh}^{i,1} - \left(\hat{\vartheta}_{lh}^{i,1} - \hat{\vartheta}_{lh}^{i,0}\right)_+$$

By substituting this expression into equation (4.40), we obtain:

$$c_l^i\langle \hat{\vartheta}_{lh}^{i,1}, -\left(\hat{\vartheta}_{lh}^{i,1} - \hat{\vartheta}_{lh}^{i,0}\right)_+\rangle \geq \langle \mathscr{F}_l^i + \eta\hat{\vartheta}_{lh}^{i,0}, -\left(\hat{\vartheta}_{lh}^{i,1} - \hat{\vartheta}_{lh}^{i,0}\right)_+\rangle. \tag{4.41}$$

$$\Rightarrow c_l^i\langle \hat{\vartheta}_{lh}^{i,1}, \left(\hat{\vartheta}_{lh}^{i,1} - \hat{\vartheta}_{lh}^{i,0}\right)_+\rangle \leq \langle \mathscr{F}_l^i + \eta\hat{\vartheta}_{lh}^{i,0}, \left(\hat{\vartheta}_{lh}^{i,1} - \hat{\vartheta}_{lh}^{i,0}\right)_+\rangle. \tag{4.42}$$

$\hat{\vartheta}_{lh}^{i,0}$ represents a solution to the following system of equations:

$$c_l^i\langle \hat{\vartheta}_{lh}^{i,0}, u_h\rangle = \langle \mathscr{F}_l^i + \eta\hat{\vartheta}_{lh}^{i,0}, u_h\rangle \quad \forall u_h \in V_h,$$

Let us assume that $u_h = \left(\hat{\vartheta}_{lh}^{i,1} - \hat{\vartheta}_{lh}^{i,0}\right)_+$ constitutes a solution to the system (4.22). Consequently, we derive:

$$c_l^i\langle \hat{\vartheta}_{lh}^{i,0}, \left(\hat{\vartheta}_{lh}^{i,1} - \hat{\vartheta}_{lh}^{i,0}\right)_+\rangle = \langle \mathscr{F}_l^i + \eta\hat{\vartheta}_{lh}^{i,0}, \left(\hat{\vartheta}_{lh}^{i,1} - \hat{\vartheta}_{lh}^{i,0}\right)_+\rangle. \tag{4.43}$$

By incorporating (4.43) into (4.42), we arrive at:

$$c_l^i\langle \hat{\vartheta}_{lh}^{i,1}, \left(\hat{\vartheta}_{lh}^{i,1} - \hat{\vartheta}_{lh}^{i,0}\right)_+\rangle \leq c_l^i\langle \hat{\vartheta}_{lh}^{i,0}, \left(\hat{\vartheta}_{lh}^{i,1} - \hat{\vartheta}_{lh}^{i,0}\right)_+\rangle.$$

$$\Rightarrow c_l^i\langle \hat{\vartheta}_{lh}^{i,1} - \hat{\vartheta}_{lh}^{i,0}, \left(\hat{\vartheta}_{lh}^{i,1} - \hat{\vartheta}_{lh}^{i,0}\right)_+\rangle \leq 0, \quad \text{where} \quad \left(\hat{\vartheta}_{lh}^{i,1} - \hat{\vartheta}_{lh}^{i,0}\right)_+ \geq 0.$$

$$\Rightarrow \hat{\vartheta}_{lh}^{i,1} - \hat{\vartheta}_{lh}^{i,0} \leq 0.$$

As a result, we can deduce that:

$$\hat{\vartheta}_{lh}^{i,1} \leq \hat{\vartheta}_{lh}^{i,0}; \quad \text{and} \quad \hat{\vartheta}_{lh}^{i,1} = \hat{\vartheta}_{jh}^{i,1} \quad \text{on } \Sigma_l; \quad \text{then} \quad \hat{\vartheta}_{lh}^{i,1} \geq 0 \quad \text{implies} \quad \hat{\vartheta}_{jh}^{i,1} \geq 0.$$

❖ **Case** $k = 1$

1. **Subdomains preceding the interface Ω_j with** $j < l$ For each $j < \mathfrak{l}$ within the subdomain Ω_j, at the step $k = 1$, we define: $\hat{\vartheta}_{jh}^{i,2}$ as the solution of the following system:
$$\begin{cases} c_j^i \langle \hat{\vartheta}_{jh}^{i,2}, u_h - \hat{\vartheta}_{jh}^{i,2} \rangle \geq \langle \mathscr{F}_j^i + \eta \hat{\vartheta}_{jh}^{i,1}, u_h - \hat{\vartheta}_{jh}^{i,2} \rangle \quad \forall u_h \in V_h, \\ \hat{\vartheta}_{jh}^{i,2} \leq \kappa + \hat{\vartheta}_{jh}^{i+1,2}, \quad u_h \leq \kappa + \hat{\vartheta}_{jh}^{i+1,2}, \\ \hat{\vartheta}_{jh}^{i,2} = \hat{\vartheta}_{lh}^{i,1} \quad \text{on } \Sigma_j, \quad u_h = \hat{\vartheta}_{lh}^{i,1} \quad \text{on } \Sigma_j. \end{cases} \tag{4.44}$$
Given that $u_h = \hat{\vartheta}_{jh}^{i,2} - v_h$ with $v_h \geq 0$, substituting this into equation (4.44) results in:
$$c_j^i \langle \hat{\vartheta}_{jh}^{i,2}, v_h \rangle \leq \langle \mathscr{F}_j^i + \eta \hat{\vartheta}_{jh}^{i,1}, v_h \rangle. \tag{4.45}$$
In the system (4.37), by setting $v_h = \hat{\vartheta}_{jh}^{i,1} - v_h$ with $v_h \geq 0$, we obtain:
$$c_j^i \langle \hat{\vartheta}_{jh}^{i,1}, v_h \rangle \leq \langle \mathscr{F}_j^i + \eta \hat{\vartheta}_{jh}^{i,0}, v_h \rangle. \tag{4.46}$$
By substituting (4.45) into (4.46), we obtain:
$$c_j^i \langle \hat{\vartheta}_{jh}^{i,2} - \hat{\vartheta}_{jh}^{i,1}, v_h \rangle \leq \langle \eta (\hat{\vartheta}_{jh}^{i,1} - \hat{\vartheta}_{jh}^{i,0}), v_h \rangle \leq 0.$$
Since we have the conditions:
$$\hat{\vartheta}_{jh}^{i,1} \leq \hat{\vartheta}_{jh}^{i,0}, \quad v_h \geq 0, \quad \eta \geq 0,$$
we can deduce that:
$$c_j^i \langle \hat{\vartheta}_{jh}^{i,2} - \hat{\vartheta}_{jh}^{i,1}, v_h \rangle \leq 0, \quad v_h \geq 0.$$
Consequently, this leads to:
$$\hat{\vartheta}_{jh}^{i,2} - \hat{\vartheta}_{jh}^{i,1} \leq 0.$$
Thus, we obtain:
$$\hat{\vartheta}_{jh}^{i,2} \leq \hat{\vartheta}_{jh}^{i,1}; \quad \text{and} \quad \hat{\vartheta}_{jh}^{i,2} = \hat{\vartheta}_{lh}^{i,1} \quad \text{on } \Sigma_j; \quad \text{then} \quad \hat{\vartheta}_{jh}^{i,2} \geq 0 \quad \text{implies} \quad \hat{\vartheta}_{lh}^{i,1} \geq 0. \tag{4.47}$$

2. **Subdomains following the interface Ω_l with** $j > l$ At the step $k = 1$, we define $\hat{\vartheta}_{lh}^{i,2}$ as the solution of the following system:
$$\begin{cases} c_l^i \langle \hat{\vartheta}_{lh}^{i,2}, u_h - \hat{\vartheta}_{lh}^{i,2} \rangle \geq \langle \mathscr{F}_l^i + \eta \hat{\vartheta}_{lh}^{i,1}, u_h - \hat{\vartheta}_{lh}^{i,2} \rangle \quad \forall u_h \in V_h, \\ \hat{\vartheta}_{lh}^{i,2} \leq \kappa + \hat{\vartheta}_{lh}^{i+1,2}, \quad u_h \leq \kappa + \hat{\vartheta}_{lh}^{i+1,2}, \\ \hat{\vartheta}_{lh}^{i,2} = \hat{\vartheta}_{jh}^{i,2} \quad \text{on } \Sigma_l, \quad u_h = \hat{\vartheta}_{jh}^{i,2} \quad \text{on } \Sigma_l. \end{cases} \tag{4.48}$$
Substituting $u_h = \hat{\vartheta}_{lh}^{i,2} - v_h$ with $v_h \geq 0$ into equation (4.48), we obtain:
$$c_l^i \langle \hat{\vartheta}_{lh}^{i,2}, v_h \rangle \leq \langle \mathscr{F}_l^i + \eta \hat{\vartheta}_{lh}^{i,1}, v_h \rangle. \tag{4.49}$$
In the system (4.40), by setting $v_h = \hat{\vartheta}_{lh}^{i,1} - v_h$ with $v_h \geq 0$, we obtain:
$$c_l^i \langle \hat{\vartheta}_{lh}^{i,1}, v_h \rangle \leq \langle \mathscr{F}_l^i + \eta \hat{\vartheta}_{lh}^{i,0}, v_h \rangle. \tag{4.50}$$
By substituting (4.49) into (4.50), we obtain:
$$c_l^i \langle \hat{\vartheta}_{lh}^{i,2} - \hat{\vartheta}_{lh}^{i,1}, v_h \rangle \leq \langle \eta (\hat{\vartheta}_{lh}^{i,1} - \hat{\vartheta}_{lh}^{i,0}), v_h \rangle \leq 0.$$

Since we have:

$$\hat{\vartheta}_{lh}^{i,1} \le \hat{\vartheta}_{lh}^{i,0}, \quad v_h \ge 0, \quad \eta \ge 0,$$

it follows that:

$$c_l^i\langle \hat{\vartheta}_{lh}^{i,2} - \hat{\vartheta}_{lh}^{i,1}, v_h\rangle \le 0, \quad v_h \ge 0.$$

Thus, we obtain:

$$\Rightarrow \hat{\vartheta}_{lh}^{i,2} - \hat{\vartheta}_{lh}^{i,1} \le 0.$$

Finally, we arrive at:

$$\hat{\vartheta}_{lh}^{i,2} \le \hat{\vartheta}_{lh}^{i,1}; \quad \text{and} \quad \hat{\vartheta}_{lh}^{i,2} = \hat{\vartheta}_{jh}^{i,2} \quad \text{on } \Sigma_l; \quad \text{then} \quad \hat{\vartheta}_{lh}^{i,2} \ge 0 \quad \text{implies} \quad \hat{\vartheta}_{jh}^{i,2} \ge 0.$$

❖ **Induction Step: for general** $k \ge 1$

1. **Subdomains preceding the interface** Ω_l **with** $j < l$ For each subdomain Ω_j with $j < l$, assuming that the property holds at step k, namely,

$$\hat{\vartheta}_{jh}^{i,k} \le \hat{\vartheta}_{jh}^{i,k-1} \quad \text{and} \quad \hat{\vartheta}_{jh}^{i,k} = \hat{\vartheta}_{lh}^{i,k-1} \quad \text{on } \Sigma_j,$$

we now verify its validity for the next step $k+1$. Let $\hat{\vartheta}_{jh}^{i,k+1}$ satisfy the following system:

$$\begin{cases} c_j^i\langle \hat{\vartheta}_{jh}^{i,k}, u_h - \hat{\vartheta}_{jh}^{i,k}\rangle \ge \langle \mathscr{F}_j^i + \eta\hat{\vartheta}_{jh}^{i,k-1}, u_h - \hat{\vartheta}_{jh}^{i,k}\rangle \quad \forall u_h \in V_h, \\ \hat{\vartheta}_{jh}^{i,k} \le \kappa + \hat{\vartheta}_{jh}^{i+1,k}, \quad u_h \le \kappa + \hat{\vartheta}_{jh}^{i+1,k}, \\ \hat{\vartheta}_{jh}^{i,k} = \hat{\vartheta}_{lh}^{i,k-1} \quad \text{on } \Sigma_j, \quad u_h = \hat{\vartheta}_{lh}^{i,k-1} \quad \text{on } \Sigma_j. \end{cases} \tag{4.51}$$

In the system (4.20), substituting $u_h = \hat{\vartheta}_{jh}^{i,k+1} - v_h$ with $v_h \ge 0$ yields:

$$c_j^i\langle \hat{\vartheta}_{jh}^{i,k+1}, v_h\rangle \le \langle \mathscr{F}_j^i + \eta\hat{\vartheta}_{jh}^{i,k}, v_h\rangle. \tag{4.52}$$

Similarly, substituting $u_h = \hat{\vartheta}_{jh}^{i,k} - v_h$ with $v_h \ge 0$ into system (4.51) for k, leads to:

$$c_j^i\langle \hat{\vartheta}_{jh}^{i,k}, v_h\rangle \le \langle \mathscr{F}_j^i + \eta\hat{\vartheta}_{jh}^{i,k-1}, v_h\rangle. \tag{4.53}$$

By subtracting equation (4.52) from equation (4.53), we obtain:

$$c_j^i\langle \hat{\vartheta}_{jh}^{i,k+1} - \hat{\vartheta}_{jh}^{i,k}, v_h\rangle \le \langle \eta(\hat{\vartheta}_{jh}^{i,k} - \hat{\vartheta}_{jh}^{i,k-1}), v_h\rangle \le 0.$$

Since $\hat{\vartheta}_{jh}^{i,k} \le \hat{\vartheta}_{jh}^{i,k-1}$, $v_h \ge 0$, and $\eta \ge 0$, we deduce that:

$$c_j^i\langle \hat{\vartheta}_{jh}^{i,k+1} - \hat{\vartheta}_{jh}^{i,k}, v_h\rangle \le 0.$$

Consequently:

$$\hat{\vartheta}_{jh}^{i,k+1} - \hat{\vartheta}_{jh}^{i,k} \le 0.$$

Hence, we deduce that:

$$\hat{\vartheta}_{jh}^{i,k+1} \le \hat{\vartheta}_{jh}^{i,k}; \quad \hat{\vartheta}_{jh}^{i,k+1} = \hat{\vartheta}_{lh}^{i,k} \quad \text{on } \Sigma_j; \quad \hat{\vartheta}_{jh}^{i,k+1} \ge 0 \Rightarrow \hat{\vartheta}_{lh}^{i,k} \ge 0.$$

2. **Subdomains following the interface** Ω_l **with** $j > l$ For each subdomain Ω_l with $j > l$, assuming that the property holds at step k, namely,

$$\hat{\vartheta}_{lh}^{i,k} \le \hat{\vartheta}_{lh}^{i,k-1} \quad \text{and} \quad \hat{\vartheta}_{lh}^{i,k} = \hat{\vartheta}_{jh}^{i,k} \quad \text{on} \quad \Sigma_l,$$

we now proceed to verify its validity for the next step $k+1$. Let $\hat{\vartheta}_{lh}^{i,k+1}$ satisfy the following system:

$$\begin{cases} c_l^i\langle\hat{\vartheta}_{lh}^{i,k}, u_h - \hat{\vartheta}_{lh}^{i,k}\rangle \geq \langle\mathscr{F}_l^i + \eta\hat{\vartheta}_{lh}^{i,k-1}, u_h - \hat{\vartheta}_{lh}^{i,k}\rangle \quad \forall u_h \in V_h, \\ \hat{\vartheta}_{lh}^{i,k} \leq \kappa + \hat{\vartheta}_{lh}^{i+1,k}, \quad u_h \leq \kappa + \hat{\vartheta}_{lh}^{i+1,k}, \\ \hat{\vartheta}_{lh}^{i,k} = \hat{\vartheta}_{jh}^{i,k} \quad \text{on } \Sigma_l, \quad u_h = \hat{\vartheta}_{jh}^{i,k} \quad \text{on } \Sigma_l. \end{cases} \tag{4.54}$$

In the system (4.20), replacing $u_h = \hat{\vartheta}_{lh}^{i,k+1} - v_h$, with $v_h \geq 0$, leads to the following expression:

$$c_l^i\langle\hat{\vartheta}_{lh}^{i,k+1}, v_h\rangle \leq \langle\mathscr{F}_l^i + \eta\hat{\vartheta}_{lh}^{i,k}, v_h\rangle. \tag{4.55}$$

In a similar manner, by inserting $u_h = \hat{\vartheta}_{lh}^{i,k} - v_h$, where $v_h \geq 0$, into the system (4.54) for k, we obtain:

$$c_l^i\langle\hat{\vartheta}_{lh}^{i,k}, v_h\rangle \leq \langle\mathscr{F}_l^i + \eta\hat{\vartheta}_{lh}^{i,k-1}, v_h\rangle. \tag{4.56}$$

By subtracting equation (4.55) from equation (4.56), we obtain:

$$c_l^i\langle\hat{\vartheta}_{lh}^{i,k+1} - \hat{\vartheta}_{lh}^{i,k}, v_h\rangle \leq \langle\eta(\hat{\vartheta}_{lh}^{i,k} - \hat{\vartheta}_{lh}^{i,k-1}), v_h\rangle \leq 0.$$

Given that $\hat{\vartheta}_{lh}^{i,k} \leq \hat{\vartheta}_{lh}^{i,k-1}$, $v_h \geq 0$, and $\eta \geq 0$, we deduce that:

$$c_l^i\langle\hat{\vartheta}_{lh}^{i,k+1} - \hat{\vartheta}_{lh}^{i,k}, v_h\rangle \leq 0.$$

As a consequence of this inequality, we derive:

$$\hat{\vartheta}_{lh}^{i,k+1} - \hat{\vartheta}_{lh}^{i,k} \leq 0.$$

Therefore, we conclude that:

$$\hat{\vartheta}_{lh}^{i,k+1} \leq \hat{\vartheta}_{lh}^{i,k}; \quad \hat{\vartheta}_{lh}^{i,k+1} = \hat{\vartheta}_{jh}^{i,k+1} \quad \text{on } \Sigma_l; \quad \hat{\vartheta}_{lh}^{i,k+1} \geq 0 \Rightarrow \hat{\vartheta}_{jh}^{i,k+1} \geq 0.$$

Comparison between upper and lower sequences

The objective is to establish a rigorous relationship between the sequences :

$$\left(\hat{\vartheta}_{jh}^{i,k+1}\right)_{j=\overline{1,q}}^{i=\overline{1,n};k\in\mathbb{N}} \quad \text{and} \quad \left(\check{\vartheta}_{jh}^{i,k+1}\right)_{j=\overline{1,q}}^{i=\overline{1,n};k\in\mathbb{N}}$$

by proving the following inequality:

$$\check{\vartheta}_{jh}^{i,k+1} \leq \hat{\vartheta}_{jh}^{i,k+1}.$$

❖ **Base cases:** $k = 0$

1. **Subdomains preceding the interface Ω_j with $j < l$** Consider the subdomain Ω_j for $j < l$. At $k = 0$, the lower sequence is initialized as

$$\check{\vartheta}_{jh}^{i,0} = 0.$$

The corresponding value of the upper sequence, $\hat{\vartheta}_{jh}^{i,0}$, is then determined by solving the following system of equations:

$$c_j^i\langle\hat{\vartheta}_{jh}^{i,0}, u_h\rangle = \langle\mathscr{F}_j^i + \eta\hat{\vartheta}_{jh}^{i,0}, u_h\rangle.$$

Since $\mathscr{F}_j^i \geq 0$, we deduce that:

$$\check{\vartheta}_{jh}^{i,0} = 0 \quad \text{and} \quad \hat{\vartheta}_{jh}^{i,0} \geq 0 \quad \text{then} \quad \hat{\vartheta}_{jh}^{i,0} \geq \check{\vartheta}_{jh}^{i,0}.$$

Consequently, we obtain:

$$\check{\vartheta}_{jh}^{i,0} \leq \hat{\vartheta}_{jh}^{i,0}.$$

2. **Subdomains following the interface Ω_l with** $j > l$ Consider the subdomain Ω_l for $j > l$. At $k = 0$, the lower sequence is initialized as

$$\check{\vartheta}_{lh}^{i,0} = 0.$$

The corresponding upper sequence value, $\hat{\vartheta}_{lh}^{i,0}$, is obtained by solving the following system of equations:

$$c_l^i \langle \hat{\vartheta}_{lh}^{i,0}, u_h \rangle = \langle \mathscr{F}_l^i + \eta \hat{\vartheta}_{lh}^{i,0}, u_h \rangle.$$

As $\mathscr{F}_l^i \geq 0$, we deduce that:

$$\check{\vartheta}_{lh}^{i,0} = 0 \quad \text{and} \quad \hat{\vartheta}_{lh}^{i,0} \geq 0 \quad \text{then} \quad \hat{\vartheta}_{lh}^{i,0} \geq \check{\vartheta}_{lh}^{i,0}.$$

Accordingly, it follows that:

$$\check{\vartheta}_{lh}^{i,0} \leq \hat{\vartheta}_{lh}^{i,0}.$$

❖ **Base cases:** $k = 1$

1. **Subdomains preceding the interface Ω_j with** $j < l$ For the subdomain Ω_j with $j < l$ and at $k = 1$, consider the system (4.37). We define

$$u_h = \hat{\vartheta}_{jh}^{i,1} - v_h, \quad \text{with } v_h \geq 0,$$

which leads to the following relation:

$$c_j^i \langle \hat{\vartheta}_{jh}^{i,1}, v_h \rangle \leq \langle \mathscr{F}_j^i + \eta \hat{\vartheta}_{jh}^{i,0}, u_h \rangle. \tag{4.57}$$

Following a similar approach, we obtain from the system (4.32):

$$c_j^i \langle \check{\vartheta}_{jh}^{i,1}, v_h \rangle \leq \langle \mathscr{F}_j^i + \eta \check{\vartheta}_{jh}^{i,0}, v_h \rangle. \tag{4.58}$$

The result follows by computing the difference between equation (4.58) and equation (4.57):

$$c_j^i \langle \check{\vartheta}_{jh}^{i,1} - \hat{\vartheta}_{jh}^{i,1}, v_h \rangle \leq \langle \eta(\check{\vartheta}_{jh}^{i,0} - \hat{\vartheta}_{jh}^{i,0}), v_h \rangle.$$

Given that $\check{\vartheta}_{jh}^{i,0} \leq \hat{\vartheta}_{jh}^{i,0}$, along with $v_h \geq 0$ and $\eta \geq 0$, we deduce that:

$$c_j^i \langle \check{\vartheta}_{jh}^{i,1} - \hat{\vartheta}_{jh}^{i,1}, v_h \rangle \leq 0.$$

As a consequence, we conclude that:

$$\check{\vartheta}_{jh}^{i,1} - \hat{\vartheta}_{jh}^{i,1} \leq 0,$$

thus, we arrive at:

$$\check{\vartheta}_{jh}^{i,1} \leq \hat{\vartheta}_{jh}^{i,1}.$$

2. **Subdomains following the interface Ω_l with** $j > l$ For the subdomain Ω_l with $j > l$ and at $k = 1$, consider the system (4.40). We define

$$u_h = \hat{\vartheta}_{lh}^{i,1} - v_h, \quad \text{with } v_h \geq 0,$$

which leads to the following relation:

$$c_l^i \langle \hat{\vartheta}_{lh}^{i,1}, v_h \rangle \leq \langle \mathscr{F}_l^i + \eta \hat{\vartheta}_{lh}^{i,0}, u_h \rangle. \tag{4.59}$$

By applying the same reasoning, we obtain from the system (4.32):

$$c_l^i\langle\check{\vartheta}_{lh}^{i,1}, v_h\rangle \leq \langle\mathscr{F}_l^i + \eta\check{\vartheta}_{lh}^{i,0}, v_h\rangle. \tag{4.60}$$

The result follows from computing the difference between equation (4.60) and equation (4.59):

$$c_l^i\langle\check{\vartheta}_{lh}^{i,1} - \hat{\vartheta}_{lh}^{i,1}, v_h\rangle \leq \langle\eta(\check{\vartheta}_{lh}^{i,0} - \hat{\vartheta}_{lh}^{i,0}), v_h\rangle \leq 0.$$

Since $\check{\vartheta}_{lh}^{i,0} \leq \hat{\vartheta}_{lh}^{i,0}$, and given that $v_h \geq 0$ and $\eta \geq 0$, it follows that:

$$c_l^i\langle\check{\vartheta}_{lh}^{i,1} - \hat{\vartheta}_{lh}^{i,1}, v_h\rangle \leq 0.$$

Consequently, we deduce that:

$$\check{\vartheta}_{lh}^{i,1} - \hat{\vartheta}_{lh}^{i,1} \leq 0,$$

hence:

$$\check{\vartheta}_{lh}^{i,1} \leq \hat{\vartheta}_{lh}^{i,1}.$$

❖ **Induction step: for general $k \geq 1$**

1. **Subdomains preceding the interface Ω_j with $j < l$**

   On the subdomain Ω_j with $j < l$, we assume that the following inequality holds at iteration k:

   $$\check{\vartheta}_{jh}^{i,k} \leq \hat{\vartheta}_{jh}^{i,k} \quad \text{on} \quad \Sigma_j.$$

   Our goal is to establish that this property remains valid for iteration $k+1$.

   Starting from the system (4.20), we introduce the definition:

   $$u_h = \hat{\vartheta}_{jh}^{i,k+1} - v_h, \quad \text{where } v_h \geq 0.$$

   By substituting this expression into the system, we obtain:

   $$c_j^i\langle\hat{\vartheta}_{jh}^{i,k+1}, v_h\rangle \leq \langle\mathscr{F}_j^i + \eta\hat{\vartheta}_{jh}^{i,k}, v_h\rangle. \tag{4.61}$$

   Following the same approach, we derive from the system (4.32) that:

   $$c_j^i\langle\check{\vartheta}_{jh}^{i,k+1}, v_h\rangle \leq \langle\mathscr{F}_j^i + \eta\check{\vartheta}_{jh}^{i,k}, v_h\rangle. \tag{4.62}$$

   The result follows by computing the difference between equation (4.62) and equation (4.61):

   $$c_j^i\langle\check{\vartheta}_{jh}^{i,k+1} - \hat{\vartheta}_{jh}^{i,k+1}, v_h\rangle \leq \langle\eta(\check{\vartheta}_{jh}^{i,k} - \hat{\vartheta}_{jh}^{i,k}), v_h\rangle.$$

   Given that $\check{\vartheta}_{jh}^{i,k} \leq \hat{\vartheta}_{jh}^{i,k}$, along with $v_h \geq 0$ and $\eta \geq 0$, we deduce that:

   $$c_j^i\langle\check{\vartheta}_{jh}^{i,k+1} - \hat{\vartheta}_{jh}^{i,k+1}, v_h\rangle \leq 0.$$

   Consequently, we arrive at the conclusion that:

   $$\check{\vartheta}_{jh}^{i,k+1} - \hat{\vartheta}_{jh}^{i,k+1} \leq 0,$$

   thus, we deduce that:

   $$\check{\vartheta}_{jh}^{i,k+1} \leq \hat{\vartheta}_{jh}^{i,k+1}.$$

2. **Subdomains following the interface Ω_l with** $j > l$ On the subdomain Ω_l with $j > l$, we assume that the inequality holds at iteration k:

$$\check{\vartheta}_{lh}^{i,k} \leq \hat{\vartheta}_{lh}^{i,k} \quad \text{on} \quad \Sigma_l.$$

Our goal is to show that this property remains valid for iteration $k+1$. Starting from the system (4.20), we set

$$u_h = \hat{\vartheta}_{lh}^{i,k+1} - v_h, \quad v_h \geq 0.$$

Substituting this expression into the system, we obtain:

$$c_l^i \langle \hat{\vartheta}_{lh}^{i,k+1}, v_h \rangle \leq \langle \mathscr{F}_l^i + \eta \hat{\vartheta}_{lh}^{i,k}, v_h \rangle. \tag{4.63}$$

Following the same approach, we deduce from the system (4.32):

$$c_l^i \langle \check{\vartheta}_{lh}^{i,k+1}, v_h \rangle \leq \langle \mathscr{F}_l^i + \eta \check{\vartheta}_{lh}^{i,k}, v_h \rangle. \tag{4.64}$$

The result follows by computing the difference between equation (4.64) and equation (4.63):

$$c_l^i \langle \check{\vartheta}_{lh}^{i,k+1} - \hat{\vartheta}_{lh}^{i,k+1}, v_h \rangle \leq \langle \eta(\check{\vartheta}_{lh}^{i,k} - \hat{\vartheta}_{lh}^{i,k}), v_h \rangle.$$

Given that $\check{\vartheta}_{lh}^{i,k} \leq \hat{\vartheta}_{lh}^{i,k}$, along with $v_h \geq 0$ and $\eta \geq 0$, we deduce that:

$$c_l^i \langle \check{\vartheta}_{lh}^{i,k+1} - \hat{\vartheta}_{lh}^{i,k+1}, v_h \rangle \leq 0.$$

As a consequence, we arrive at the conclusion that:

$$\check{\vartheta}_{lh}^{i,k+1} - \hat{\vartheta}_{lh}^{i,k+1} \leq 0,$$

this implies the following conclusion:

$$\check{\vartheta}_{lh}^{i,k+1} \leq \hat{\vartheta}_{lh}^{i,k+1}.$$

Finally, the proof is completed by analyzing the limit au temps final $T = m\Delta t$:

$$\lim_{k\to\infty} \check{\vartheta}_{jh}^{i,k} = \lim_{k\to\infty} \hat{\vartheta}_{jh}^{i,k} = \vartheta_h^i, \quad i = \overline{1,n}.$$

Thus, it converges to the unique solution of the discrete problem.

4.3.4 Asymptotic behavior analysis in L^∞

In this section, we will analyze the convergence using the infinity norm and the geometric convergence theorem of the generalized Schwarz algorithm. To simplify the calculations, we introduce specific notations as follows:

$$|\cdot|_i = \|\cdot\|_{L^\infty(\Sigma_j)} \quad \text{and} \quad \|\cdot\|_j = \|\cdot\|_{L^\infty(\Omega_j)}, \quad j = \overline{1,q}.$$

Lemma 4.3.1: [38]

If $\mathbb{C} = (c_{zs})_{z,s=\overline{1,N}}$ is an M-matrix, then for every $k \geq 0$, there exist constants $\kappa_1, \kappa_2, \ldots, \kappa_q$ such that for $j = \overline{1, q-1}$ and $l = \overline{2, q}$ with $j < l$:

$$\kappa_j = \sup \{w_h(x) : x \in \Sigma_j\} \in (0,1), \quad \kappa_l = \sup \{w_h(x) : x \in \Sigma_l\} \in (0,1).$$

Additionally, the following bounds hold:

$$\sup_{\Sigma_j} \left|\vartheta_{jh} - \vartheta_{jh}^{k+1}\right|_j \leq \kappa_j \sup_{\Sigma_j} \left|\vartheta_{jh} - \vartheta_{jh}^{k}\right|_j , \tag{4.65}$$

and

$$\sup_{\Sigma_l} \left|\vartheta_{lh} - \vartheta_{lh}^{k+1}\right|_l \leq \kappa_l \sup_{\Sigma_l} \left|\vartheta_{lh} - \vartheta_{lh}^{k}\right|_l . \tag{4.66}$$

Remark 4.3.2

The proof of the above lemma is adapted from [38], originally formulated for the variational inequality problem. The result remains valid for the problem introduced in this thesis.

Geometric convergence of the generalized algorithm

The convergence of the Schwarz iterative procedure can be formalized as follows:

Theorem 4.3.4: [38]

The sequences $\left(\vartheta_{jh}^{k+1}\right)$ and $\left(\vartheta_{lh}^{k+1}\right)$, produced by the Schwarz alternating method for $k \geq 0$, converge at a geometric rate to the exact solution ϑ of the HJB equation (4.8). More precisely, there exist constants $\kappa_1, \ldots, \kappa_q \in (0,1)$, determined by the subdomains (Ω_j, Σ_j) and (Ω_l, Σ_l), such that for $j = \overline{1, q-1}$, $l = \overline{2, q}$ with $j < l$, the following estimates hold for all $k \geq 0$:

$$\begin{aligned} \sup_{\bar{\Omega}_j} \left|\vartheta_{jh} - \vartheta_{jh}^{k+1}\right|_j &\leq \kappa_j^{k+1} \kappa_l^{k+1} \sup_{\Sigma_j} \left|\vartheta_{jh} - \vartheta_{jh}^{0}\right|_j , \\ \sup_{\bar{\Omega}_l} \left|\vartheta_{lh} - \vartheta_{lh}^{k+1}\right|_l &\leq \kappa_j^{k+1} \kappa_l^{k} \sup_{\Sigma_l} \left|\vartheta_{lh} - \vartheta_{lh}^{0}\right|_l . \end{aligned} \tag{4.67}$$

Asymptotic behavior analysis of the generalized domain decomposition method

Theorem 4.3.5

Let ϑ denote the exact solution of problem (4.8). For $j = \overline{1, q-1}$ and $l = \overline{2, q}$ with $j < l$, there exists a constant C, independent of h and the iteration index k, such that

$$\left\|\vartheta_j^\infty - \vartheta_{jh}^m\right\|_\infty \leq C\, h^2 |\log h|^3, \tag{4.68}$$

and

$$\|\vartheta_l^\infty - \vartheta_{lh}^m\|_\infty \leq C\, h^2 |\log h|^3, \tag{4.69}$$

Proof

We structure the proof into several steps in order to clarify the asymptotic behavior argument.

Step 1: Consider first the case Ω_j. The total error can be decomposed as:

$$\left\|\vartheta_j^\infty - \vartheta_{jh}^{k+1}\right\|_\infty \leq \|\vartheta_j - \vartheta_{jh}\|_\infty + \left\|\vartheta_{jh} - \vartheta_{jh}^{k+1}\right\|_\infty.$$

Step 2: Using theorem 4.2.1 for the discretization error and theorem 4.3.4 for the geometric decay of the Schwarz iterations, with $\rho = \max(\kappa_j, \kappa_l)$, we obtain:

$$\begin{aligned}\left\|\vartheta_j - \vartheta_{jh}^{k+1}\right\|_\infty &\leq C_1 h^2 |\log h|^3 + \rho^{k+1} \left\|\vartheta_{jh} - \vartheta_{jh}^0\right\|_\infty \\ &\leq C_1 h^2 |\log h|^3 + \rho^{k+1} \Big(\|\vartheta_j - \vartheta_{jh}\|_\infty + \left\|\vartheta_j - \vartheta_{jh}^0\right\|_\infty \Big).\end{aligned}$$

Step 3: Assuming the existence of a constant C_2, we deduce:

$$\left\|\vartheta_j - \vartheta_{jh}^{k+1}\right\|_\infty \leq C_1 h^2 |\log h|^3 + \rho^{k+1} \|\vartheta_j - \vartheta_{jh}\|_\infty + \rho^{k+1} \left\|\vartheta_j - \vartheta_{jh}^0\right\|_\infty.$$

$$\left\|\vartheta_j - \vartheta_{jh}^{k+1}\right\|_\infty \leq C h^2 |\log h|^3 + \rho^{k+1} \left\|\vartheta_j - \vartheta_{jh}^0\right\|_\infty.$$

Step 4: We study the asymptotic behavior in the L^∞-norm for the parabolic quasi-variational inequalities by evaluating the difference between $\vartheta_h(x, T)$, the discrete solution at the final time $T = m\Delta t$, and ϑ^∞, the asymptotic continuous solution. Since $\rho \in (0, 1)$, the term ρ^{k+1} tends to zero as k approaches to infinity. Therefore, the iterative error vanishes and the asymptotic estimate becomes:

$$\left\|\vartheta_j^\infty - \vartheta_{jh}^m\right\|_\infty \leq C\, h^2 |\log h|^3.$$

The same arguments apply to the case Ω_l, leading to an identical estimate following the same reasoning steps.

Remark 4.3.3

Although the theoretical analysis is centered on the noncoercive case, the numerical experiments indicate that the convergence rate remains essentially unaffected whether the problem is coercive or noncoercive. This confirms that the proposed domain decomposition method provides consistent accuracy across both types of problems. Specifically, Theorem (4.3.4) ensures that

$$\left\|\vartheta_j^{\infty} - \vartheta_{jh}^{m}\right\|_{\infty} \leq Ch^2|\log h|^3.$$

4.4 Numerical illustration for the parabolic HJB problem

In this section, we demonstrate the efficiency of the overlapping Schwarz domain decomposition algorithm applied to the time-discretized coercive reformulation of a non-coercive parabolic Hamilton–Jacobi–Bellman (HJB) problem.

4.4.1 Model problem: parabolic HJB formulation

The spatial domain is discretized using a conforming finite element method, while temporal integration employs the backward Euler scheme. At each time step, the nonlinear problem is addressed using the previously developed domain decomposition strategy, assuming a uniform spatial grid and a constant time step Δt. Iterations are continued until the L^{∞}-norm of successive iterates falls below a tolerance of 10^{-6}.

We consider a solution $\vartheta(x,t)$ satisfying [13]:

$$\begin{cases} \max\limits_{1\leq i\leq 2}\left(\dfrac{\partial\vartheta}{\partial t} + \mathbb{A}^i\vartheta - \mathbb{F}^i\right) = 0, & (x,t)\in[0,1]\times[0,2],\\ \vartheta(x,0) = \varphi(x), & x\in[0,1],\\ \vartheta(0,t) = \vartheta(1,t) = 0, & t\in[0,2], \end{cases}$$

where the diffusion parameter is set as $J = 0.5$.

The operators are defined by:

$$\mathbb{A}^1\vartheta = J\frac{\partial^2\vartheta}{\partial x^2}, \quad \mathbb{A}^2\vartheta = J\frac{\partial^2\vartheta}{\partial x^2} + \vartheta.$$

To respect the nonlinear structure of the HJB problem, the source terms are set as:

$$\mathbb{F}^1 = \mathbb{F}^2 = \max\left(\mathbb{A}^1\vartheta^*, \mathbb{A}^2\vartheta^*\right),$$

with:

$$\eta = \mu + \theta, \quad \mu = 0 \text{ (coercivity parameter)}, \quad \theta = \frac{1}{\Delta t} \text{ (temporal contribution)}.$$

An analytical solution is chosen as:

$$\vartheta^*(x,t) = (x^4 - x^5)\sin(10x)\cos(20\pi t),$$

from which the initial condition is obtained via:

$$\varphi(x) = \vartheta(x,0) = (x^4 - x^5)\sin(10x).$$

Variational formulation: following standard finite element procedures and integration by parts, the bilinear forms associated with the operators $\mathbb{A}^1$ and $\mathbb{A}^2$ are:

$$a^1\langle \vartheta, u\rangle = \int_\Omega J\,\vartheta'(x)\,u'(x)\,\mathrm{d}x,$$

$$a^2\langle \vartheta, u\rangle = \int_\Omega \left(J\,\vartheta'(x)\,u'(x) + \vartheta(x)\,u(x)\right)\,\mathrm{d}x.$$

Linear forms for source terms: the linear functionals corresponding to the source terms are expressed as:

$$\mathbb{F}^i(u) = \int_\Omega \mathbb{F}^i(x)\,u(x)\,\mathrm{d}x, \quad i = 1, 2.$$

4.4.2 Finite element discretization

This section describes the finite element approximation of the time-dependent HJB problem. The approach relies on constructing a finite-dimensional subspace of $H_0^1(\Omega)$ using piecewise linear functions, which forms the basis for spatial discretization.

- **Mesh Cconstruction:**
  The spatial domain $\Omega = [0, 1]$ is subdivided into $N + 1$ equal sub intervals of length h:

  $$h = \frac{1}{N+1}, \quad x_z = z\,h, \quad z = 0, 1, \ldots, N + 1.$$

  The nodes $\{x_z\}$ define the discrete mesh on $[0, 1]$.

- **Definition of the Finite Element Space:**
  We introduce the conforming finite element space $V_h \subset H_0^1(\Omega)$ as:

  $$V_h = \left\{u_h \in C^0([0,1]) \;\middle|\; u_h|_{[x_z, x_{z+1}]} \in P_1,\ u_h(0) = u_h(1) = 0\right\},$$

  where P_1 denotes polynomials of degree one. Functions in this space are continuous, piecewise linear, and vanish at the boundary points.

- **Basis functions:**
  A natural basis for V_h is given by the standard hat functions $\{\varphi_z\}_{z=1}^N$:

  - ❖ $\varphi_z(x_s) = \delta_{z,s}$ with $\delta_{z,s}$ as the Kronecker delta,
  - ❖ φ_z is piecewise linear on $[x_{z-1}, x_{z+1}]$ and vanishes elsewhere,
  - ❖ Each φ_z has compact support, nonzero only on two adjacent subintervals.

- **Interpolation representation:**
  Any function $u_h \in V_h$ can be written as

  $$u_h(x) = \sum_{z=1}^{N} u_z\,\varphi_z(x),$$

  where $u_z = u_h(x_z)$ are the nodal values. On each element $[x_z, x_{z+1}]$, this reduces to the linear interpolation formula:

  $$u_h(x) = u_z + \frac{x - x_z}{h}\left(u_{z+1} - u_z\right), \quad x \in [x_z, x_{z+1}].$$

  This construction provides a structured framework for implementing the finite element approximation. The basis functions are local, linearly independent, and yield a sparse system when the variational form of the HJB problem is discretized.

4.4.3 Construction of finite element basis functions

In this section, we describe the construction of linear finite element basis functions and how they determine the structure of the resulting stiffness matrix. We provide explicit formulas for both the diffusion-only and diffusion-reaction cases, along with the computation of integrals that define the matrix entries.

Definition and properties of basis functions

Let V_h denote the finite element space introduced previously. The basis functions $\varphi_z(x)$, commonly referred to as *hat functions*, are defined with the following characteristics:

- $\varphi_z \in P_1$ over each subinterval $[x_{z-1}, x_z]$ and $[x_z, x_{z+1}]$,
- Nodal property: $\varphi_z(x_s) = \delta_{z,s}$, where $\delta_{z,s}$ is the Kronecker delta,
- Compact support: $\mathrm{supp}(\varphi_z) = [x_{z-1}, x_{z+1}]$,
- Boundary conditions: $\varphi_z(0) = \varphi_z(1) = 0$.

Graphical illustration of basis functions

Figure (4.3) shows a single linear finite element basis function, while Figure (4.4) illustrates three neighboring basis functions, emphasizing their local support and overlap, which is crucial for the sparsity of the stiffness matrix.

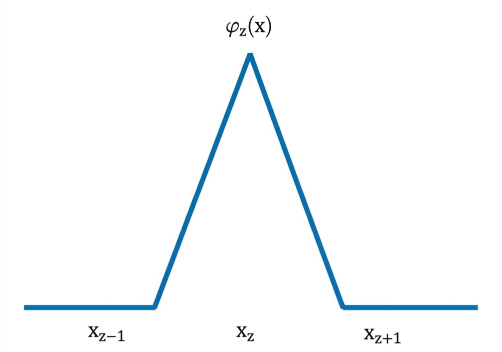

Figure 4.3: **Single basis function φ_z.**

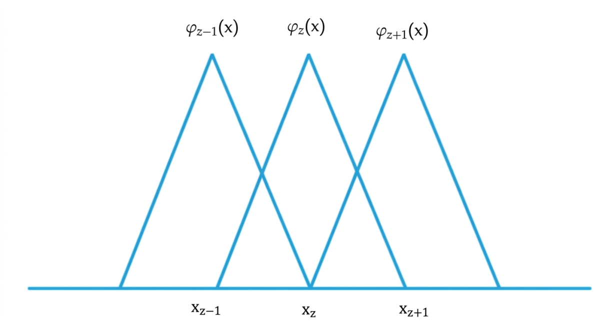

Figure 4.4: **Three overlapping basis functions.**

Piecewise linear form

On each subinterval, the hat function $\varphi_z(x)$ can be expressed explicitly as:

$$\varphi_z(x) = \begin{cases} \dfrac{x - x_{z-1}}{h}, & x \in [x_{z-1}, x_z], \\ \dfrac{x_{z+1} - x}{h}, & x \in [x_z, x_{z+1}], \\ 0, & \text{otherwise.} \end{cases}$$

The function is linear on each subinterval and vanishes outside the local support. Its derivative is constant in each interval:

$$\varphi_z'(x) = \begin{cases} \dfrac{1}{h}, & x \in [x_{z-1}, x_z], \\ -\dfrac{1}{h}, & x \in [x_z, x_{z+1}], \\ 0, & \text{otherwise.} \end{cases}$$

Stiffness matrix structure

The local support of the basis functions implies that the stiffness matrix $\mathscr{A}^i$ is tridiagonal. Entries corresponding to non-overlapping functions vanish:

$$a^i\langle\varphi_z,\varphi_s\rangle = 0, \quad \text{for } |z-s| \geq 2.$$

The nonzero entries are computed as:

$$\begin{cases} a^i\langle\varphi_z,\varphi_z\rangle = \int_{x_{z-1}}^{x_{z+1}} \left[J(x)(\varphi_z')^2 + C(x)\varphi_z^2\right]dx, \\ a^i\langle\varphi_z,\varphi_{z+1}\rangle = \int_{x_z}^{x_{z+1}} \left[J(x)\varphi_z'\varphi_{z+1}' + C(x)\varphi_z\varphi_{z+1}\right]dx, \\ a^i\langle\varphi_z,\varphi_{z-1}\rangle = \int_{x_{z-1}}^{x_z} \left[J(x)\varphi_z'\varphi_{z-1}' + C(x)\varphi_z\varphi_{z-1}\right]dx. \end{cases}$$

Explicit calculation for uniform mesh

Assuming a uniform mesh of step size h and constant coefficients J and C, we have:

$$a^1\langle\varphi_z,\varphi_z\rangle = J\frac{2}{h}, \quad a^1\langle\varphi_z,\varphi_{z\pm1}\rangle = -J\frac{1}{h}.$$

When the reaction term is included:

$$a^2\langle\varphi_z,\varphi_z\rangle = J\frac{2}{h} + \frac{2h}{3}, \quad a^2\langle\varphi_z,\varphi_{z\pm1}\rangle = -J\frac{1}{h} + \frac{h}{6}.$$

Numerical integration

In practice, integrals involving general functions $\mathscr{F}(x)$ can be approximated using the trapezoidal rule:

$$\int_0^1 \mathscr{F}(x)\varphi_z(x)dx \approx h\,\mathscr{F}(x_z).$$

Self-interaction coefficient

The diagonal entry of the stiffness matrix corresponding to φ_z is:

$$a^1\langle\varphi_z,\varphi_z\rangle = J\int_0^1 (\varphi_z'(x))^2\,dx.$$

Splitting the integral over the support intervals yields

$$a^1\langle\varphi_z,\varphi_z\rangle = J\left(\int_{x_{z-1}}^{x_z} \frac{1}{h^2}\,dx + \int_{x_z}^{x_{z+1}} \frac{1}{h^2}\,dx\right) = J\frac{2}{h}.$$

Neighbor interaction coefficients

The interaction between adjacent basis functions involves integrals of the form:

$$a^1\langle\varphi_z,\varphi_{z+1}\rangle = J\int_{x_z}^{x_{z+1}} \varphi_z'(x)\varphi_{z+1}'(x)\,dx = -J\frac{1}{h},$$

$$a^1\langle\varphi_z,\varphi_{z-1}\rangle = J\int_{x_{z-1}}^{x_z} \varphi_z'(x)\varphi_{z-1}'(x)\,dx = -J\frac{1}{h}.$$

These relations confirm the sparsity of the resulting stiffness matrix, as only neighboring entries are nonzero.

Inclusion of reaction term

When a reaction or interaction term is included, the bilinear form for the diagonal entry becomes

$$a^2\langle\varphi_z,\varphi_z\rangle = J\int_0^1 (\varphi_z'(x))^2\,dx + \int_0^1 \varphi_z^2(x)\,dx.$$

The first integral is the same as before, while the second integral evaluates to:

$$\int_0^1 \varphi_z^2(x)\,dx = \int_{x_{z-1}}^{x_z}\left(\frac{x-x_{z-1}}{h}\right)^2 dx + \int_{x_z}^{x_{z+1}}\left(\frac{x_{z+1}-x}{h}\right)^2 dx = \frac{h}{3}.$$

Therefore, the complete diagonal entry reads:

$$a^2\langle\varphi_z,\varphi_z\rangle = J\frac{2}{h} + \frac{h}{3}.$$

Off-diagonal entries with reaction term

The off-diagonal entries corresponding to neighboring basis functions are:

$$a^2\langle\varphi_z,\varphi_{z+1}\rangle = J\int_{x_z}^{x_{z+1}} \varphi_z'(x)\varphi_{z+1}'(x)\,dx + \int_{x_z}^{x_{z+1}} \varphi_z(x)\varphi_{z+1}(x)\,dx = -J\frac{1}{h} + \frac{h}{6}.$$

By symmetry, we also have:

$$a^2\langle\varphi_z,\varphi_{z-1}\rangle = -J\frac{1}{h} + \frac{h}{6}.$$

Numerical integration considerations

For more general functions $\mathscr{F}(x)$, it may be necessary to approximate integrals numerically. A common approach is the trapezoidal or midpoint rule:

$$\int_0^1 \mathscr{F}^i(x)\varphi_z(x)\,dx \approx h\,\mathscr{F}^i(x_z),$$

where h is the uniform mesh size and $\mathscr{F}(x_z)$ denotes the function evaluated at the node.

4.4.4 Global system matrices in finite element discretization

Once the local stiffness and mass contributions of each finite element have been computed, the next step is to assemble them into global matrices that encode the coupling between all nodes of the discretized domain. These global matrices are sparse, symmetric, and structured, and they play a crucial role in the numerical resolution of the resulting variational problem.

We first consider the stiffness matrix $\mathscr{A}^1$, derived from the diffusion (or rigidity) operator alone, and then the augmented matrix $\mathscr{A}^2$, which includes both stiffness and mass effects.

Stiffness matrix $\mathscr{A}^1$

The global stiffness matrix associated with the discretization of the Laplacian operator is tridiagonal and given by:

$$\mathscr{A}^1_{z,z} = \frac{2J}{h}, \quad \mathscr{A}^1_{z,z\pm1} = -\frac{J}{h}, \quad \mathscr{A}^1_{z,s} = 0 \quad \text{for } |z-s|>1.$$

The numerical structure of $\mathscr{A}^1$ can be summarized as follows:

Matrix $\mathscr{A}^1$	$\frac{J}{h}\times$	$\begin{bmatrix} 2 & -1 & & & \\ -1 & 2 & -1 & & \\ & \ddots & \ddots & \ddots & \\ & & -1 & 2 & -1 \\ & & & -1 & 2 \end{bmatrix}$

Table 4.1: **Global stiffness matrix $\mathscr{A}^1$**

Mass matrix $\mathscr{M}$

The consistent mass matrix $\mathscr{M}$ in the finite element context is symmetric and captures the integral contributions of the basis functions over the elements. Its main and adjacent diagonals are defined as:

$$\mathscr{M}_{z,z} = \frac{2h}{3}, \quad \mathscr{M}_{z,z\pm 1} = \frac{h}{6}, \quad \mathscr{M}_{z,s} = 0 \quad \text{for } |z-s| > 1.$$

This leads to the following matrix form:

Matrix $\mathscr{M}$	$\dfrac{h}{6}\times$	$\begin{bmatrix} 4 & 1 & & & \\ 1 & 4 & 1 & & \\ & \ddots & \ddots & \ddots & \\ & & 1 & 4 & 1 \\ & & & 1 & 4 \end{bmatrix}$

Table 4.2: **Consistent mass matrix $\mathscr{M}$**

Augmented matrix $\mathscr{A}^2$: stiffness + mass

By combining the stiffness and mass matrices, we construct the global matrix:

$$\mathscr{A}^2 = \mathscr{A}^1 + \mathscr{M}.$$

Numerically, this corresponds to:

Matrix $\mathscr{A}^2$	$\frac{J}{h}$	$\begin{bmatrix} 2 & -1 & & & \\ -1 & 2 & -1 & & \\ & \ddots & \ddots & \ddots & \\ & & -1 & 2 & -1 \\ & & & -1 & 2 \end{bmatrix}$	$+\frac{h}{6}$	$\begin{bmatrix} 4 & 1 & & & \\ 1 & 4 & 1 & & \\ & \ddots & \ddots & \ddots & \\ & & 1 & 4 & 1 \\ & & & 1 & 4 \end{bmatrix}$

Table 4.3: **Global matrix $\mathscr{A}^2 = \mathscr{A}^1 + \mathscr{M}$**

For numerical stability and to ensure monotonicity in solving HJB problems, we define:

$$\mathcal{C}^1 = \mathscr{A}^1 + \eta I, \quad \mathcal{C}^2 = \mathscr{A}^2 + \eta I, \quad ,$$

such that $\eta = \mu + \theta$, where $\theta > 0$ is a penalization parameter and I denotes the identity matrix, ensuring stability and monotonicity in the discretization of controlled diffusion operators.

4.4.5 Numerical investigation of the asymptotic behavior in the L^∞-norm

This section presents the main numerical contribution of this work and investigates the asymptotic behavior of the proposed overlapping domain decomposition method for the parabolic quasi-variational inequality associated with the Hamilton–Jacobi–Bellman equation. The analysis is carried out in the L^∞-norm in order to examine:

- the asymptotic stability and long-time behavior of the numerical approximation;
- the convergence properties of the method, including the effects of spatial and temporal refinements, the overlap transmission between subdomains, and the Schwarz iterative process.

Each numerical experiment is presented separately and followed by a brief discussion of the observed results.

Initialization and numerical configuration

The computational framework is defined as follows:

- The iterative procedure is initialized from either a subsolution or a supersolution.
- The spatial discretization is performed on a uniform mesh with:
$$h = \frac{1}{100}.$$
- The temporal evolution is computed using:
$$\Delta t = 0.05.$$
- Since the coercivity parameter satisfies: $\mu = 0$ the stabilization coefficient is chosen as:
$$\eta = \mu + \frac{1}{\Delta t}.$$

This numerical configuration guarantees the coercive reformulation required by the overlapping decomposition procedure and provides a stable framework for studying the asymptotic behavior of the solution in the L^∞-norm.

Temporal evolution of the solution profiles

Several solution profiles are represented at different time levels in order to analyze the temporal propagation of the approximation.

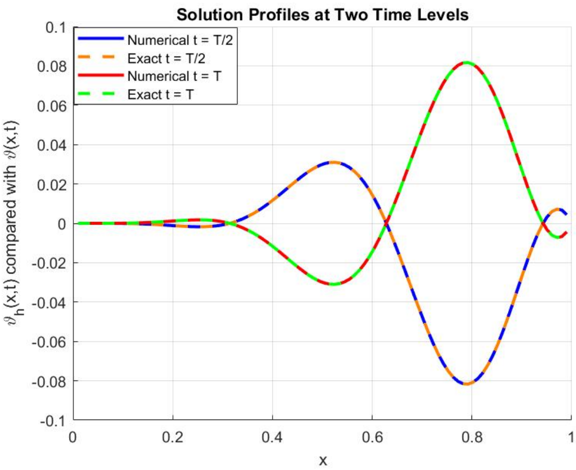

Figure 4.5: **Temporal evolution of the exact and numerical solution profiles.**

The numerical approximation accurately reproduces the oscillatory structure of the exact solution throughout the simulation. The results show:

- the preservation of amplitude and phase,
- the temporal stability of the discretization,
- and the robustness of the iterative procedure over long-time evolution.

Asymptotic convergence of the Schwarz iterations

The following figures illustrate the progressive construction of the numerical solution through the overlapping domain decomposition algorithm.

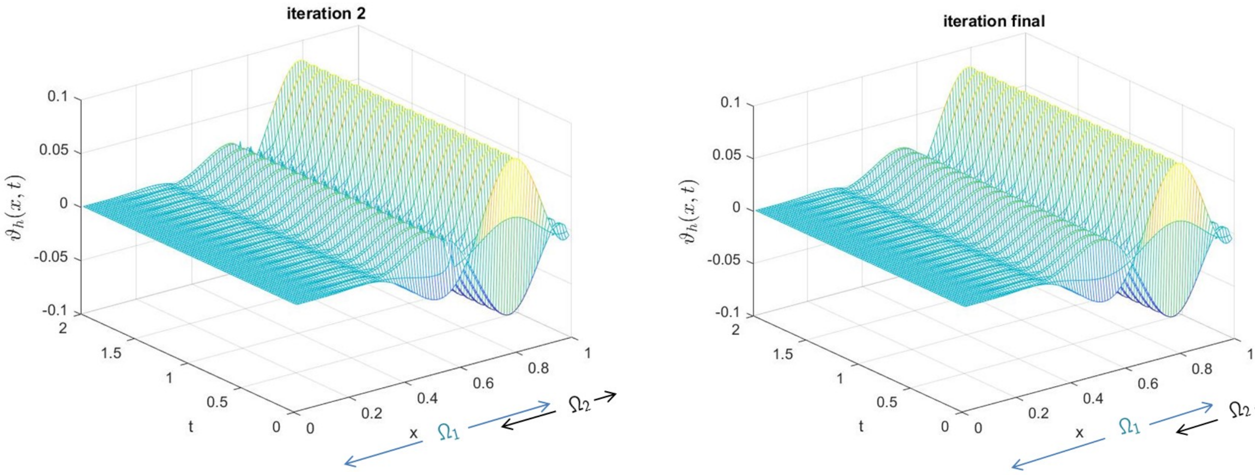

Figure 4.6: **Evolution of the Schwarz iterative sequences toward the final-time solution.**

These numerical iterations clearly demonstrate:

- the propagation of information through the overlap region,
- the progressive stabilization of the approximation,
- the convergence of the Schwarz sequences,

- and the reconstruction of the global solution at the final time.

The final iteration confirms the asymptotic convergence of the overlapping decomposition process toward the exact solution.

Spatial asymptotic convergence

The spatial convergence behavior is analyzed by computing the L^∞-error at the final time for several mesh refinements.

Table 4.4: **Maximum L^∞-error under spatial refinement.**

Mesh size h	$\|\vartheta_h^m(x,T) - \vartheta^\infty\|_\infty$
$1/50$	4.0190×10^{-8}
$1/100$	1.1795×10^{-8}
$1/200$	3.6944×10^{-9}

The obtained results indicate:

- a regular decay of the numerical error,
- a stable asymptotic behavior under mesh refinement,
- and a convergence pattern consistent with the theoretical estimates established previously.

Temporal asymptotic convergence

The effect of temporal discretization is investigated by reducing the time step while keeping the spatial mesh fixed.

Table 4.5: **Maximum L^∞-error under time refinement.**

Time step Δt	$\|\vartheta_h^m(x,T) - \vartheta^\infty\|_\infty$
0.10	3.7763×10^{-8}
0.05	1.1795×10^{-8}
0.025	1.0101×10^{-8}
0.0125	6.6577×10^{-9}

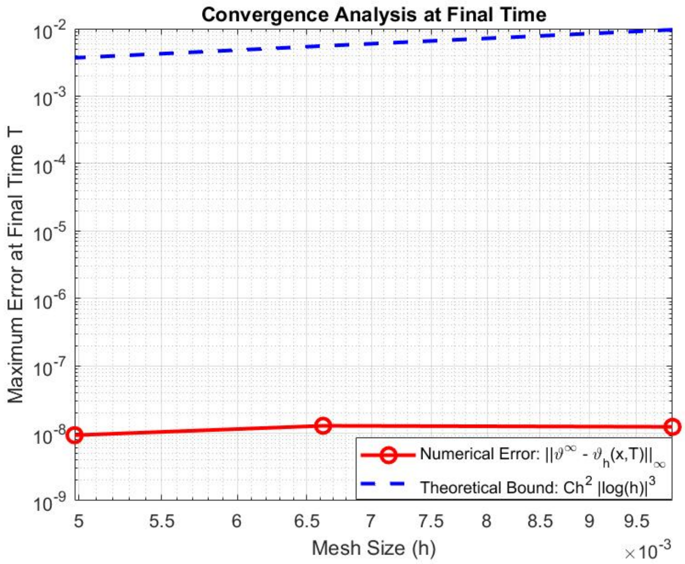

Figure 4.7: **Asymptotic decay of the numerical error under temporal refinement.**

The reduction of the time step produces:

- a systematic decrease of the approximation error,
- a stable long-time numerical behavior,
- and a temporal convergence consistent with the theoretical asymptotic estimates.

Influence of the overlap on the asymptotic regime

The effect of the overlap width is analyzed by measuring the approximation error in each subdomain at the final time.

Table 4.6: **Influence of the overlap width on the L^∞-error.**

Overlap Width	$\|\boldsymbol{\vartheta_{1h}^m(x,T)-\vartheta_1^\infty}\|_\infty$ over Ω_1	$\|\boldsymbol{\vartheta_{2h}^m(x,T)-\vartheta_2^\infty}\|_\infty$ over Ω_2	$\|\boldsymbol{\vartheta_h^m(x,T)-\vartheta^\infty}\|_\infty$ over Ω
No Overlap	2.60×10^{-9}	8.30×10^{-8}	7.66×10^{-8}
Small Overlap	1.25×10^{-10}	4.84×10^{-8}	4.43×10^{-8}
Large Overlap	3.68×10^{-11}	1.18×10^{-8}	1.18×10^{-8}

The numerical results show that increasing the overlap width:

- improves the transmission of information between subdomains,
- reduces interface errors,
- accelerates the convergence of the Schwarz iterations,
- and stabilizes the asymptotic regime at the final time.

Conclusion and perspectives

In this thesis, we investigated the asymptotic behavior of parabolic quasi-variational inequality systems associated with Hamilton–Jacobi–Bellman equations. The principal objective was to develop a robust numerical framework capable of accurately approximating the long-time behavior of nonlinear parabolic problems while preserving stability, convergence, and consistency at the discrete level.

The proposed methodology was based on an overlapping domain decomposition strategy formulated through a sequential Schwarz iterative procedure. The study demonstrated that the combination of domain decomposition techniques with monotone iterative sequences provides an efficient framework for the analysis of nonlinear parabolic quasi-variational inequalities. In particular, the construction of upper and lower sequences allowed us to establish stability properties and asymptotic convergence results in the L^∞-norm.

A significant part of this work was devoted to the treatment of non-coercive parabolic Hamilton–Jacobi–Bellman problems. By introducing a semi-implicit backward Euler discretization, the original evolutionary problem was transformed into a sequence of coercive elliptic quasi-variational inequalities. This reformulation made it possible to extend elliptic analytical techniques to the parabolic setting while maintaining rigorous control of the asymptotic behavior of the numerical approximation.

The numerical investigations confirmed the theoretical analysis developed throughout the thesis. The obtained results demonstrated the convergence of the Schwarz iterative sequences toward the final-time solution and highlighted the important role played by the overlap region in stabilizing the numerical process. The overlapping structure significantly improved the transmission of information between neighboring subdomains, reduced interface discrepancies, and accelerated convergence toward the asymptotic regime.

Beyond the theoretical and numerical contributions, this work emphasizes the effectiveness of overlapping domain decomposition methods for nonlinear parabolic problems arising in optimal control, diffusion processes, and evolutionary systems governed by Hamilton–Jacobi–Bellman equations. The developed framework provides a reliable approach for studying long-time asymptotic behavior in complex nonlinear settings.

Several research perspectives naturally emerge from this study. A first direction concerns the extension of domain decomposition methods to geometrically more complex configurations, particularly domains with fractal or self-similar structures. Such geometries appear in porous media, heterogeneous materials, irregular diffusion processes, and complex transport phenomena. The analysis of the asymptotic behavior and convergence properties in these irregular geometrical settings constitutes a challenging and promising continuation of the present work. In particular, future investigations may focus on the impact of fractal geometries on the stability, transmission conditions, and convergence speed of overlapping decomposition algorithms.

Another important perspective concerns the development of adaptive and scalable numerical strategies for high-dimensional nonlinear parabolic problems. Combining overlapping domain decomposition methods with multilevel techniques, adaptive discretizations, or parallel computing strategies could significantly improve computational efficiency for large-scale applications.

Finally, extending the present framework to more general classes of nonlinear evolutionary systems and coupling it with modern computational approaches represents a promising direction for future research in the numerical analysis of parabolic quasi-variational inequalities and Hamilton–Jacobi–Bellman problems.

Research and publications

- **Publications in international journals:**

  - **Samar Chebbah**, Sofiane Madi, Mohamed Haiour. *Overlapping Domain Decomposition Methods for Noncoercive Hamilton-Jacobi-Bellman Equation. European journal of pure and applied mathematics*, Vol. 18, Issue 2, Article Number 6070, 2025. ISSN 1307-5543. Published by New York Business Global.
  - **Samar Chebbah**, Mohamed Haiour, Ahmed Himadan, Ulviye Demirbilek. *Fractal Scaling Laws and Asymptotic Behavior for Schwarz Domain Decomposition of Parabolic Hamilton–Jacobi–Bellman with AI-Driven Adaptivity. Fractals*, Fractal Geometry and Scaling Laws in the Era of AI, April 2026.
    https://doi.org/10.1142/S0218348X27400019.

- **National conferences:**

  - **The 1st national conference on applied algebra**
    Date: 06 june 2023
    Location: university center Si El Haouse, Barika, Algeria
    Presented paper: "Schwarz method for variational inequalities"
    Presentation type: communication
  - **The national seminar on modern mathematics and applications - MMA24**
    Date: 06–08 october 2024
    Location: Université Badji Mokhtar, Annaba, Algeria
    Presented paper: "Schwarz method for bilateral obstacle problem"
    Presentation type: poster
  - **4th national conference of mathematics and applications (CNMA - 2024)**
    Date: 07–08 december 2024
    Location: centre universitaire Abdelhafid Boussouf, Mila, Algeria
    Presented paper: "Schwarz method for HJB equation"
    Presentation type: communication
  - **The first national symposium on innovative mathematics: retrospective and perspectives**
    Date: 11–12 december 2024
    Location: université Abdelhamid Ibn Badis, Mostaganem, Algeria
    Presented paper: "Additive Schwarz method for coercive variational inequalities"
    Presentation type: communication

- **International conferences:**

  - **1st International workshop on applied mathematics (IWAM 2022)**
    Date: 6–8 december 2022
    Location: université Frères Mentouri Constantine 1, Constantine, Algeria

Presented paper: "Error estimate on the uniform norm of the Schwarz method for variational inequalities with nonlinear source terms"
Presentation type: poster

- **The fourth international conference on applied algebra**
  Date: 17–18 september 2024
  Location: university center Si El Haouse, Barika, Algeria
  Presented paper: "The Schwarz alternating method for obstacle problems"
  Presentation type: communication

- **1st international symposium on applied mathematics and mathematical modeling (MAMM-2024)**
  Date: 12 november 2024
  Location: university Chadli Bendjedid, El-Tarf, Algeria
  Presented paper: "Schwarz method for unilateral obstacle problems"
  Presentation type: communication

- **International conference on mathematics and its applications in science and technology (ICMAST'2024)**
  Date: 15–16 december 2024
  Location: Setif 1 University Ferhat Abbas, Setif, Algeria
  Presented paper: "Restricted additive Schwarz method for variational inequalities"
  Presentation type: communication

Seminars and workshops:

- **Mathematics and applications seminar**
  Date: 06 february 2022
  Location: Abdelhafid Boussouf University Center, Mila, Algeria
  Presented paper: "Variational inequalities with non-coercive operator"
  Presentation type: communication

- **The university week for mathematics**
  Date: 12–14 march 2023
  Location: centre universitaire Abdelhafid Boussouf, Mila, Algeria
  Presented paper: "On variational inequalities with the nonlinear second member"
  Presentation type: poster

Bibliography

[1] M. Allaoua. *Approximation par la Méthode de Décomposition en sous Domaines d'une Classe d'Inéquation Quasi-Variationnelle Elliptique*. Thèse de doctorat en sciences, Université Badji Mokhtar–Annaba, Algeria, 2015.

[2] S. A. Belbas and I. D. Mayergoyz. Application des méthodes du point fixe aux équations de Hamilton-Jacobi-Bellman discrètes et aux inéquations quasi-variationnelles discrètes. *C. R. Acad. Sci. Paris*, Serie I, 7, 1984.

[3] M. A. Bencheikh Le Hocine, S. Boulaaras, and M. Haiour. An Optimal L^{∞}-error Estimate for an Approximation of a Parabolic Variational Inequality. *Numerical Functional Analysis and Optimization*, 37(1):1–18, 2016.

[4] M. A. Bencheikh Le Hocine, S. Boulaaras, and M. Haiour. On finite element approximation of system of parabolic quasi-variational inequalities related to stochastic control problems. *Cogent Mathematics*, 3, Article: 1251386, 2016.

[5] M. A. Bencheikh Le Hocine and M. Haiour. Algorithmic Approach for the Asymptotic Behavior of a System of Parabolic Quasi-Variational Inequalities. *Applied Mathematical Sciences*, 7(19):909–921, 2013.

[6] M. A. Bencheikh Le Hocine and M. Haiour. L^{∞}-Error Analysis for Parabolic Quasi-Variational Inequalities Related to Impulse Control Problems. *Computational Mathematics and Modeling*, 28(1), 2017.

[7] A. Bensoussan and J.-L. Lions. *Applications des Inéquations Variationnelles en Contrôle Stochastique*. Dunod, Paris, France, 1978.

[8] A. Bensoussan and J.-L. Lions. *Impulse Control and Quasi-Variational Inequalities*. Gauthier-Villars, 1984.

[9] S. Boulaaras, M. E. A. Bencheikh Le Hocine, and M. Haiour. A New Error Estimate on Uniform Norm of a Parabolic Variational Inequality with Nonlinear Source Terms via the Subsolution Concepts. *Journal of Inequalities and Applications*, 2020(78), 2020.

[10] S. Boulaaras, K. Habita, and M. Haiour. Asymptotic Behavior and A Posteriori Error Estimates for the Generalized Overlapping Domain Decomposition Method for Parabolic Equation. *Boundary Value Problems*, 124, 2015.

[11] S. Boulaaras, K. Habita, and M. Haiour. A Posteriori Error Estimates for the Generalized Overlapping Domain Decomposition Method for Parabolic Equation With Mixed Boundary Condition. *Boletim da Sociedade Paranaense de Matemática*, 38(4):157–174, 2020.

[12] S. Boulaaras and M. Haiour. L^∞-Asymptotic Behavior for a Finite Element Approximation in Parabolic Quasi-Variational Inequalities Related to Impulse Control Problem. *Applied Mathematics and Computation*, 217(14):6443–6450, March 2011.

[13] S. Boulaaras and M. Haiour. The finite element approximation of evolutionary Hamilton–Jacobi–Bellman equations with nonlinear source terms. *Indagationes Mathematicae*, 24(1):161–173, 2013.

[14] S. Boulaaras and M. Haiour. The Maximum Norm Analysis of an Overlapping Schwarz Method for Parabolic Quasi-Variational Inequalities Related to Impulse Control Problem with the Mixed Boundary Conditions. *Applied Mathematics & Information Sciences*, 7(1):343–353, 2013.

[15] S. Boulaaras and M. Haiour. The theta time scheme combined with a finite element spatial approximation of Hamilton–Jacobi–Bellman equation with Linear Source Terms. *Computational Mathematics and Modeling*, 25(3):423–438, 2014.

[16] S. Boulaaras and M. Haiour. A General Case for the Maximum Norm Analysis of an Overlapping Schwarz Method of Evolutionary HJB Equation with Nonlinear Source Terms with the Mixed Boundary Conditions. *Applied Mathematics & Information Sciences*, 9(3):1247–1257, 2015.

[17] S. Boulaaras and M. Haiour. A New Proof for the Existence and Uniqueness of the Discrete Evolutionary Hamilton–Jacobi–Bellman Equations. *Applied Mathematics and Computation*, 262:42–55, 2015.

[18] S. Boulaaras, M. A. Bencheikh Le Hocine, and M. Haiour. The Finite Element Approximation in a System of Parabolic Quasi-Variational Inequalities Related to Management of Energy Production with Mixed Boundary Condition. *Computational Mathematics and Modeling*, 25(4):530–543, 2014.

[19] S. Boulaaras, M. A. Bencheikh Le Hocine, and M. Haiour. L^∞-Error Estimate of a Parabolic Quasi-Variational Inequalities System Related to Management of Energy Production Problems via the Subsolution Concept. *Boletín de la Sociedad Matemática Mexicana*, 24:439–461, 2017.

[20] S. Boulaaras, M. A. Bencheikh Le Hocine, and M. Haiour. L^∞-error estimates of finite element methods with Euler time discretization scheme for an evolutionary HJB equation with nonlinear source terms. *Journal of Applied Mathematics and Computational Mechanics*, 16(1):19–31, 2017.

[21] M. Boulbrachene, Ph. Cortey-Dumont, and J. C. Miellou. La notion de acontraction. Applications. *Comptes Rendus de l'Académie des Sciences de Paris, Série I*, 302(16):591–594, 1986.

[22] M. Boulbrachene and M. Haiour. The finite element approximation of Hamilton-Jacobi-Bellman equations. *Computers and Mathematics with Applications*, 41(7-8):993–1007, 2001.

[23] M. Boulbrachene and H. Sissaoui. On the finite element approximation of variational inequalities related to ergodic control problems. *International Journal of Computers and Mathematics with Applications*, 31:137–141, 1996.

[24] H. Brézis. *Analyse fonctionnelle: Théorie et applications.* Masson, Paris, New York, Barcelone, Milan, Mexico, Sao Paulo, 1987.

[25] S. Chebbah, M. Haiour, A. Himadan, and U. Demirbilek. Fractal Scaling Laws and Asymptotic Behavior for Schwarz Domain Decomposition of Parabolic Hamilton–Jacobi–Bellman with AI-Driven Adaptivity. *Fractals*, 2026.

[26] S. Chebbah, M. Haiour, and S. Messaoudi. A Generalized Schwarz Method for Systems of Quasi-Variational Inequalities. *The Pečarić Journal of Mathematical Inequalities*, 1:49–58, 2025.

[27] S. Chebbah, S. Madi, and M. Haiour. Overlapping Domain Decomposition Methods for Noncoercive Hamilton–Jacobi–Bellman Equation. *European Journal of Pure and Applied Mathematics*, 18(2):Article 6070, 2025.

[28] P. G. Ciarlet and J.-L. Lions, editors. *Handbook of Numerical Analysis, Vol. II: Finite Element Methods (Part I).* North-Holland, 1991.

[29] P. G. Ciarlet and P. A. Raviart. Maximum principle and uniform convergence for the finite element method. *Computer Methods in Applied Mechanics and Engineering*, 2(1):17–31, 1973.

[30] Ph. Cortey-Dumont. Contribution à l'analyse numérique des inéquations variationnelles sans principe du maximum discret. *Comptes Rendus de l'Académie des Sciences - Series I*, 1983.

[31] Ph. Cortey-Dumont. On finite element approximation in the L^∞-norm of variational inequalities. *Numerische Mathematik*, 47(1):45–58, 1985.

[32] Ph. Cortey-Dumont. Sur les inéquations variationnelles à opérateur non coercif. *M2AN. Mathematical Modelling and Numerical Analysis – Modélisation Mathématique et Analyse Numérique*, 19(2):195–212, 1985.

[33] Ph. Cortey-Dumont and J. C. Nedelec. Sur l'analyse numérique des équations de Hamilton-Jacobi-Bellman. *Mathematical Methods in Applied Sciences*, 9(1):198–209, 1987.

[34] L. Djemaoune and M. Haiour. Overlapping domain decomposition method for a noncoercive system of quasi-variational inequalities related to the Hamilton–Jacobi–Bellman equation. *Computational Mathematics and Modeling*, 27:217–227, 2016.

[35] L. C. Evans and A. Friedman. Optimal stochastic switching and the Dirichlet problem for the Bellman equations. *Transactions of the American Mathematical Society*, 253:365–389, 1979.

[36] M. J. Gander. Schwarz Methods over the Course of Time. *Electronic Transactions on Numerical Analysis (ETNA)*, 31:228–255, 2008.

[37] R. Glowinski. *Numerical Methods for Nonlinear Variational Problems.* Springer, 1984.

[38] M. Haiour and S. Boulaaras. Overlapping domain decomposition methods for elliptic quasi-variational inequalities related to impulse control problem with mixed boundary conditions. *Proceedings of the Indian Academy of Sciences (Mathematical Sciences)*, 121(4):481–493, 2011.

[39] M. Haiour and S. Boulaaras. The Finite Element Approximation of Parabolic Quasi-Variational Inequalities Related to Impulse Control Problem. *International Journal of Numerical Methods and Applications*, 5:123–139, 2011.

[40] R. H. W. Hoppe. Multi-grid methods for Hamilton-Jacobi-Bellman equations. *Numerische Mathematik*, 49:239–254, 1986.

[41] P.-L. Lions. On the Schwarz Alternating Method. I. In *First International Symposium on Domain Decomposition Methods for Partial Differential Equations*, pages 1–42, Philadelphia, PA, 1988. SIAM.

[42] P. L. Lions and J. L. Menaldi. Optimal control of stochastic integrals and Hamilton-Jacobi-Bellman equations (Part II). *SIAM Journal on Control and Optimization*, 20:82–95, 1982.

[43] P. L. Lions and B. Mercier. Approximation numérique des équations de Hamilton-Jacobi-Bellman. *RAIRO. Analyse Numérique*, 14(4):369–393, 1980.

[44] J. Nitsche. L^∞-convergence of finite element approximations. In *Mathematical Aspects of Finite Element Methods*, volume 606 of *Lecture Notes in Mathematics*, pages 261–274. 1977.

[45] H. A. Schwarz. Über einen Grenzübergang durch alternierendes Verfahren. *Vierteljahrsschrift der Naturforschenden Gesellschaft in Zürich*, 15:272–286, 1870.

[46] M. Sun. Domain decomposition algorithms for solving Hamilton-Jacobi-Bellman equations. *Numerical Functional Analysis and Optimization*, 14(1–2):145–166, 1993.

[47] S. Zhou and Z. Zou. A relaxation scheme for Hamilton–Jacobi–Bellman equations. *Applied Mathematics and Computation*, 186(1):806–813, 2007.

[48] S. Zhou and Z. Zou. An iterative algorithm for a quasi-variational inequality system related to HJB equation. *Journal of Computational and Applied Mathematics*, 219:1–8, 2008.